STABLY LAYERED FLUIDS

A thesis

submitted for the degree

of

Doctor of Philosophy in Mathematics

in th

University of Canterbury

by

A.K. Laing

University of Canterbury

Christchurch, New Zealand

May 1978

To Janice

CONTENTS

Page

ABSTRACT

Various problems associated with a stably layered fluid are studied.

Firstly, the flow of a layered fluid from a reservoir is considered. Steady solutions are sought and found to depend on the flow at the critical points, that is, points at which the long wave speeds for the different modes of gravity wave propagation vanish. For certain distributions of the layers' depths it is found that there are too many critical points, and hence the flow is overdetermined and no steady solutions are possible. Thus, when reservoir conditions are slowly altered so as to pass from one depth ratio to another, the flow will not necessarily change slowly too.

A closed three layered fluid with small density differences between the layers is also studied. The non-linear interactions between the two, closely related, internal wave modes are investigated, and general evolution equations are obtained for small disturbances at the interfaces. Permanent solutions involving one mode alone are calculated, but it is found that at certain wavelengths the slower mode permanent waves resonantly generate harmonics of the faster mode.

When the group velocity of a train of faster mode waves is the same as the phase velocity of a slower mode wave there is significant interaction leading to a permanent wave structure comprising a group of permanent envelope and a carrier wave also of permanent shape. For each wavelength

the theory predicts several forms of structure. However, numerical solutions were only obtained for some of the simpler forms.

CHAPTER 1

INTRODUCTION

This thesis deals with various problems associated with a stably layered fluid. In general the systems considered comprise a rigid lower boundary with homogeneous layers of fluid arranged in order of decreasing density and bounded above by either a free surface or a rigid lid.

The most important areas within these fluids are the regions of density discontinuity, or the interfaces, and it is here that a disturbance within the fluid will manifest itself. If a free surface is considered an interface whose upper layer is of zero density, then a system with n interfaces will allow n different modes by which a given disturbance may propagate. Each of these n modes has an associated long wave speed. Hence, a long wave could propagate at any of n speeds.

Suppose each layer is moving steadily, then we define a Froude number as less than unity when long waves at the interfaces can propagate both upstream and downstream, and greater than unity when they can propagate downstream only. Consequently, if there are n wave modes, there will be n different Froude numbers and each will be less or greater than unity depending on whether or not its associated long wave speed is sufficient to propagate a disturbance upstream. If a Froude number is less than unity then the flow is said to be subcritical with respect to that wave mode, and if greater than unity it is said to be supercritical. When a

Froude number is unity then the flow is critical, and it is in the regions of critical or near-critical flow that most of the interesting problems lie.

For a fluid with variations of the flow speed in the direction of flow, there arises the possibility of the fluid passing through critical conditions at some points. These discrete points are called critical points and play an important role in solving the flow. If the flow is backed up by an infinite reservoir and there is a smooth geometry of contraction of the flow channel, then there will be steady downstream increase in flow velocity and a number of critical points may exist. For a steady system WOOD (1968 and 1970), WOOD and LAI (1972a and 1972b), and LAI and WOOD (1973) provide examples of the use of critical points in solving flows. BRYANT (1974), and BRYANT and WOOD (1976) further developed this idea and applied it to a situation in which steady flow solutions are bounded by unsteady regions in which the theory predicts and excessive number of critical points. Chapter two is an application of the same techniques to a slightly more complicated structure, and there are several different features revealed.

The question of critical points is continued into Chapter three to clarify both the role of critical points in unsteady flows, and the association of critical points with the interfaces.

The latter question introduces the problem of systems with more than one internal mode of wave propogation. The linear analysis in Chapter three shows the close relation between internal modes in contrast to the fairly well

defined identities of the modes in internal/surface systems. The latter part of this thesis concentrates on the non-linear theory of the system with two internal modes. The close relation of the modes causes effects not evident in studies where the interacting parts are well identified such as in the interactions between waves with vastly different modes of propogation.

The aim of this nonlinear analysis is ultimately to seek waves of permanent form which may exist within this system. Permanent waves and permanent wave structures are indeed found with features definitely attributable to the closely related, internal nature of the two modes.

As with the earlier part of the thesis, the problem is historically derived from flows of a critical nature. The concept of permanent waves began with the discovery of solitary waves, that is, isolated pulses with constant shape. The wavelengths of these "solitons" is effectively infinite and they travel at speeds near the longwave speed [in actual fact the speed is $\{g(h+a)\}^{\frac{1}{2}}$ where h is the fluid depth and a the amplitude of the wave] which characterises the critical conditions for a fluid. In other words, if a fluid contains a critical point, then a solitary wave would be stationary and permanent in form near that critical point.

The theory of permanent waves originated in the reconciliation of two distinct classical treatments of gravity waves on homogeneous, incompressible, irrotational fluids. Defining a, ℓ and h as scales of amplitude, wavelength and fluid depth respectively, the two approaches

are based on the two parameters $\varepsilon = a/h$ and $\mu = h/\ell$. The first is an initially infinitessimal theory involving expansions based on the small parameter $\varepsilon (\ll \mu^2)$. This can be Fourier analysed and to a first approximation describes linear dispersive wave motion. The other method is the long wave (or shallow water) theory for which $\mu^2 (\ll \varepsilon)$ is the small parameter. Distortion and breaking of waves are features of this approach. However, when $\varepsilon/\mu^2 = 0(1)$ these effects attain a balance, and waves whose shape is conserved can exist. Initial investigations were pursued in this field by SCOTT-RUSSELL(1844), BOUSSINESQ (1871), RAYLEIGH (1876), and KORTEWEG and DE VRIES (1895).

The Korteweg - de Vries equation which describes the evolution of waves under these conditions has been found relevant for many physical problems besides small, finite amplitude water waves. These include: Magneto-hydromagnetic waves in cold plasma; Rotating flow in a tube; Pressure waves in liquid gas bubble mixtures; Ion accoustic waves in an anharmonic crystal; Longtitudonal vibrations of a harmonic discrete mass string; and Longtitudonal dispersive waves in elastic rods [see KRUSKAL (1974) for references].
One of the features of the Korteweg - de Vries equation is that it accommodates solutions of permanent form.

Internal waves of permanent form were not considered until much later [KEULEGAN (1953), LONG (1956)] when solitary waves at a lone interface in a two layer system with fixed upper and lower boundaries were investigated. PETERS and STOKER (1960) extended the problem to include both free surface and internal solitary waves, and BENJAMIN

(1966), using a flow force perturbation expansion, provides a generalised theory for internal permanent waves allowing arbitrary vertical density and velocity distributions, and either a free upper surface or a rigid upper boundary.

The interaction of different wavetrains has long been a topic of interest, particularly in oceanography. The concept of radiation stress was used by LONGUET-HIGGINS and STEWART (1960) to study the effect of a wavetrain of long waves on another of short waves. The variation in energy of the short waves is found to correspond to the work done by the longer waves against the radiation stress of the short waves. This study has later been extended to a two layer system with a free surface to see the effect of long interfacial waves on a wavetrain of short free-surface waves [GARGETT and HUGHES (1972)]. The drawback of this method in relation to the present study is the prescribing of the long waves.

However, the present approach is based on a general method proposed by BENNEY (1966) for studying long non-linear waves and their interactions without prior knowledge of the wave profiles. Generalised expansions in both parameters ε and μ^2 are found and solutions sought in the neighbourhood of $\varepsilon = \mu^2 = 0$. Korteweg - de Vries type evolution equations are predicted for the amplitudes of disturbances and permanent forms of waves are found. In subsequent papers (1970, 1973, 1974a and 1974b) BENNEY has further investigated interactions of long non-linear waves and in a 1977 paper produced a generalised approach to non-linear interactions between long and short waves.

In the present study several features make BENNEY'S approach preferable to BENJAMIN'S.

Benjamin's analysis is primarily a steady flow analysis based on an expansion of the wave resistance in a small displacement parameter ε. The problem then yields solutions which are shown to be derived from the $0(\varepsilon^2)$ terms. Such solutions are of necessity permanent in form.

However, Benney's method is initially an unsteady expansion of the general problem. Thus, evolution equations can be found for which solutions of permanent form are special cases. This method provides a better basis for studying non-linear wave interactions since the notion of wave propagation is present until the final step.

The former approach retains very close contact with its physical interpretation. However, mathematically the flow force is regarded as an integral equation to be solved by successive approximation. On the other hand Benney writes partial differential equations for the non-linear perturbation equations. These can be solved using fairly standard techniques, and generally seem more manageable than integral equations.

One development incorporated in the present study is that used by BRYANT (1973) [and in subsequent papers] where the wavelength parameter μ is unrestricted, and so the expansion is in terms of ε but allows a wide range of μ.

This μ-exact approach means that Stokes' waves, Cnoidal waves, and Solitary waves can all be found from the theory. For small μ (long waves) Benney's results can be recovered and Korteweg - de Vries type equations

give the evolution of the interfacial amplitudes.

The significance of the non-linear effects incorporated into the analysis is in the quadratic interactions they represent between the various wave harmonics present. These interactions are particularly significant if resonance or near-resonance occurs. If k is a wavenumber, and $\omega(k)$ the associated linear frequency of a wave, then the resonance conditions for quadratic interactions require that

$$k_1 + k_2 + k_3 = 0 \tag{1.1}$$

$$\omega(k_1) + \omega(k_2) + \omega(k_3) = 0. \tag{1.2}$$

In the presence of more than one mode of propagation the frequencies may be of any mode, hence a wide range of possibilities is present. For near-resonance the relation in (1.2) is a near equality in which case there is still an appreciable transfer of energy possible between elements of the near-resonant triad - For a conservative system, at resonance the energy within a triad is conserved but can be readily transferred between the component harmonics.

For a closed three layered system there are two interfaces and two internal modes for wave propagation. The non-linear interactions between harmonics of both modes and their contribution to the formation of permanent waves and groups of waves with permanent envelopes are studied in chapters four and five. Chapter four concentrates on developing the relevant evolution equations and using these to solve for permanent waves consisting of one mode only or predominantly one mode. Chapter five extends this to include the interactions with groups of waves of the faster

mode, and the resulting permanent structures, consisting of groups of permanent envelope travelling at the same speed as their "carrier" waves (which also have permanent form), are found.

CHAPTER II

CRITICAL POINTS IN THE FLOW OF A LAYERED FLUID FROM A RESERVOIR

The properties of critical points are instrumental in solving certain types of flow. If a layered fluid flows with uniformly increasing velocity in the downstream direction, and the correct number of critical points exists, solutions for the flow can be found at these points and consequently anywhere in the fluid. At the critical points the geometry of the channel containing the fluid determines the flow. Hence the naming of the critical points as controls.

WOOD (1968) analysed the flow from a stably-layered reservoir through an open channel with a horizontal contraction. The method he established was used later for various reservoir outlet problems including: lock exchange flows (WOOD 1970), layered fluid flow over a weir (WOOD & LAI 1972a), layered fluid flow from a reservoir into a closed conduit (WOOD & LAI 1972b), and two-layered flow through a contraction (LAI & WOOD 1973). The critical point corresponding to the fastest wave mode, which occurs at the point of minimum width, is called the control, whilst the upstream critical points are called virtual controls.

BRYANT (1974b) and BRYANT & WOOD (1976) show for a problem of withdrawal through a contraction with a closed

conduit that if the withdrawal is steady there may be discontinuous changes to the flow ratios between the layers. In fact, for some configurations it is shown that no steady solutions exist, whilst for others there is the possibility of more than one solution. The involvement of critical points is all important and this chapter further investigates this role using a slightly more complicated model. The work was begun as part of a Masters Thesis by the author (1975).

Consider a large Reynold's number (inviscid), non-diffusive, stably layered fluid, flowing in the positive-x direction through a smooth horizontal contraction with a point of minimum width at x = 0. A weir is placed in the contraction so that its maximum height is at x = 0. Assume the flow is backed up by a reservoir so that the time for a fluid particle to travel through the contraction is small compared to the time for the streamline patterns to change. This is effectively a system of steady flow with reservoir conditions that can be prescribed. Also assume the hydrostatic approximation, which is reasonable provided the reservoir outlet's dimensions change only gradually so that vertical accelerations are negligible compared to horizontal accelerations.

§2.1. The aim of this chapter is to explore the involvement of critical points in the limiting conditions for steady solutions of a reservoir outlet flow regime. Mathematically, for a stable system there is a fixed number of critical points (not exceeding the number of flowing layers).

However, there are situations in which an excessive number of critical points tends to form and so cause over-determination of the system, and hence instability.

Consider the system depicted in figure (2.1) with two flowing layers above a third stagnant layer. Both the height and width of the channel are functions of x and the geometry of the channel is determined by the relation $h(x) + b(x) =$ a constant, where $b(x)$ is the channel width and $h(x)$ the height of the weir above some datum. The flowing layers are represented by the subscripts 1 and 2 for lower and upper layers respectively, whilst the non-flowing layers by 0 and 3. The thicknesses of layers are y_i, the fluxes Q_i, the velocities u_i, and the densities ρ_i where $\rho_0 > \rho_1 > \rho_2 > \rho_3$. Also, the undisturbed layer thicknesses are Y_i, and the maximum height of the weir (at $x = 0$) is H.

This system has three main points of interest: a control at the point of minimum width (MW) which is also the weir crest, a virtual control (VC) somewhere upstream at $x = x_{VC}$, and a point of contact between the lower interface and the weir (C) which is also upstream of MW, at $x = x_C$. Suppose the interface levels can be altered. For example, if the reservoir is slowly drained (very slowly so as not to upset the steady flow approximations made), then the positions of VC and C will change. The interesting question is whether conditions can be found for which no steady solutions are possible. That is, as the critical points move from one part of the geometry to another, the flow experiences an unsteady transition.

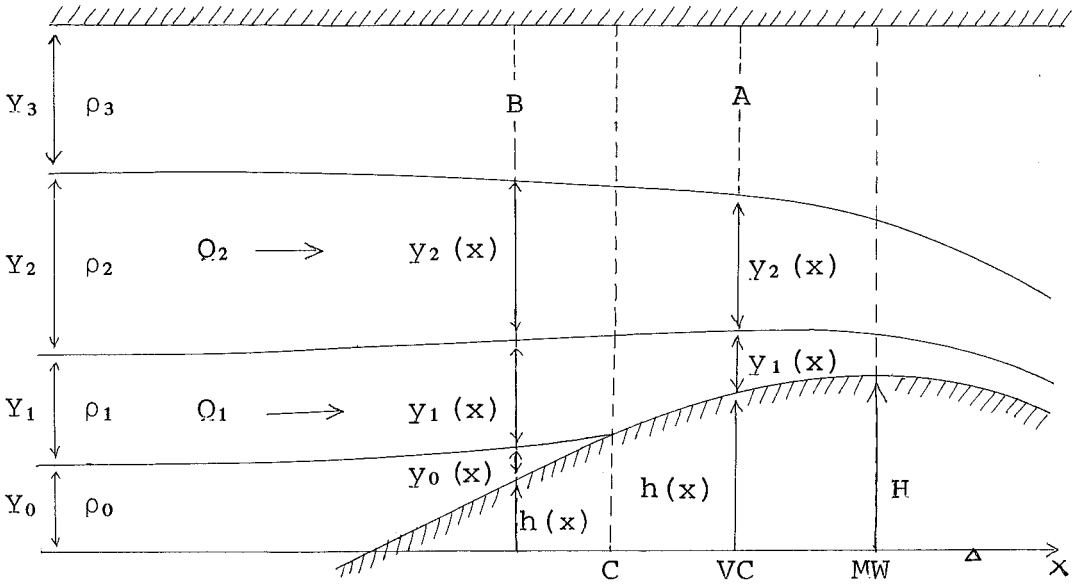

Elevation

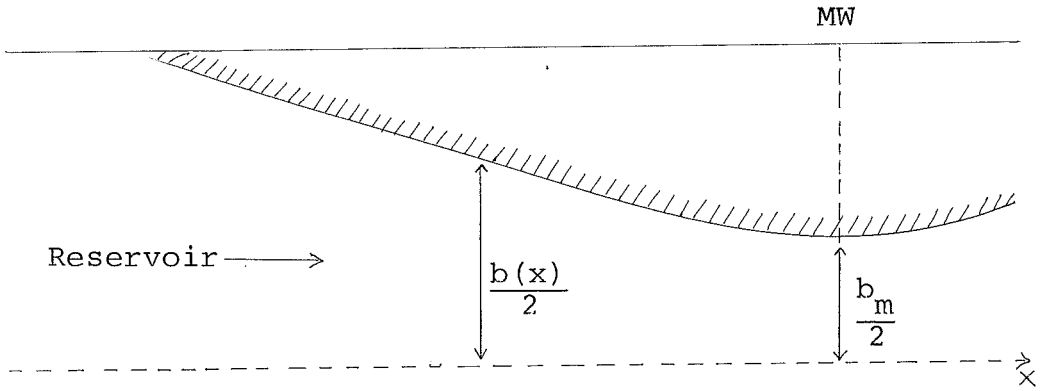

Plan

Figure 2.1

Geometry is $b_m + H = b + h$

The flow regime may be subdivided into two types: flows with the virtual control upstream or downstream of the point of contact respectively ($x_{VC} \lesseqgtr x_C$). The regions with $|x_{VC} - x_C|$ small are of particular interest since the proximity may well influence the solutions. In this section the model is analysed theoretically. A discussion of possible experimental situations is included in the presentation of the results in §2.3.

§2.1:1. Firstly consider $x_C < x_{VC} < x_{MW}$.

The energy equations at the interfaces yield

$$\tfrac{1}{2} y_2 G_2^2 = Y_0 + Y_1 + Y_2 - y_1 - y_2 - h \tag{2.1}$$

$$\tfrac{1}{2} y_1 G_1^2 = \tfrac{1}{2} y_2 \frac{\rho_{23}}{\rho_{12}} G_2^2 + Y_0 + Y_1 - y_1 - h \tag{2.2}$$

where $\rho_{ij} = \rho_i - \rho_j$ and G_i^2 is the dimensionless quantity $\dfrac{\rho_i Q_i^2}{gb^2 y_i^3 (\rho_i - \rho_j)}$ ($j = 3$ if $i = 2$, $j = 2$ if $i = 1$).

Clearly further equations are required, so the condition that the layers must vary smoothly is used. Differentiating equations (2.1) and (2.2) and solving;

$$\frac{dy_1}{dx} = \frac{1}{b}\frac{db}{dx}\frac{|D_1|}{|D_0|}, \quad \frac{dy_2}{dx} = \frac{1}{b}\frac{db}{dx}\frac{|D_2|}{|D_0|} \tag{2.3}$$

where $|D_0| = (1 - G_1^2)(1 - G_2^2)\dfrac{\rho_{12}}{\rho_{23}} - G_2^2$,

$$\frac{1}{b}\frac{db}{dx}|D_1| = (1 - G_2^2)\left[\frac{1}{b}\frac{db}{dx}\left(G_1^2 y_1 \frac{\rho_{12}}{\rho_{23}} - G_2^2 y_2\right) - \frac{\rho_{12}}{\rho_{23}}\frac{dh}{dx}\right] - G_2^2\left(G_2^2 y_2 \frac{1}{b}\frac{db}{dx} - \frac{dh}{dx}\right),$$

and $$\frac{1}{b}\frac{db}{dx}|D_2| = \frac{1}{b}\frac{db}{dx}\left(G_2^2 y_2 - G_1^2 y_1 \frac{\rho_{12}}{\rho_{23}}\right) + \frac{\rho_{12}}{\rho_{23}}\frac{dh}{dx} + \frac{\rho_{12}}{\rho_{23}}(1 - G_1^2)\left(G_2^2 y_2 \frac{1}{b}\frac{db}{dx} - \frac{dh}{dx}\right).$$

The points at which D_0 is singular are the critical points one of which is at $x = 0$ and the other at $x = x_{VC}$. To invoke the finiteness condition on $\frac{dy_1}{dx}$ and $\frac{dy_2}{dx}$ requires that either $\frac{db}{dx} = 0$ or $|D_1| = |D_2| = 0$ at the critical points. Obviously at the control $\frac{db}{dx} = 0$ and so we must have that D_1 and D_2 are also singular at the virtual control.

[Notes: (1) An unsteady analysis of the same configuration would give long wave speeds vanishing under the same condition of singularity of D_0. Briefly, the characteristic directions for unsteady propogations ($\dot{x}_k$) are defined by singularity of a coefficient matrix $D(\dot{x})$; so $|D(\dot{x})| = 0$. Now $\dot{x}_k$ corresponds to the long wave speed of one of the interfacial modes, and thus, for steady flow, the points at which $\dot{x} = 0$ correspond to the critical points. This is born out by the observation that $|D(\dot{x} = 0)| = 0 \Rightarrow |D_0| = 0$. This relation between the characteristics and critical points is clarified in Chapter III.

(2) D_0, D_1, and D_2 differ only in one column. Given that $|D_i| = 0$ for any two $i \in \{0,1,2\}$ then, means that $|D_i|$ will vanish for all $i \in \{0,1,2\}$. Hence, smoothness of y_i gives only two independent conditions at the virtual control,

$$|D_0| = |D_1| = 0.].$$

Thus far: at VC, equations (2.1) and (2.2) along with

$$|D_0| = |D_1| = 0;$$

at MW, equations (2.1) and (2.2) along with

$$|D_0| = 0;$$

and at C, equations (2.1) and (2.2) with

$$-y_1 G_1^2 - \frac{\rho_{01}}{\rho_{12}} (Y_0 - h) = 0$$

or $$\rho_{01}(Y_0 - h) + \rho_{12}(Y_0 + Y_1 - y_1 - h) + \rho_{23}(Y_0 + Y_1 + Y_2 - h - y_1 - y_2) = 0 \qquad (2.5)$$

are the equations.

The first seven of these at VC and MW are sufficient to solve for Q_1, Q_2, y_{1VC}, y_{2VC}, y_{1MW}, Y_{2MW} and h_{VC} (or x_{VC}), and once these have been obtained the final three equations at C will give y_{1C}, y_{2C} and h_C.

Consider now the limiting conditions for this type of flow. If the model is solved for various levels of the upper interface while the other external parameters are held constant, a dependence of this type of solution on the interface level is deduced. The higher the interface, the further downstream the contact point and the further upstream the virtual control. (This is true for most cases although exceptions are found later.) In the region of small $x_{VC} - x_C$ three alternatives are suggested:

(1) $|x_C - x_{VC}|$ vanishes with no discontinuity to the solutions and so there is continuity between the solutions with $x_C > x_{VC}$ and those with $x_C < x_{VC}$, at $|x_C - x_{VC}| = 0$.

(2) Critical conditions are reached at C or some point upstream of C while VC and C are still distinct.

(3) As $|x_C - x_{VC}|$ vanishes, C ceases to exist and this regime is "continuous" with a regime of three layers flowing.

The first suggestion is extremely unlikely since different equations are used to solve the two regimes and

continuity at C is unlikely. This was indeed verified by the results. The other possibilities may be tested as follows:

(2) By calculating the "critical matrix", analogous to D_0, for the three layer region upstream of C and evaluating its determinant as $x \to x_C$. If a point upstream of C becomes critical while $x < x_C$, then C will become super-critical with respect to this speed (or mode) and testing this determinant for a change of sign at C will suffice.

(3) By calculating $\frac{dy_0}{dx}$ at C over a range of interface levels. If, as the interface rises, $\frac{dy_0}{dx}$ passes smoothly through zero at C, while conditions are still subcritical with respect to this mode, then the lower interface must become tangential to the weir, and the third layer begins to flow. By the same token, given a three-flowing-layer regime and a falling interface, at this point the third layer will cease to flow.

Note that as the third layer flows a third wave mode forms with an associated critical point which appears at C. So C is critical with respect to this new mode, but still subcritical with respect to the second mode considered above.

The above tests necessitate setting up equations for the region $x < x_C$:

$$\tfrac{1}{2} y_2 G_2^2 = Y_0 + Y_1 + Y_2 - y_0 - y_1 - y_2 - h \tag{2.6}$$

$$y_1 \frac{\rho_{12}}{\rho_{23}} G_1^2 = y_2 G_2^2 + \frac{\rho_{12}}{\rho_{23}} (Y_0 + Y_1 - y_0 - y_1 - h) \tag{2.7}$$

$$-y_1 \frac{\rho_{12}}{\rho_{23}} G_1^2 = \frac{\rho_{01}}{\rho_{23}} (Y_3 - y_0 - h). \tag{2.8}$$

Differentiating,

$$\begin{bmatrix} 1-G_2^2 & 1 & 1 \\ G_2^2 & \frac{\rho_{12}}{\rho_{23}}(1-G_1^2) & \frac{\rho_{12}}{\rho_{23}} \\ 0 & \frac{\rho_{12}}{\rho_{23}} G_2^2 & \frac{\rho_{01}}{\rho_{23}} \end{bmatrix} \begin{bmatrix} \frac{dy_2}{dx} \\ \frac{dy_1}{dx} \\ \frac{dy_0}{dx} \end{bmatrix}$$

$$= \begin{bmatrix} G_2^2 y_2 \frac{1}{b}\frac{db}{dh} - 1 \\ \left(\frac{\rho_{12}}{\rho_{23}} G_1^2 y_1 - G_2^2 y_2\right)\frac{1}{b}\frac{db}{dh} - \frac{\rho_{12}}{\rho_{23}} \\ -\frac{1}{b}\frac{db}{dh}\frac{\rho_{12}}{\rho_{23}} G_1^2 y_1 - \frac{\rho_{01}}{\rho_{23}} \end{bmatrix} \frac{dh}{dx} . \qquad (2.9)$$

Thence, $\frac{dy_0}{dx}$ is readily found, and since y_{1C}, y_{2C}, and h_C are known, $\left.\frac{dy_0}{dx}\right|_{x=x_C}$ can be calculated. Furthermore, the matrix on the left hand side of equation (2.9) is the "critical matrix" to be tested for singularity at C. Call this D. Note that the flow will be subcritical upstream of C, so $|D| > 0$ in the reservoir, and so at C, $|D|$ will decrease towards zero as $|x_{VC} - x_C|$ becomes small.

These calculations therefore suffice to give the nature of limiting conditions to this type of flow.

What might happen physically in case (2) above requires a little speculation. Since x_C and x_{VC} are distinct, three critical points are implied for a two-moving-layer fluid. This flow is overdetermined and no steady solutions exist. Some breakdown must occur.

Also, if the upper interface is low, eventually the lower flowing layer must cease to flow and the virtual control is close to the point of minimum width.

Thus, if these solutions, for which $x_C < x_{VC} < x_{MW}$, are referred to as "type A" solutions, the range of interface levels over which they exist will be bounded by low upper interface levels where cessation of flow in layer 1 occurs, and also by high interface levels where (2) or (3) above occurs.

§2.1:2. *Now consider* $x_{VC} < x_C < x_{MW}$.

At the point of minimum width equations (2.1), (2.2) and $|D_0| = 0$ hold, while at the virtual control the equations are (2.6), (2.7) and (2.8), which after elimination of $Y_0 - y_0$ give

$$\tfrac{1}{2} y_2 G_2^2 + \tfrac{1}{2} y_1 G_1^2 \frac{\rho_{12}}{\rho_{01}} = Y_1 + Y_2 - y_1 - y_2 \qquad (2.10)$$

$$\tfrac{1}{2} y_1 \frac{\rho_{12}}{\rho_{23}} \frac{\rho_{02}}{\rho_{01}} G_1^2 - \tfrac{1}{2} y_2 G_2^2 = \frac{\rho_{12}}{\rho_{23}} (Y_1 - y_1). \qquad (2.11)$$

Differentiating,

$$\begin{bmatrix} 1-G_2^2 & 1 - \frac{\rho_{12}}{\rho_{01}} G_1^2 \\ G_2^2 & \frac{\rho_{12}}{\rho_{23}} - \frac{\rho_{02}}{\rho_{01}} \frac{\rho_{12}}{\rho_{23}} G_1^2 \end{bmatrix} \begin{bmatrix} \frac{dy_2}{dx} \\ \frac{dy_1}{dx} \end{bmatrix}$$

$$= \begin{bmatrix} G_2^2 y_2 + \frac{\rho_{12}}{\rho_{01}} G_1^2 y_1 \\ \frac{\rho_{02}}{\rho_{01}} \frac{\rho_{12}}{\rho_{23}} G_1^2 y_1 - G_2^2 y_2 \end{bmatrix} \frac{1}{b} \frac{db}{dx} . \qquad (2.12)$$

Call the matrix on the left hand side of equation (2.12) B, then the critical condition at VC is $|B| = 0$ and the finiteness conditions on $\frac{dy_1}{dx}$, $\frac{dy_2}{dx}$ give

$$\frac{1 - G_2^2}{G_2^2} = \frac{1 - \frac{\rho_{12}}{\rho_{01}} G_1^2}{\frac{\rho_{12}}{\rho_{23}} - \frac{\rho_{02}}{\rho_{01}} \frac{\rho_{12}}{\rho_{23}} G_1^2} = \frac{G_2^2 y_2 + \frac{\rho_{12}}{\rho_{01}} G_1^2 y_1}{\frac{\rho_{02}}{\rho_{01}} \frac{\rho_{12}}{\rho_{23}} G_1^2 y_1 - G_2^2 y_2} . \qquad (2.13)$$

Solutions can be found from equations (2.10), (2.11) and (2.13). [Note that the matrix D from (2.9) can be written using elementary row operations as

$$\text{constant} \times \begin{vmatrix} & & 0 \\ & B & \\ & & 0 \\ 0, & \frac{\rho_{12}}{\rho_{23}} G^2, & \frac{\rho_{01}}{\rho_{23}} \end{vmatrix}$$

and this is singular iff $|B| = 0$. So the elimination of $Y_0 - y_0$ is a matter of choice. Also note that $|D_0| \neq 0$ for $x_C < x < x_{MW}$ and $|B| \neq 0$ for $x < x_C$, $x \neq x_{VC}$.]

Again the limiting conditions for this type of flow are sought. For various levels of the upper interface $\frac{dy_0}{dx}\Big|_{x=x_C}$ and $|D_0|_{x=x_C}$ are calculated. As $|x_C - x_{VC}|$ becomes small, provided $|D_0| < 0$, there will be well-determined solutions.

Call this type of solution, for $x_{VC} < x_C < x_{MW}$, a "type B" solution.

§2.2:1. Solutions to the type-A problem in §2.1.1 cannot be found analytically if the problem is to be kept general. For a similar situation WOOD & LAI (1972a) manage to decouple the crest equations (at MW) from the virtual control equations by setting h_{VC} as zero, making the datum unknown, and proceed to solve analytically at VC. Thence a numerical method obtains solutions at MW and finally $H - h_{VC}$ can be determined. However, if reservoir conditions are to be prescribed along with the geometry (including the crest height H), the datum needs to be prescribed and all

the equations at C (viz (2.1), (2.2) and (2.5)) and MW (viz (2.1), (2.2) and $|D_0| = 0$) have to be solved simultaneously. For this purpose a Newton-Raphson numerical method is used once the equations have been analytically reduced as far as possible. Once solved, the conditions at C can be found from equations (2.9), (2.10) and (2.11) with $y_0 = 0$.

§2.2:2. For the type-B problem in §1.1:2

notice that there is no explicit h(x) dependence at VC (unlike the type-A problem for which this is quite evident). The number of unknowns is reduced by virtue of the fact that Q_i and x in the form of b(x) always appear together as $\frac{Q_i^2}{b^2}$. The equations can be decoupled and analytical solutions found at VC from equations (2.10), (2.11) and (2.13).

From (2.13) $G_2^2 = \frac{R}{1+R+y}$, $G_1^2 = \frac{yR'}{(1+y)(R+R') - R}$ (2.14)

where $y = \frac{Y_2}{Y_1}$, $R = \frac{\rho_{12}}{\rho_{23}}$ and $R' = \frac{\rho_{01}}{\rho_{23}}$.

Substitution into (2.10) and (2.11), and elimination of y_1, leads to a single equation

$$\left(\frac{Y_2}{Y_1} - y\right)[2y(R+R')(1+R+y) + 2R'(1+R+y) + Ry(1+R+R')] = 0 \qquad (2.15)$$

whence

$$y = \frac{y_{2VC}}{y_{1VC}} = \frac{Y_2}{Y_1} .$$

(The other possibility gives $y < 0$ and is non-physical.)

Furthermore

$$\frac{Y_2}{Y_2} = \frac{Y_1}{Y_1} = \frac{[(1+\alpha)(R+R') - R](1+R+\alpha)}{(1+R)[2\alpha(R+R') + R'] + \alpha^2(R+R')} ,$$

where $\alpha = \frac{Y_2}{Y_1}$, and also

$$\left(\frac{Q_2}{Q_1}\right)^2 = \frac{\rho_1}{\rho_2}\frac{G_2^2\, y_2^3}{G_1^2\, y_1^3} = \alpha^2 \frac{R}{R'}\,\frac{[(1+\alpha)(R+R') - R]}{(1+R+\alpha)}\,.$$

Consider now any $x \leqslant x_C$. Since $\frac{Q_2}{Q_1}$ is a constant, then

$$\frac{\rho_2\, y_1^3 Q_2^2}{\rho_1\, y_2^3 Q_1^2} = \frac{G_2^2}{G_1^2} = \left(\frac{y_1}{y_2}\right)^3 \alpha^2 \frac{R}{R'}\,\frac{[(1+\alpha)(R+R') - R]}{(1+R+\alpha)}\,. \qquad (2.16)$$

Also from equations (2.6), (2.7) and (2.8)

$$\frac{G_2^2}{G_1^2} = \left(\frac{y_1}{y_2}\right)\frac{R}{R'} \cdot \frac{R(Y_1-y_1) + (R+R')(Y_2-y_2)}{(1+R)(Y_1-y_1) + (Y_2-y_2)}\,. \qquad (2.17)$$

Using (2.16) and (2.17) and writing $\beta = \frac{y_2}{y_1}$, we eventually get

$$(\alpha - \beta)\,.\,\{(\alpha+\beta)(1+R+\alpha)[R'+\alpha(R+R')] + \frac{y_1}{Y_1}[(\alpha^2+\alpha\beta+\beta^2)\,.$$

$$(R+R')(1+R) + \alpha\beta(\alpha+\beta)(R+R') + (\alpha+\beta)R'(1+R)$$

$$+ \alpha\beta R']\} = 0. \qquad (2.18)$$

The only physical solution to this is $\alpha = \beta$,

so $$\frac{y_{2C}}{y_{1C}} = \frac{y_{2VC}}{y_{1VC}} = \frac{Y_2}{Y_1} = \alpha. \qquad (2.19)$$

This result in fact is true for all $x \leqslant x_C$ since equations (2.16) and (2.17) are quite general for the type-B situation.

At MW any attempts to solve analytically become too involved algebraically and numerical computation is necessary. The ratio in (2.19) does not hold at MW or for any $x > x_C$. These results are not surprising as the type-B situation is very similar to the two layer selective withdrawal problem for which WOOD (1968) found self-similar solutions with $\frac{y_2}{y_1}$ constant throughout. However for points downstream of C the flowing layers come into contact with the weir and this influences the solutions.

§2.3. *Results and Discussion.*

It is useful to present the results in the light of experimental possibilities and so a hypothetical experiment is considered. Assume all the external parameters are held constant except Y_1 and Y_2. The upper interface is allowed to drop. This is achieved by allowing free draining over the weir but replenishing the upper layer in the reservoir to maintain a constant depth. BRYANT (1974b) allowed control over all three layers whilst BRYANT & WOOD (1976) preferred complete draining with no replenishing. However, the models all represent reservoir outlet schemes and thus some inflow is likely. Hence, replenishing the upper layer to keep constant depth is considered acceptable although, from the laboratory point of view, less readily reproduced than complete draining.

The varying parameter as the interface falls is taken as Y_2, which increases. Firstly the ranges of Y_2 for solutions of both type-A and type-B have been found. This was done for a variety of values of R and R' to show the effect of density difference ratios on the limiting conditions. Figures (2.2), (2.3) and (2.4) show the ranges of Y_2 for which these solutions exist for the geometries with crest heights H = 0.5, 0.6 and 0.7 respectively. Note that all heights and depths are measured as proportions of $Y_0 + Y_1 + Y_2$. In all cases the width of the channel has a minimum of 0.1, $h + b = H + 0.1$ determines the geometry, and $Y_0 = 0.2$. The limits of the regimes are denoted by solid lines or regularly broken lines (that is ——— or ----) if flow becomes overdetermined through the presence of an extra

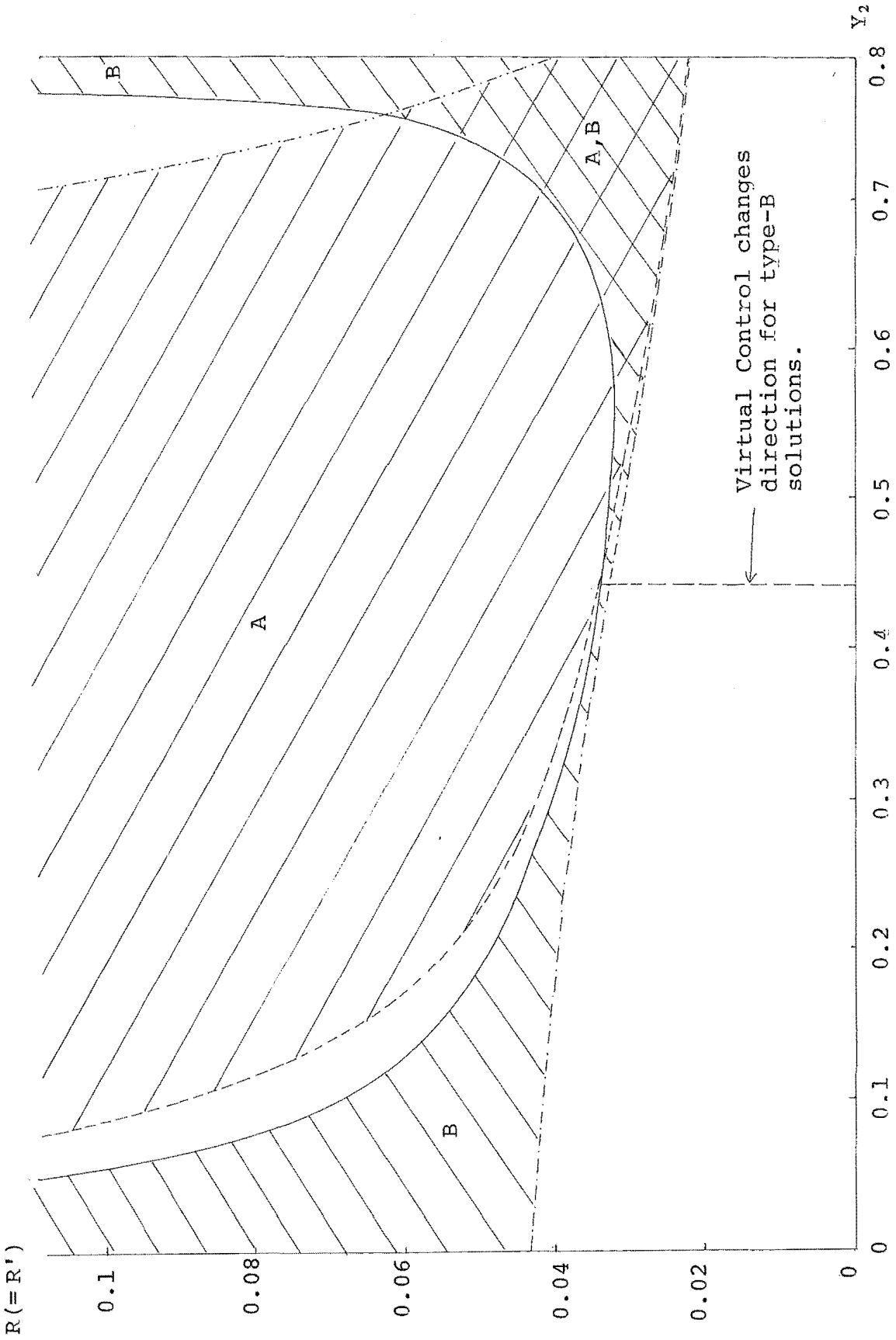

Figure 2.2

Ranges of Y_2 for Type-A and Type-B solutions to exist.

Y_0 = 0.2 and H = 0.5.

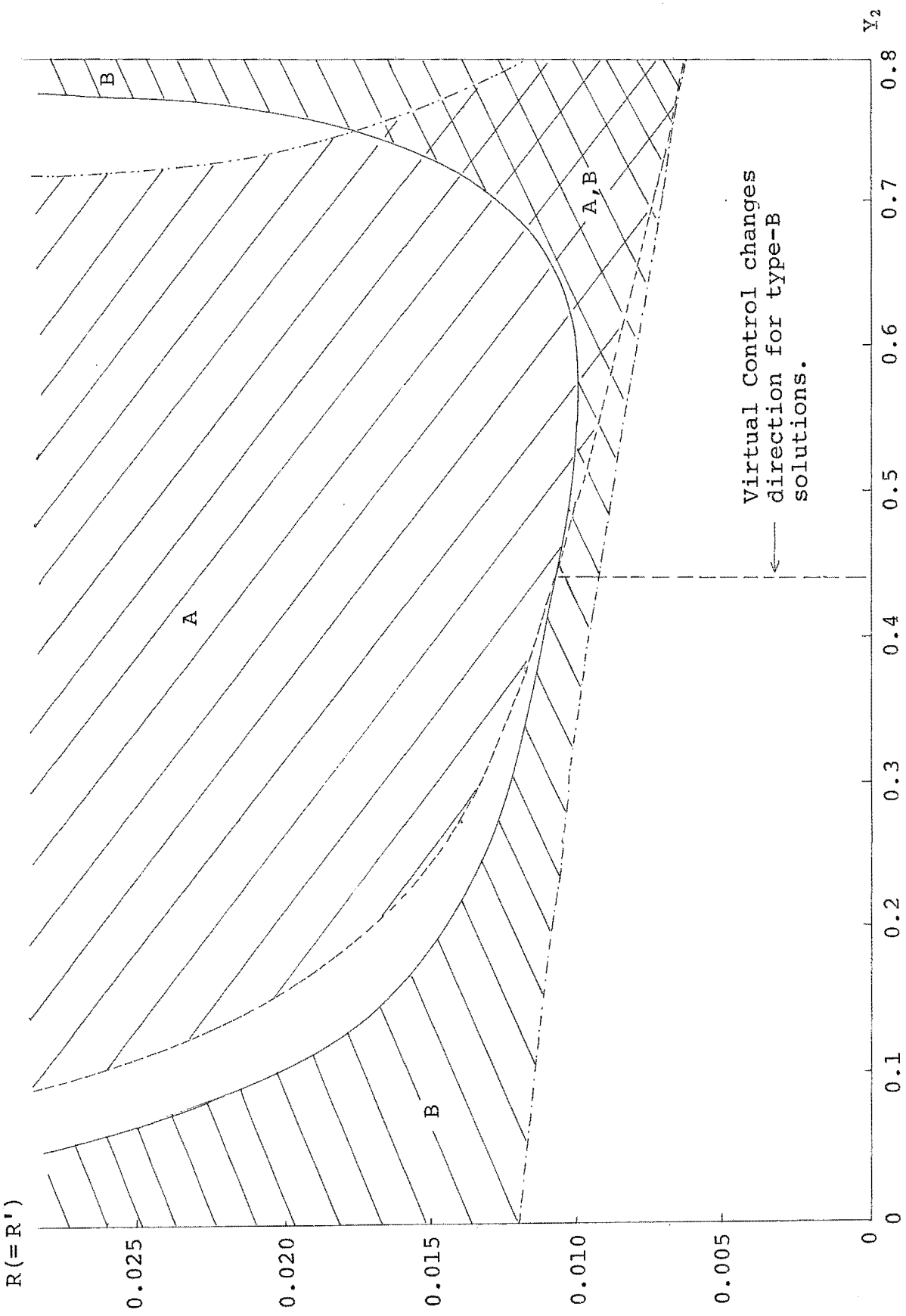

Figure 2.3

Ranges of Y_2 for Type-A and Type-B solutions to exist.

Y_0 = 0.2 and H = 0.6.

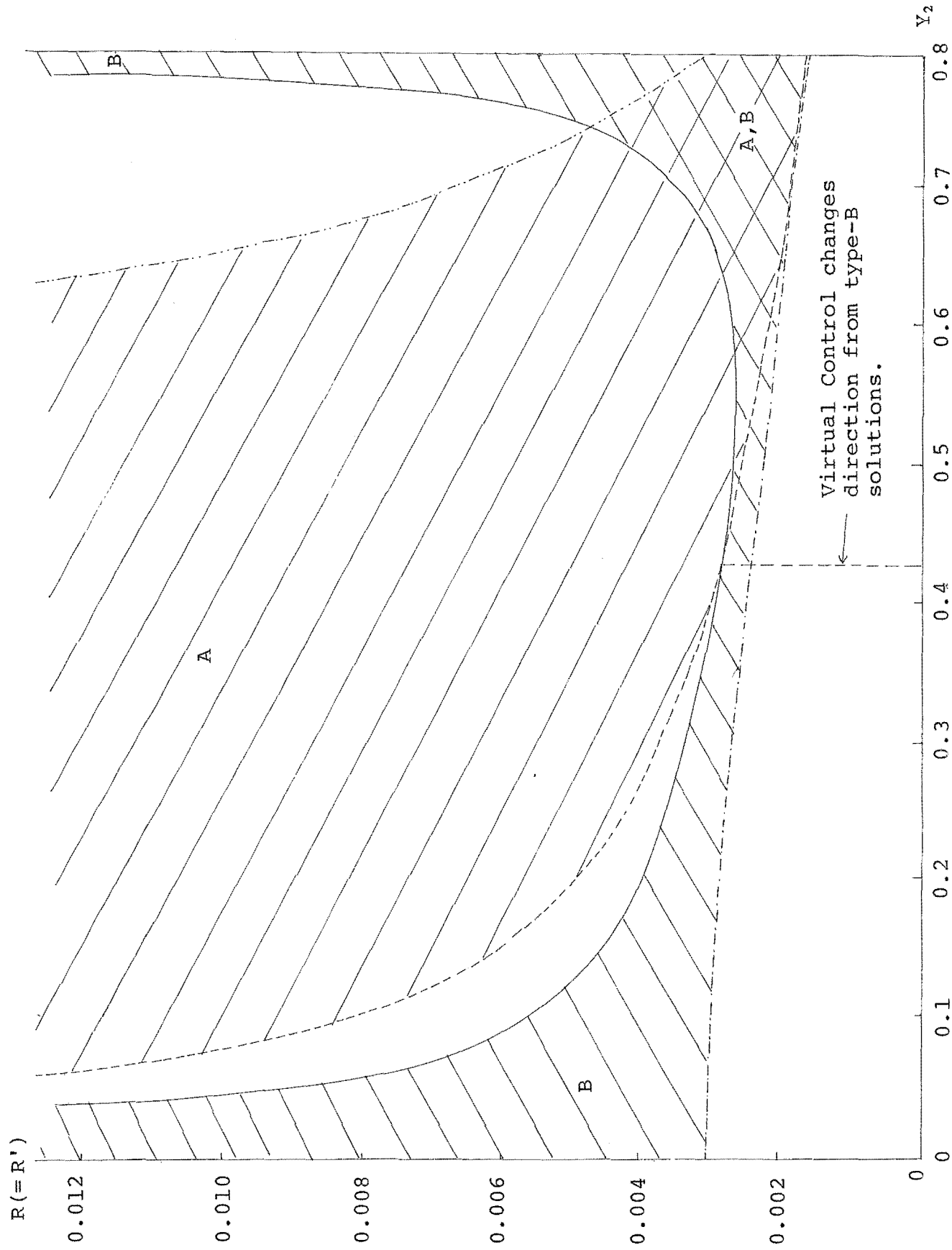

Figure 2.4

Ranges of Y_2 for Type-A and Type-B solutions to exist.

Y_0 = 0.2 and H = 0.7.

critical point, by (-·-·-·) if three-flowing-layer solutions are continuous with the two-flowing-layer solutions, and by (-·-·-·-·-·) when the lower layer ceases to flow because Y_1 has become too small.

Several features are notable:

(1) Lowering the crest height means the values of the density difference ratios for which the problem is of interst are higher. Since Boussinesq fluids are of most interest and ρ_3 is taken as being very small (even $\rho_3 = 0$ for a free surface), then the smaller R and R' are, the better. Subsequently the configuration with H = 0.7 will be used in preference to the others.

Several solutions were also obtained for reduced Y_0 (down to 0.1), but the effect of this was the same as lowering the crest and nothing extra was revealed.

(2) In every case for small $|x_C - x_{VC}|$ the limiting factor was the tendency to form an extra critical point. It thus follows that in each case there will be an unsteady break-down of the flow pattern at the boundary (to the two-flowing-layer regimes) for which the virtual control and contact point are close.

(3) For the type-B solutions there are two regions. If $Y_2 < 0.445$, 0.440 and 0.430 (in Figures (2.2), (2.3) and (2.4) respectively), x_{VC} increases as the interface drops, whilst for Y_2 larger than these values, x_{VC} decreases. These regions correspond to two branches of type-B solutions. For example if H = 0.7, and R = R' = 0.008, there are two

ranges of Y_2 for which type-B solutions exist.

If $Y_2 \in (0, 0.06)$, x_{VC} increases with Y_2, but for

$Y_2 \in (0.77, 0.80)$, x_{VC} decreases as Y_2 increases.

Figure (2.5), which has been included to show the dependence of x_{VC} and x_C on Y_2, makes these distinctions clear. This figure is drawn for the three density difference ratios $R = R' = 0.006$, 0.0036 and 0.0026. For the first two values the two regions of type-B solution are distinct, whilst for the latter value they are continuous, meeting at a point where h_{VC} (and hence x_{VC}) reaches a maximum.

This phenomenon is accountable if the experimental situation is considered. Firstly, it is reasonable to assume when one of the flowing layers is shallow that proportional changes in velocity for a small drop in the upper interface are small compared to the proportional changes in the layer thicknesses. That is, for velocity u and thickness y, $y\delta u \ll u\delta y$, so for purposes of small change in layer thickness assume the velocities in the thin layers are constant. Secondly, given the long wave approximation, the narrower any layer becomes, the slower the critical speed becomes (assuming the layer velocities constant). This of course refers to the slow mode since the fast mode's critical point is at MW. [This is a general comment. For example, the two layer system with layer depths y_1 and y_2 confined between rigid planes, has a single mode with wave velocity proportional to $1/(\rho_1 \coth ky_1 + \rho_2 \coth ky_2)$. In the long wave limit and as either y_1 or y_2 becomes very small this obviously

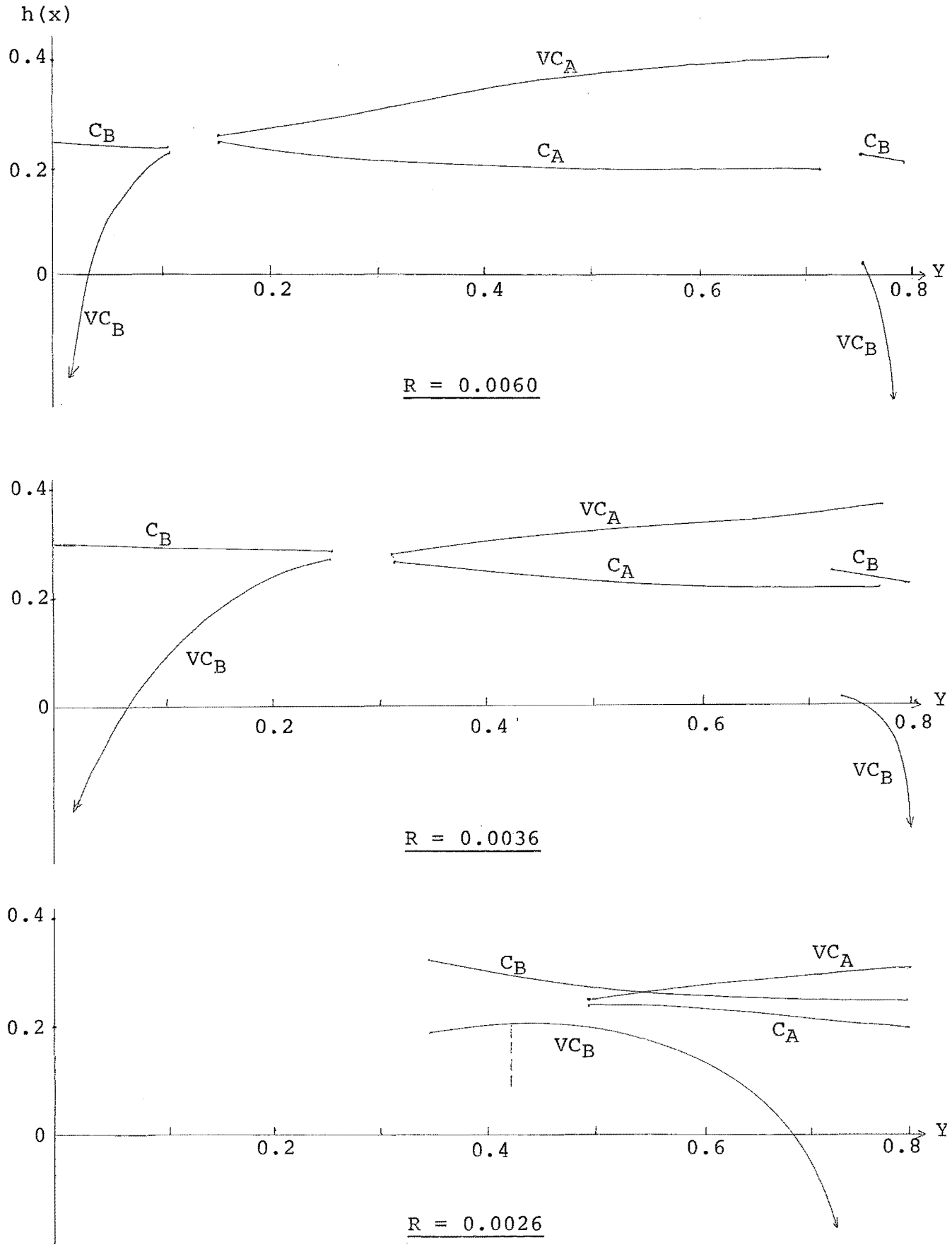

Figure 2.5

Positions of Virtual Control (VC) and Contact point (C) for various levels of the upper interface. Both types of solution are included and are denoted by the subscripts A and B. H = 0.7 and Y_0 = 0.2.

decreases. For two layers with a free surface and a rigid base the smaller of the two modes' speeds (in the long wave limit and with $y_1 + y_2$ a constant, say 1) is

$$\left\{\frac{\rho_1 \rho_2}{y_1 y_2} - \left[\frac{\rho_1^2 \rho_2^2}{y_1^2 y_2^2} - 4\left(\rho_2^2 + \frac{\rho_1 \rho_2}{y_1 y_2}\right)\rho_2 (\rho_1 - \rho_2)\right]\right\} \div \left(2\,\frac{\rho_1 \rho_2}{y_1 y_2} + \rho_2^2\right)$$

which also decreases for either y_1 or y_2 small. This case is akin to the present situation.]

Thus, at the beginning of the "experiment" the interface is still high and Y_2 small, so the critical speed is slow and the critical point well upstream. As the reservoir drains the interface drops, and Y_2 increases with an increase in the critical speed and a downstream movement of x_{VC} towards the contact point at x_C. At the other end of the scale, as Y_2 becomes large, Y_1 is small and decreasing. For small enough Y_1 the critical speed will be slow again and the critical point well upstream, getting further upstream as Y_1 diminishes.

This means two regions of type-B solutions exist, as $(x_C - x_{VC})$ will be large enough depending on Y_1 or Y_2 being small enough. For some parameters the critical speed never becomes sufficiently large (as the interface drops) for x_{VC} to be close enough to x_C for a breakdown. In this situation the type-B solutions are continuous but with a reversal in the direction of x_{VC}. This is the case for $R = R' = 0.0026$ in figure (2.5).

It is possible to deduce the above analytically. For $x \leqslant x_C$, write the critical determinant, $|B|$, from

equations (2.12), using (2.16) and (2.19), as

$$|B| = \text{positive constant} \cdot \left| G_1^2 - \frac{\alpha R'}{\alpha(R+R')+R'} \right| \cdot \left| \frac{R}{R'}(1+R+R')G_1^2 - (1+R+\alpha) \right| . \qquad (2.20)$$

Upstream and immediately downstream of x_{VC} the second factor on the right hand side of equation (2.20) is negative and so for a given $x = x_0$, as α varies the sign of the first factor in (2.20) will determine the sign of $|B|$ and hence whether x_0 is upstream or downstream of x_{VC}. If $G_1^2(\alpha;x)$ and $\frac{\alpha R'}{\alpha(R+R')+R'}$ are both sketched versus α and x in a three dimensional figure, it is not too difficult to establish that for x small enough, $|B| \geqslant 0$ when $\alpha \leqslant$ some α_0 or when $\alpha \geqslant$ some α_1, and where $|B| = 0$, x_{VC} is respectively increasing and decreasing.

One further point worth noting is the overlapping of type-A and type-B solutions in figures (2.2), (2.3) and (2.4). This implies that for some interface levels in certain distributions of the external parameters, both regimes may exist. Under experimental conditions the actual form of the solutions would probably be determined by the flow history. That is, as the interface lowers, the type-B solutions will most likely persist until breakdown occurs at the upper limits depicted in the diagrams. Similarly if the overlap were approached in the opposite manner, the type-A solutions would be expected to continue until their lower boundary is reached.

Thus, beginning with small Y_2 and allowing the system to drain, maintaining constant total depth, if only two layers are flowing then the virtual control will be upstream

of the point of contact and steady type-B solutions will exist. As Y_2 increases a point is reached where steady solutions no longer exist. The flow becomes overdetermined due to the presence of an extra critical point. In the diagrams this is represented by the gaps between regions of type-B and type-A solutions. Where the external parameters lie in one of these gaps, no steady solutions exist and as Y_2 traverses these values unsteadiness prevails. For larger Y_2, type-A solutions, with the critical point now upstream of the point of contact, appear. This brings a return to steady flow and these solutions continue until the interface drops so far as to cut off all flow in the lower layer.

If, for small Y_2, three layer flow exists, then as the upper layer drops, the third critical point will move downstream to the point at which the lowest layer stops flowing. Here, the third critical point vanishes, and a point of contact between the lower interface and the weir appears with the lower interface tangential to the surface of the weir. Two layer flow of type-B ensues, and as Y_2 gets larger there is either an unsteady transition to type-A solutions as before, or the possibility of overlap in which case type-B solutions are most likely to persist. The transformation of the third critical point to a contact point, or vice versa, is evident in the results by simultaneous vanishing of $\frac{dy_0}{dx}$ and the determinant of the critical matrix for three layer flow, whilst the two layer flow matrix remains non-singular.

Upper branch type-B solutions could only be evident in a reverse situation. Supposing it were possible to raise

the upper interface by replacing the second layer only, then at low levels of the interface solutions of type-B could exist. However, it should be noticed from figures (2.2), (2.3) and (2.4) that this upper branch always overlaps with either one layer flow or type-A solutions. Raising the interface would bring about either an unsteady breakdown and reversion to one layer flow or type-A flow, or a steady transition to three layer flow, depending on the parameters R and R'. Assuming that the flow history governs the form of solution where overlapping occurs, upper branch type-B solutions are unlikely to be encountered if the upper interface is falling since type-A solutions will persist with a possible transition to single layer flow.

As this is a model for a reservoir outlet, there is considerable importance in the discharges for each layer. For solutions within the steady type-A or type-B regions small changes in the external parameters are reflected in small changes in the discharges. However, as the unsteady boundaries to these regions are crossed the flow ratios cannot necessarily be expected to change smoothly and slowly. In the regions of unsteady solutions the flow ratios also oscillate unsteadily.

The dependence of flux on the upper interface level is plotted in figure (2.6). The nondimensional quantities

$$q_1 = \frac{\rho_1 Q_1^2}{\rho_{12}\, g (Y_0 + Y_1 + Y_2)^5} \quad \text{and} \quad q_2 = \frac{\rho_2 Q_2^2}{\rho_{23}\, g (Y_0 + Y_1 + Y_2)^5}$$

are drawn for different values of the density difference ratios R and R'. Only the type-A solutions are drawn. For a given set of reservoir conditions, there is very little

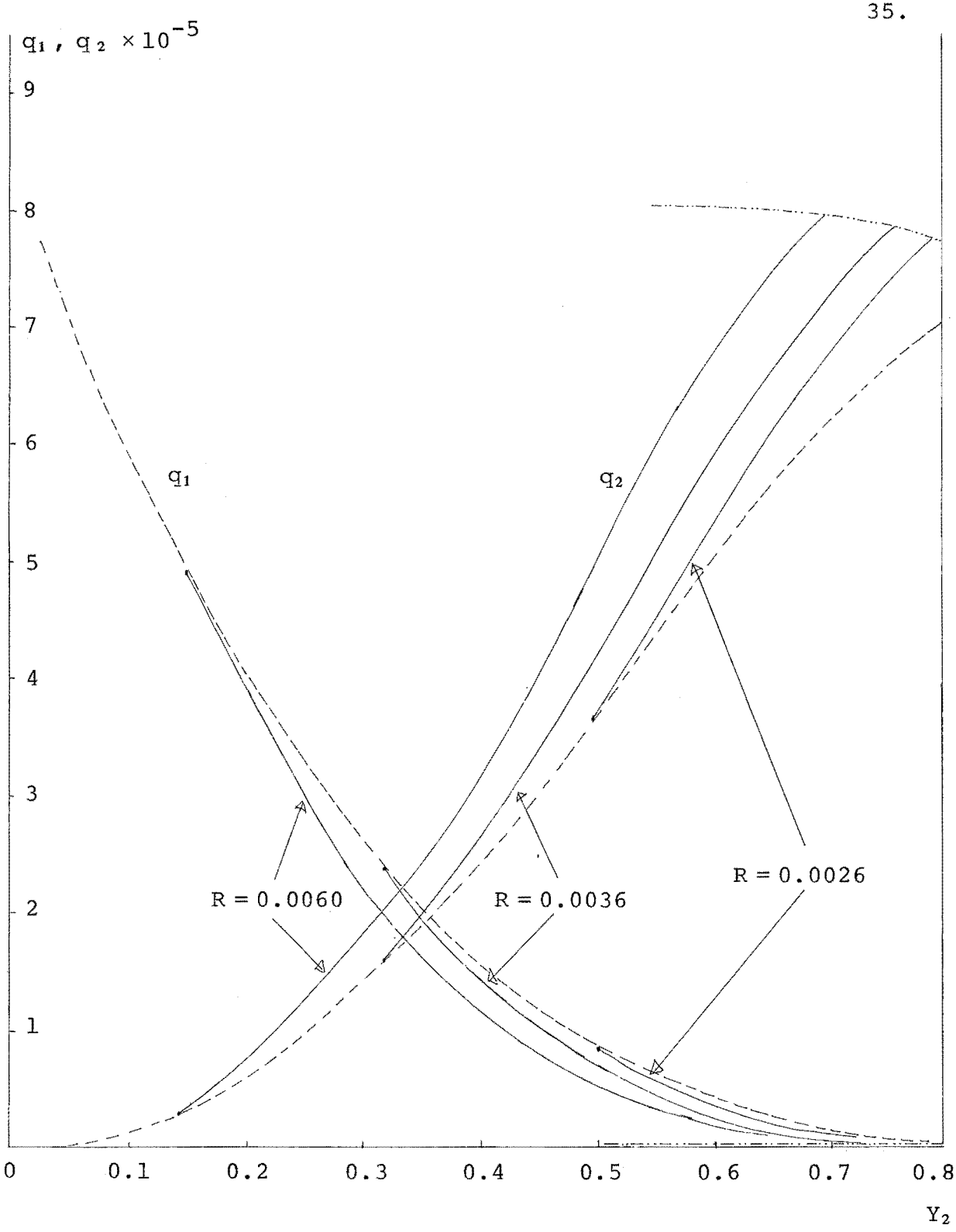

Figure 2.6

Fluxes in both flowing layers as functions of the upper interface level. The fluxes are plotted only for the ranges in which type-A solutions exist. The lower limit of Y_2 for a given R(= R') is denoted by -----, and the upper limit by -·-·-·- as in figure (2.4) (H = 0.7).

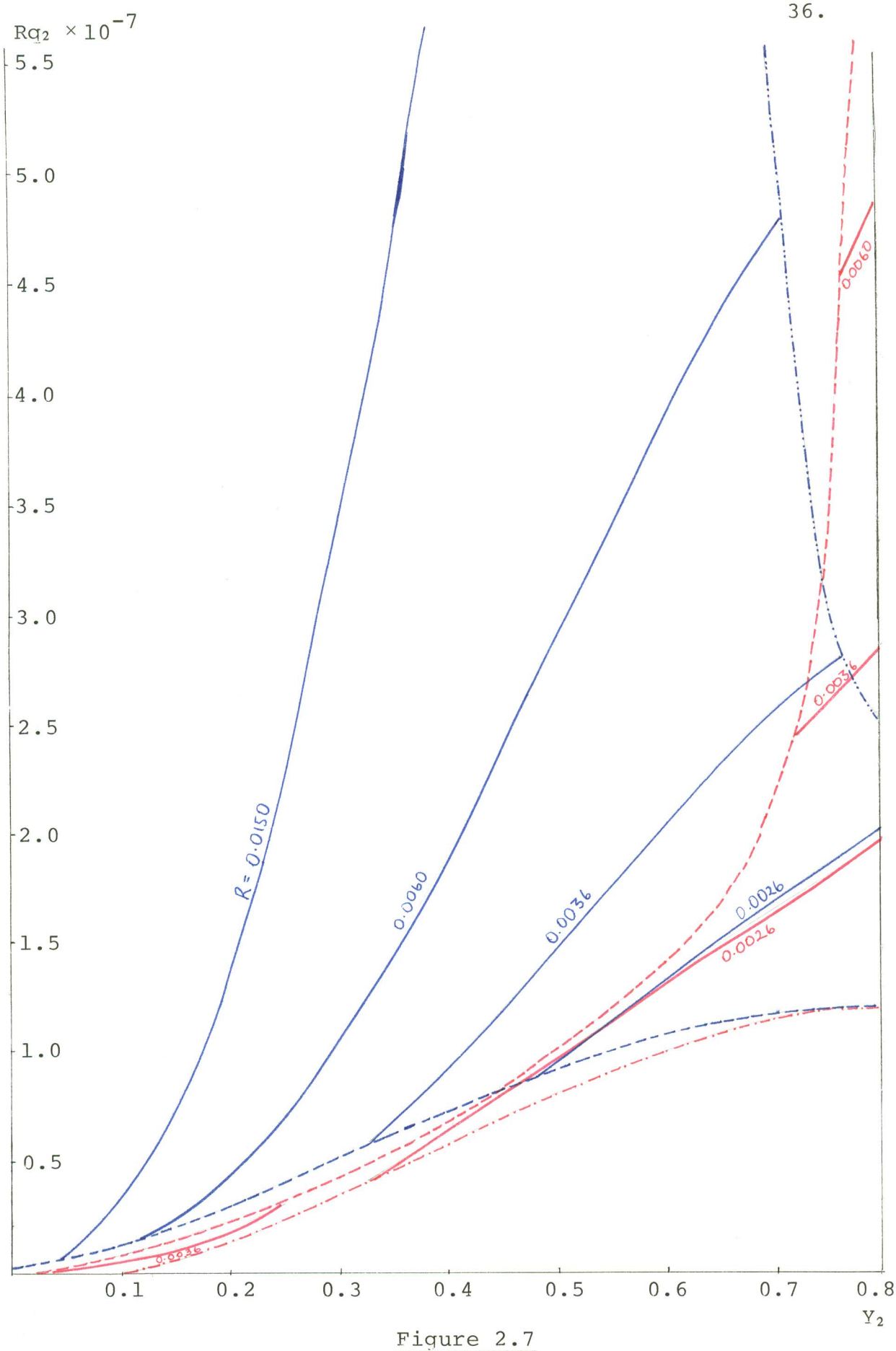

Figure 2.7

Weighted flux in the upper flowing layer for both types of solution (H = 0.7)

——— = Type-A solutions.
——— = Type-B solutions.

Boundaries to the ranges of Y_2 for which each type of solution is valid are indicated in the same way as in figure (2.4).

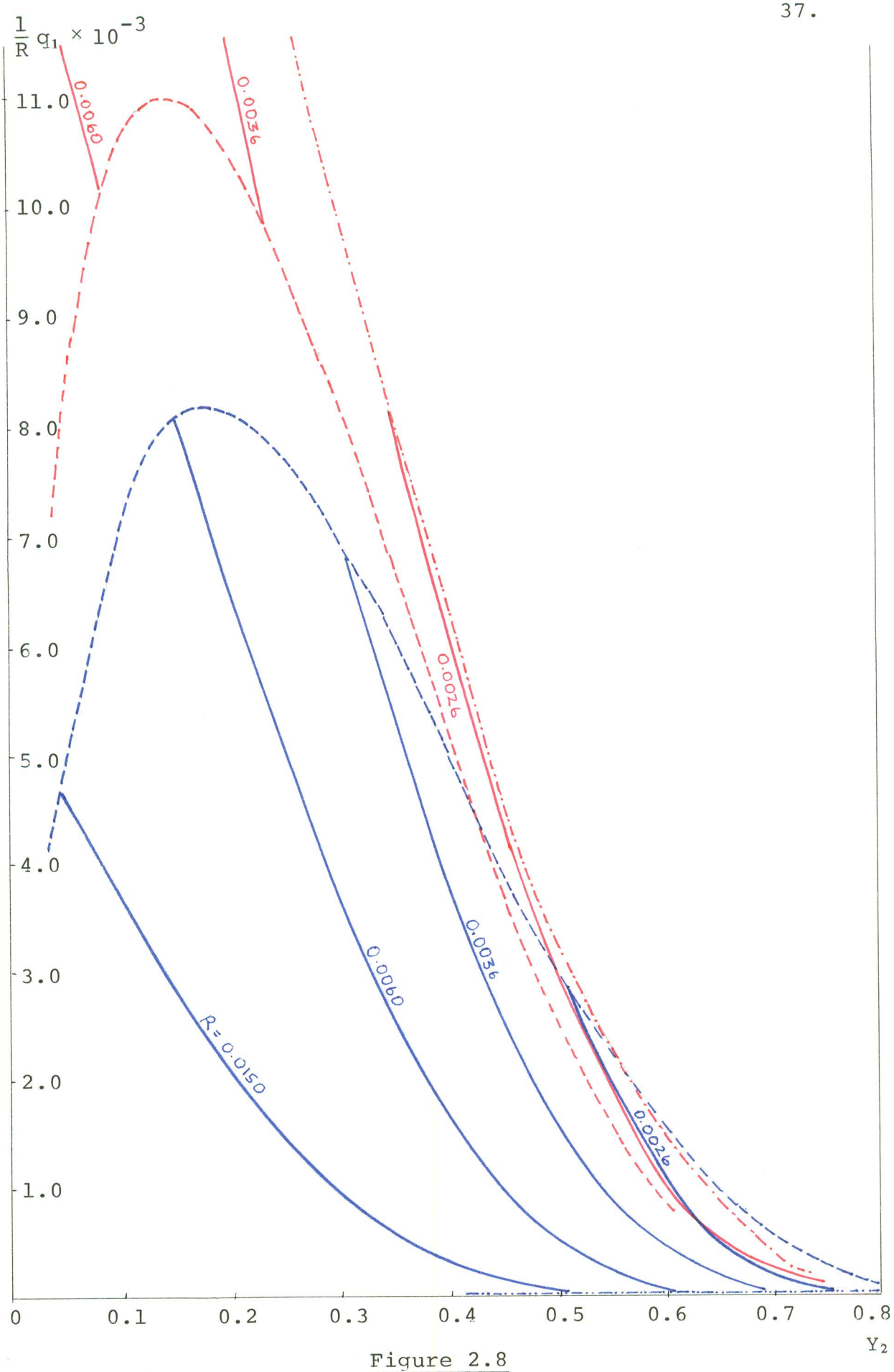

Figure 2.8

Weighted flux in lower flowing layer for both types of solution (H = 0.7)

——— = Type-A solutions.

——— = Type-B solutions.

Boundaries to the ranges of Y_2 for which each type of solution is valid are indicated in the same way as in figure (2.4).

spread in the flux. The density difference ratios appear to have limited influence. However, the closeness of the curves is a little misleading. There is a substantial vertical spread but over a large variation in the density difference ratios. For example for $Y_2 = 0.6$, $q_2 = 5.15 \times 10^{-5}$ at $R = 0.0026$ and 6.60×10^{-5} at $R = 0.0060$, which is a 30% variation in flux over an alteration in R of 0.0034 (a 230% change). Although the density difference ratios are a good indication of the "Boussinesq nature" of the fluid, their function as a measure of density variation is not so good. In order to rectify this and appreciate the discontinuities in the solutions, weighting factors of R for q_2, and $\frac{1}{R}$ for q_1 are used. Figures (2.7) and (2.8) plot $R\ q_2$ and $\frac{1}{R}\ q_1$ respectively for $H = 0.7$.

The regions of overlap and discontinuity in these diagrams can be easily identified with those in figure (2.4). For a given ratio R (and R') the solid lines are traversed from left to right. For small values of Y_2 the best picture is obtained from figure (2.8), whilst for large Y_2 figure (2.7) is best. The description of the experiment is the same as made previously. Note that an expression for total flux requires evaluation of $q_2^{\frac{1}{2}} + (R\frac{\rho_2}{\rho_1})^{\frac{1}{2}} q_1^{\frac{1}{2}}$. For most cases likely to be considered experimentally $\rho_3 \simeq 0$, $\rho_1 \simeq 1$ and $\rho_1 \simeq \rho_2$, so that $q_2^{\frac{1}{2}} + R^{\frac{1}{2}} q_1^{\frac{1}{2}}$ would suffice.

§2.4. *Generalisation.*

As a conclusion to this study a general n-layered situation is discussed. Number the layers from 0 to n + 1 upwards from the channel floor, and the interfaces similarly

from 0 to n. Layers 0 and n + 1 are non-flowing. The method for dealing with such multilayered systems is derived from that of WOOD (1968). The energy equations evaluated upstream of the contact point of the lowest interface and the weir (C_0) give the differences

$$\tfrac{1}{2}\rho_k u_k^2 - \tfrac{1}{2}\rho_{k+1} u_{k+1}^2 = g(\rho_k - \rho_{k+1}) \cdot \left[\sum_{i=0}^{k} Y_i - \sum_{i=0}^{k} y_i - h \right] \quad k = 1,2,\ldots n-1, \qquad (2.21)$$

for the upper most interface

$$\tfrac{1}{2}\rho_n u_n^2 = g(\rho_n - \rho_{n+1}) \left[\sum_{i=0}^{n} Y_i - \sum_{i=0}^{n} y_i - h \right] , \qquad (2.22)$$

and for the lowest interface

$$-\tfrac{1}{2}\rho_1 u_1^2 = g(\rho_0 - \rho_1)(Y_0 - y_0 - h). \qquad (2.23)$$

There are no geometrical restrictions except for the shape of the channel and weir, for which $h = h(x)$ and $b = b(x)$ with $\frac{dh}{dx} = \frac{db}{dx} = 0$ at $x = 0$, and the invariance of the quantities $\sum_{i=0}^{n+1} Y_i$ and $\sum_{i=0}^{n+1} y_i + h$.

Also used is the condition that the derivatives $\frac{dy_i}{dx}$ for $i = 0,1 \ldots n+1$ must be finite, that is, that y_i must vary smoothly.

Differentiating equations (2.21) - (2.23), after using the substitution $u_k^2 = \frac{Q_k^2}{b^2 y_k^2}$, we have

$$\begin{bmatrix} c_{00} & c_{01} & 0 & 0 & \cdot & \cdot & \cdot & 0 \\ c_{10} & c_{11} & c_{12} & 0 & & & & \cdot \\ \cdot & & & & & & & \cdot \\ \cdot & & & & & & & \cdot \\ \cdot & & & & & & & \cdot \\ c_{\ell 0} & c_{\ell 1} & c_{\ell 2} & \cdots & c_{\ell,\ell} & c_{\ell,\ell+1} & 0 \cdots & 0 \\ \cdot & & & & & & & \cdot \\ \cdot & & & & & & & \cdot \\ \cdot & & & & & & & \cdot \\ c_{n0} & c_{n1} & c_{n2} & & \cdot & \cdot & \cdot & c_{n,n} \end{bmatrix} \begin{bmatrix} \frac{dy_0}{dx} \\ \frac{dy_1}{dx} \\ \cdot \\ \cdot \\ \cdot \\ \frac{dy_\ell}{dx} \\ \cdot \\ \cdot \\ \cdot \\ \frac{dy_n}{dx} \end{bmatrix}$$

$$= \begin{bmatrix} d_0 \\ d_1 \\ \cdot \\ \cdot \\ \cdot \\ d_n \end{bmatrix} \qquad (2.24)$$

where $c_{00} = g(\rho_0 - \rho_1)$

$$c_{01} = \frac{\rho_1 Q_1^2}{b_1^2 y_1^3}$$

$$c_{kk} = g(\rho_k - \rho_{k+1}) - \frac{\rho_k Q_k^2}{b^2 y_k^3} \qquad k = 1,2,\ldots n$$

$$c_{k,k+1} = \frac{\rho_{k+1} Q_{k+1}^2}{b^2 y_{k+1}^3} \qquad k = 1,2,\ldots n-1$$

$$c_{k,\ell} = (\rho_k - \rho_{k+1})g \qquad \ell = 1,2,\ldots k-1$$

$$k = 1,2,\ldots n.$$

$$d_0 = (\rho_0 - \rho_1)g \frac{dh}{dx} + \frac{\rho_1 Q_1^2}{b^3 y_1^2} \frac{db}{dx} .$$

$$d_k = g(\rho_k - \rho_{k-1}) \frac{dh}{dx} + \left[\frac{\rho_{k+1} Q_{k+1}^2}{b^3 y_{k+1}^2} - \frac{\rho_k Q_k^2}{b^3 y_k^2} \right] \frac{db}{dx}$$

$$k = 1,2,\ldots n$$

and $d_n = g(\rho_n - \rho_{n-1})\frac{dh}{dx} + \frac{db}{dx}(-\frac{\rho_n Q_n^2}{b^3 y_n^2})$.

From equation (2.24) we have

$$\frac{dy_i}{dx} = \frac{|D_i|}{|D|}\frac{db}{dx} \qquad i = 0,1,\ldots n \qquad (2.25)$$

where D is the n+1 × n+1 matrix on the left hand side of (2.24) and the D_i are obtained by replacing the ith column of D with the vector on the right hand side of (2.24).

Upstream of C_0, D is singular at no more than n - 1 points. These are critical points or virtual controls at which the long wave velocities of the slower modes vanish.

Downstream of C_0 the equations (2.21) - (2.25) all hold with the adjustment made that all terms subscripted with 0 are omitted. From D and D_i form the n × n matrices E and E_i respectively by omitting the first row and column. E is singular at no more than n - 1 points between C_0 and the crest of the weir. These are the remaining virtual controls corresponding to the points where the faster mode long wave velocities vanish. E also is singular at x = 0 which is the control and corresponds to the fastest mode. At x = 0 the finiteness condition is clearly satisfied as $\frac{dh}{dx} = \frac{db}{dx} = 0$, but at the virtual controls downstream of C we require that the E_i matrices are also singular. By an argument similar to that preceding equation (2.4) this results in two independent conditions at each virtual control, viz $|E| = |E_i| = 0$ for any one $i \in \{1,2,\ldots n\}$. Similarly at the virtual controls upstream of C_0 the conditions are that $|D| = |D_i| = 0$ for any one $i \in \{0,2,\ldots n\}$. For steady flow the total number of virtual controls in both parts of the

flow is exactly n - 1 since only then is the system well determined. In principle there can be up to n - 1 critical points in each part of the flow and so it is easy to conceive how the total number in both parts of the flow upstream of $x = 0$ could exceed n - 1. The flow would then become over-determined, solutions would fail and the flow become unsteady.

Gradual alteration of the interface levels causes the virtual controls to move, and as any one of them approaches C_0 this type of overdetermination is likely. The resulting unsteadiness would persist until steady solutions are again possible. The new solutions would be characterised by the appearance of one of the virtual controls on the side of C_0 opposite to that it occupied prior to the breakdown.

Thus, steady alteration of interface levels results in a progression of steady phases, in which the flow ratios change smoothly, punctuated by unsteady periods as the virtual controls pass through C_0.

The above discussion assumes layers 1 to n are all flowing, but it is possible for the lowest layer to stop. In this case C_1 will form at the position where the virtual control corresponding to the appropriate mode vanishes. The situation is now exactly the same as before except that n - 1 layers flow with n - 2 virtual controls (in steady flows) and the relevant contact point is now C_1.

[Notes. (1) All results for such layered flow problems are reasonably valid only if the layer depths are not too small. For a thin layer, boundary-layer effects will invalidate the inviscid assumption, so layer thicknesses must be chosen much greater than boundary-layer widths.

(2) The analysis was for steady flow so that when an interface level is altered and the virtual controls move etc, the change in the layer depths is slow enough so that the time for the streamline patterns to change is very large compared to the time for flow through the outlet.

(3) As the flow enters the contraction, the speed in each layer increases and the points of critical speed will be progressively passed until at the control the flow becomes completely supercritical. It would seem plausible that critical conditions pertain to particular interfaces and an association can be made between each critical point and an interface. However, it is shown in chapter III that this assignment is very weak and throughout the preceding chapter any such associations have been avoided.

(4) Where $|D| = 0$ or $|E| = 0$, in the general example above, one of the properly constituted Froude numbers passes through unity.]

CHAPTER III

SOME FURTHER FEATURES OF CRITICAL POINTS

The preceding chapter raises some interesting questions. The importance of critical points in solving steady flows has been displayed and it would be useful to investigate any dependence unsteady flows may have on similar phenomena in order to generalise the concept. Furthermore, for a multi-layered system as encountered in chapter two there are several critical points possible, and the question arises as to whether any correspondence can be assumed between particular interfaces and particular critical points.

§3.1. *Association of Critical points with Interfaces.*

It has already been noted in chapter one that a critical point in a steady flow is a point at which the speed of a long wave relative to the flow becomes equal to the speed of the flow itself, so that disturbances emanating from somewhere downstream of a critical point cannot propagate upstream. For an n-layered system contracting downstream as in the example of chapter two, there are n wave modes possible and n critical points. There is a one-to-one correspondence between the possible long wave speeds and the critical points, since if the wave speeds are ordered, $C_1 < C_2 < C_3 < \ldots < C_n$, as are the critical points, $x_1 < x_2 < x_3 < \ldots < x_n$ (flow is in direction of increasing x), the fastest mode, C_n, will be associated with x_n and so on. Thus, association of a critical point with an inter-

face is the same as association of a long wave speed, and hence a wave mode, with an interface. Consequently a relatively simple multilayered system with no contraction can be used to seek a definite pairing of modes and interfaces.

YIH (1965 Chapter 2 §12.4) considers that this association is not ambiguous and is possible if the wave speeds C_i are known as functions of the density discontinuities $\Delta\rho_i$. If C_k vanishes with $\Delta\rho_k$ then the mode whose speed is C_k belongs to the interface whose density difference is $\Delta\rho_k$. In principle this is all very well but the association is dependent on limiting conditions as the $\Delta\rho_i$ vanish. From a practical point of view a simple comparison of amplitudes of the modes at each interface should give results valid everywhere.

Consider three uniform layers of fluid bounded above and below by rigid barriers with decreasing densities $\rho_1 > \rho_2 > \rho_3$ and undisturbed depths h_1, h_2 and h_3, as depicted in figure (3.1). Let the interfacial disturbances be η and ξ at the lower and upper interfaces respectively, and introduce a potential function for each layer ϕ_i $i = 1,2,3$. Then the equations are

$$\nabla^2\phi_1 = \nabla^2\phi_2 = \nabla^2\phi_3 = 0, \tag{3.1}$$

with the boundary conditions

$$\frac{\partial\phi_3}{\partial y} = 0 \qquad \text{on } y = h_1 + h_2 + h_3 \tag{3.2}$$

$$\frac{\partial\phi_1}{\partial y} = 0 \qquad \text{on } y = 0$$

$$\frac{\partial\phi_2}{\partial y} = \left.\frac{D\eta}{Dt}\right|_1 = \left.\frac{D\eta}{Dt}\right|_2 = \frac{\partial\phi_2}{\partial y} \qquad \text{on } y = h_1 + \eta$$

$$\frac{\partial\phi_2}{\partial y} = \left.\frac{D\xi}{Dt}\right|_2 = \left.\frac{D\xi}{Dt}\right|_3 = \frac{\partial\phi_3}{\partial y} \qquad \text{on } y = h_1 + h_2 + \xi$$

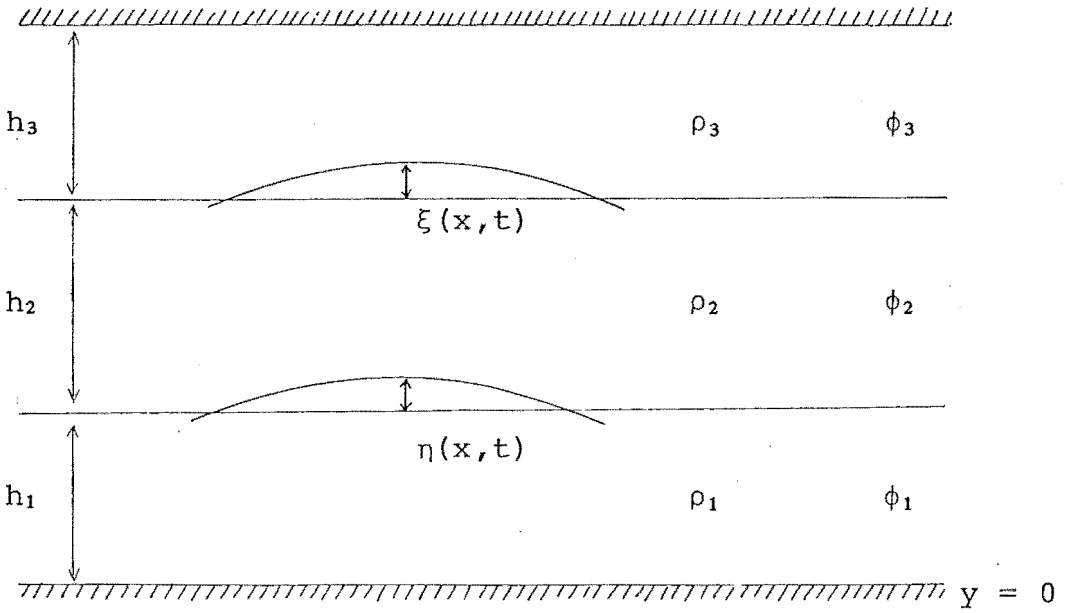

Figure 3.1

and from pressure continuity at the interfaces

$$P_1 = P_2 \text{ on } y = h_1 + \eta$$

$$P_2 = P_3 \text{ on } y = h_1 + h_2 + \xi.$$

Taking a first approximation, neglecting terms in squares and products of η, ξ, and ϕ_i $i = 1,2,3$, and their derivatives

$$\frac{\partial \phi_1}{\partial y} = \frac{\partial \eta}{\partial t} = \frac{\partial \phi_2}{\partial y} \quad \text{on } y = h_1 \tag{3.4}$$

$$\frac{\partial \phi_2}{\partial y} = \frac{\partial \xi}{\partial t} = \frac{\partial \phi_3}{\partial y} \quad \text{on } y = h_1 + h_2 \tag{3.5}$$

$$\rho_1 \frac{\partial \phi_1}{\partial t} + \rho_1 g \eta = \rho_2 \frac{\partial \phi_2}{\partial t} + \rho_2 g \eta \quad \text{on } y = h_1 \tag{3.6}$$

$$\rho_2 \frac{\partial \phi_2}{\partial t} + \rho_2 g \xi = \rho_3 \frac{\partial \phi_3}{\partial t} + \rho_3 g \eta \quad \text{on } y = h_1 + h_2 \tag{3.7}$$

Since the problem is linear, using solutions for (3.1), represent the disturbances at the interfaces by sinusoidal progressive waves in the positive-x direction.

Thus,

$$\phi_j(x,t) = R\{F_j(y) \exp i(kx-\omega t)\} \quad \text{for } j = 1,2,3$$

$$\eta(x,t) = R\{b \exp i(kx-\omega t)\},$$

$$\xi(x,t) = R\{a \exp i(kx-\omega t)\}.$$

Substituting into equations (3.2) - (3.4) eventually yields

$$\frac{a}{b} = -[(\rho_1 - \rho_2)gk - \omega^2(\rho_2 \coth kh_2 + \rho_1 \coth kh_1)] \cdot \sinh kh_2/\rho_2 \omega^2 \qquad (3.8)$$

where there are two values of the frequency ω given by the positive solutions of the dispersion relation

$$[(\rho_1 - \rho_2)gk - \omega^2(\rho_1 \coth kh_1 + \rho_2 \coth kh_3)] \times (\rho_2 - \rho_3)gk - \omega^2(\rho_2 \coth kh_2 + \rho_3 \coth kh_3)] = \frac{\rho_2^2 \omega^4}{\sinh^2 kh_2} \qquad (3.9)$$

viz: $\omega_1(k)$ and $\omega_2(k)$ where $\omega_1 > \omega_2$. These are the frequencies of the two natural modes.

The ratio in equation (3.8) is convenient and represents the ratio of amplitudes at upper and lower interfaces for a given mode. Let $r_1(k) = \frac{a}{b}$ when $\omega = \omega_1(k)$ and $r_2(k) = \frac{a}{b}$ when $\omega = \omega_2(k)$.

A little manipulation of equations (3.8) and (3.9) gives the relation

$$r_1 r_2 = -\frac{(\rho_1 - \rho_2)}{(\rho_2 - \rho_3)} . \qquad (3.10)$$

It is instructive to realise that equation (3.9) describes a composite system comprising

(i) the upper boundary and interface with $\rho_1 \to \rho_2$, $h_1 + h_2 \to h_2$, and

(ii) the lower boundary and interface with $\rho_3 \to \rho_2$,

$h_2 + h_3 \to h_2$.

These systems individually have the respective frequencies

$$\omega^2_{(i)} = \frac{gk(\rho_2 - \rho_3)}{\rho_2 \coth kh_2 + \rho_3 \coth kh_3},$$

$$\omega^2_{(ii)} = \frac{gk(\rho_1 - \rho_2)}{\rho_2 \coth kh_2 + \rho_1 \coth kh_1}, \tag{3.11}$$

which are precisely the zeros of the left hand side of equation (3.9). Thus, regard $\frac{\rho_2^2 \omega^4}{\sinh^2 kh_2}$ as a "link" term. As $h_2 \to \infty$, $\frac{1}{\sinh^2 kh_2} \to 0$, and equation (3.9) gives the unlinked systems described in (3.11). This is relevant since it gives another criterion for associating a mode with an interface. As the link term increases, the modes in (3.11) are distorted. The present question is whether these distorted modes retain their identity with the interfaces they were associated with in the unlinked systems. Note that this criterion gives the same mode/interface correspondence as Yih's density limits do.

The presence of two modes necessitates rewriting

$$\eta(x,t) = R\{b_1 \exp i(kx-\omega_1 t) + b_2 \exp i(kx-\omega_2 t)\},$$

$$\xi(x,t) = R\{a_1 \exp i(kx-\omega_1 t) + a_2 \exp i(kx-\omega_2 t)\},$$

whence, equation (3.8) describes the ratios $r_1(k) = \frac{a_1}{b_1}$ when $\omega = \omega_1(k)$, and $r_2(k) = \frac{a_2}{b_2}$ when $\omega = \omega_2(k)$.

To convincingly associate a mode with an interface requires that one interface is consistently affected most by one mode. In other words, for the fast mode to be associated with the upper interface requires that $|r_1(k)| > 1$ always, and hence a fast mode disturbance shows more strongly at the upper interface. Similarly for the

slow mode to belong to the lower interface requires that $|r_2(k)| < 1$ always.

Reference to equation (3.10) shows it is convenient to consider the relationships of $|r_1(k)|$ and $|r_2(k)|$ to $\left(\frac{\rho_1 - \rho_2}{\rho_2 - \rho_3}\right)$, since there is no great loss of generality in choosing $(\rho_1 - \rho_2) = (\rho_2 - \rho_3)$ and thus relating these ratios to unity.

Firstly note that

(1) For $k \to \infty$, that is, very short waves, the solutions to equation (3.9) give $\frac{\omega_i^2}{gk} \to \frac{\rho_1 - \rho_2}{\rho_1 + \rho_2}$ or $\frac{\rho_2 - \rho_3}{\rho_2 + \rho_3}$ where if $i = 1$ the limit is the larger ratio and if $i = 2$ it is the smaller. Also from equation (3.8)

$$r_1(k) \to \left| \frac{(\rho_1 - \rho_2)(\rho_2 + \rho_3) - (\rho_2 - \rho_3)(\rho_1 + \rho_2)}{2(\rho_2 + \rho_3)} \right| \frac{\exp(k h_2)}{\rho_2 \omega_i^2}$$

which becomes large as $k \to \infty$. Similarly $r_2(k)$ becomes very small, so for large k, $|r_1| \gg 1$ and $|r_2| \ll 1$.

(2) For the fast mode the interfacial disturbances are always in phase, whilst for the slow mode they are π out of phase, so that $r_1(k) > 0$ and $r_2(k) < 0$.

Using equation (3.10)

$$r_1 > \left(\frac{\rho_1 - \rho_2}{\rho_2 - \rho_3}\right) \quad \text{if and only if} \quad r_2 > -\left(\frac{\rho_1 - \rho_2}{\rho_2 - \rho_3}\right)$$

that is $$r_1 + r_2 > 0.$$

Upon using equation (3.8) and the solutions for ω_1 and ω_2 from (3.9) eventually we get the condition:

$r_1 > -r_2$ if and only if

$$\frac{\rho_2 \coth kh_2 + \rho_1 \coth kh_1}{\rho_1 - \rho_2} > \frac{\rho_2 \coth kh_2 + \rho_3 \coth kh_3}{\rho_2 - \rho_3}. \quad (3.12)$$

Also from (3.10) it is clearly possible in the general case that both r_1 and $-r_2$ are larger than unity if $\rho_1 - \rho_2 > \rho_2 - \rho_3$.

Condition (3.12) is very weak and implies that it is erroneous to assume that a particular mode will be "strongest" at one interface.

When the density discontinuities are made equal, (3.12) becomes

$$r_1 > 1 > -r_2 \text{ if and only if } \rho_1 \coth kh_1 > \rho_3 \coth kh_3 \quad (3.13)$$

which is relatively easy to reverse by careful selection of h_1, h_2 and h_3.

To relate this result back to the critical points it is necessary to consider the long wave velocities. Take $k \to 0$, then (3.12) becomes

$$r_1 > \left(\frac{\rho_1 - \rho_2}{\rho_2 - \rho_3}\right) \text{ if and only if } \frac{\frac{\rho_2}{h_2} + \frac{\rho_1}{h_1}}{\rho_1 - \rho_2} > \frac{\frac{\rho_2}{h_2} + \frac{\rho_3}{h_3}}{\rho_2 - \rho_3}. \quad (3.14)$$

By the same means as above this shows that examples can be found for which $r_1 > 1 > -r_2$ is not valid and so the assignment of critical points to particular interfaces is not a sure process.

The above arguments show the danger of assuming these associations. However, in many cases the parameters ρ_1, ρ_2, ρ_3, h_1, h_2 and h_3 are in fact such that $r_1 > 1 > -r_2$. For example, suppose $\rho_3 \to 0$, as for a free surface system, then (3.12) becomes

$$r_1 > -r_2 \text{ if and only if } \rho_2 \coth kh_2 + \rho_1 \coth kh_1 > (\rho_1 - \rho_2) \coth kh_2.$$

and for Boussinesq type fluids this condition is satisfied. An example of such a fluid would be a two layer free surface system with a density discontinuity due to a salinity difference.

If h_1 becomes very large ($\& \rho_3 = 0$), an infinite two layered free surface system results. For the fast mode $\frac{a_1}{b_1} = e^{kh_2} > 1$ whence the free surface is strongly favoured, and for the slow mode $-\frac{b_2}{a_2} = (\frac{\rho_1}{\rho_2} - 1)e^{kh_2}$ whence the interface is favoured.

In conclusion, the critical point associated with a particular mode cannot be assumed to belong to one interface. In a physical situation the critical nature of a fluid will relate to a whole vertical cross section. For example, in a system contracting so that the velocity increases from zero as the channel becomes narrow, select a point where just sub-critical conditions prevail and increase the velocity so as to pass through critical conditions here. The fluid then becomes critical throughout the whole fluid at this point and not just at one interface. If an unsteady breakdown occurs as in chapter two, then it occurs over all the interfaces, although it may be more evident at one particular interface. This interface may vary according to the external parameters.

At a critical point, x, the long wave speed of one of the modes has become stationary through all the layers. Since the layers travel at different speeds then the particular mode in question will have different long wave speeds, C_i, relative to each layer i, so that $u_i(x) = C_i$.

At a point upstream of the critical point corresponding to the slowest mode, the whole fluid, and not just one interface or layer, will be subcritical with respect to all the modes, but as the velocity progresses through the speeds of the modes then the fluid becomes supercritical with respect to progressively more of the modes.

Clearly it is possible to establish criteria for critical point/interface associations as YIH (1965) has done, but these tend to be restricted to special cases involving limiting conditions on external parameters.

The above discussion naturally relates also to Froude numbers. At each of the critical points one of the Froude numbers will pass through unity. However, the Froude number is a measure of the state of a whole vertical section of the fluid in relation to a wave speed, and hence has no associations with particular layers or interfaces.

[Often a non-dimensional quantity related to the ratio of a layer's velocity to the square root of the layer's depth is quoted as a Froude number for that layer, but there is more physical meaning in a "wave speed" definition.]

§3.2. *Relation of Critical Points to Unsteady Flows.*

As an attempt to understand critical points in a more general context, it is appropriate to clarify their relation to non-steady analysis. The two-layer dam-break problem provides a useful basis for the discussion.

For linearised unsteady problems the question is one of first order partial differential equations, and the method of solution is through the establishment of characteristics

and conditions along these characteristics. Consider a two layer system originally confined to the region $x \leqslant 0$ with a rigid base at $y = 0$, a free surface at $y = h_1 + h_2$, an interface at $y = h_1$, and a dam at $x = 0$ which is removed at $t = 0$. Let ρ_1 and ρ_2 be the densities, y_1 and y_2 the heights, and u_1 and u_2 the speeds of the lower and upper layers respectively. The characteristic directions are found to be given by $\dot{x}$ where

$$[(\dot{x} - u_1)^2 - y_1 g][(\dot{x} - u_2)^2 - y_2 g] - \frac{\rho_2}{\rho_1} y_1 y_2 = 0 \qquad (3.15)$$

along which

$$\rho_1[dy_1(\dot{x} - u_1) + y_1 du_1][y_2 g - (u_2 - \dot{x})] +$$

$$\rho_2 y_1 g[dy_2(u_2 - \dot{x}) - y_2 du_2] = 0 \ . \qquad (3.16)$$

For the same system the dispersion relation for the frequencies $\omega(k)$ of long wave disturbances is the limit as $k \to 0$ of

$$[(\rho_1 - \rho_2)gk - (u_2 k - \omega)^2 \rho_2 \coth ky_2 - (u_1 k - \omega)^2 \rho_1 \coth ky_1]$$

$$\times [gk - (u_2 k - \omega)^2 \coth ky_2] = \frac{\rho_2 (u_2 k - \omega)^4}{\sinh^2 ky_2} \ . \qquad (3.17)$$

All information is propogated at the long wave velocities so these velocities, $\lim\limits_{k \to 0} \frac{\omega(k)}{k}$ from (3.17), will correspond to the speeds of propogation, $\dot{x}$, given by equation (3.15), that is

$$\dot{x} = \frac{\omega(k)}{k} \quad \text{in the long wave limit.}$$

This is easily checked to be consistent.

Flow is critical at the points where long waves become stationary in their upstream motion, whence $\lim\limits_{k \to 0} \frac{\omega(k)}{k} = 0$.

This is the same as stipulating that $\dot{x}$ in equation (3.15) vanishes, or one of the characteristics in the (x,t) plane is vertical.

Putting $\dot{x} = 0$ into equation (3.15) yields

$$(u_1^2 - gy_1)(u_2^2 - gy_2) - \frac{\rho_2}{\rho_1} g^2 y_1 y_2 = 0 \qquad (3.18)$$

which is precisely the critical condition obtained in the steady analysis of WOOD & LAI (1972a, 1972b, 1973) for a two layer system with a free surface. From equation (3.16) there is no analogous steady condition at the critical point, but notice from the aforementioned examples that this condition for steady flow is dependent on geometry (channel shape). This is then easily remedied by considering the dambreak problem in a contracting channel of width b(x). The condition analogous to (3.16) then reduces to an expression for steady flow, like $D_1 \frac{db}{dx} = 0$, which is the same form as WOOD and LAI obtained [D_1 is a function of x].

Within an unsteady flow the critical points thus satisfy equation (3.18), and also (3.16) for $\dot{x} = 0$,

viz: $\rho_1 [y_1 du_1 - u_1 dy_1](y_2 g - u_2) + \rho_2 y_2 g[dy_2 u_2 - y_2 du_2]$

$$= 0 \qquad (3.19)$$

Here, one of the characteristics is tangentially vertical and, as time increases, the critical points are not necessarily stationary. In the two-layer dambreak situation both critical points originate at $x = 0$, and as one progresses upstream the other goes downstream, leaving a region in between which is supercritical with respect to the slow wave mode but which will still allow upstream motion in the fast mode.

If one of the characteristic speeds always vanishes at some $x = x_c$ then this characteristic is always vertical in the (x,t) plane and conditions at x_c are always critical. In the single layer dam-break problem the characteristic at the origin is always vertical and hence solutions can be found here. Also in this case the characteristics are all straight lines so solutions for any part of the fluid can be obtained analytically.

Thus, it appears that the critical points of steady analyses are limiting points of the characteristics as unsteady flow becomes asymptotically steady. In the same sense that a steady flow is a special case of more general flow which is not necessarily steady, the critical points are special cases of characteristics for which one of the characteristics has $\dot{x} = 0$. Whereas an unsteady flow is determined by its characteristics, (3.15), and the conditions along them as expressed in (3.16), a steady flow is determined by its critical points and the conditions at these points. [Assuming a model for which critical points exist in the steady state.]

CHAPTER IV

PERMANENT WAVES IN A CLOSED THREE LAYERED FLUID

§4.1. For a stably layered fluid with three layers of similar density confined between rigid planes, there are two interfaces and two closely related modes of propagation for gravity waves. The main difference between the modes is that the faster mode displaces both interfaces in phase while the slower mode displaces them in antiphase. When one mode only is present there can be non-linear interactions between the harmonics of that mode, and when both modes are present, non-linear interactions can be between harmonics of both modes. These interactions are dominated by those that are resonant or nearly resonant. When the significant non-linear interactions are in balance with linear dispersive effects, permanent waves or permanent wave structures containing one or more modes may occur.

In most systems previously considered when dealing with non-linear interactions of two different types of wavetrain there is not such close relation between their modes of propagation. Rather, the wave speeds of the interacting wavetrains differ significantly. In particular, BENNEY (1976) for free-surface interactions between gravity and capillary waves, and BRYANT (1977) for interactions between free-surface and internal gravity waves, deal with systems in which the identity of the interacting parts is unambiguous. For the latter case there is a very definite identity of wave mode with interface or free-

surface (see chapter III).

However, for the present case the two modes cannot be assigned decisively to particular interfaces. The two long wave velocities can be similar. Ultimately this means that in the analysis the system cannot be conveniently divided into two parts, considering each mode separately, except in special cases. In fact it is found that the proximity of the phase and group velocities of the modes necessitates including a much wider range of interactions in the analysis.

For capillary-gravity wave interactions BENNEY (1976) showed the non-linear interaction was resonant when the phase velocity of a low-wavenumber gravity wave harmonic equalled the group velocity of a fast high-wavenumber capillary wave harmonic. For BRYANT (1977)'s free surface-interface model, this parallels equating the phase velocity of a slow low-wavenumber interfacial harmonic with the group velocity of a fast high-wavenumber free-surface harmonic. In the vicinity of such resonances the non-linear interactions are significant and permanent wave structures can be found comprising a free-surface wave group (in Benney's case a group of capillary waves) of permanent envelope travelling at the same speed as a permanent carrier wave at the interface (in Benney's case a surface gravity wave). Also single mode permanent waves exist for both modes.

The overall features of the present investigation are similar except that both the group envelope and the carrier wave will appear at both interfaces. The permanent waves and wave structures result from the significant non-linear interactions of closely related *internal* modes only, and

the wavenumbers of the interacting harmonics do not differ so much between the modes.

The method employed in the following allows both interfacial waves to be of unknown shape. Assuming wave motion is unidirectional and spatially periodic, both modes of interfacial wave are represented by Fourier series whose coefficients vary slowly with time. Evolution equations are obtained for the Fourier amplitudes such that all quadratic interactions between Fourier amplitudes are included. Permanent waves and structures can be found from these equations when the significant quadratic interactions and linear dispersive terms are in balance. This method is akin to that employed in the treatment of interactions between internal and free surface waves by BRYANT (1977), and has advantages over many previous studies of non-linear intermodal interactions in which radiation stress concepts are used to study the response of a surface wave to the presence of a *prescribed* internal wave and its velocity field (see LONGUET-HIGGINS and STEWART (1960), GARGETT and HUGHES (1972), LEWIS LAKE and KO (1974)).

The importance of resonant interactions lies in the means they provide for transferral of energy between the various resonating elements. If k and ℓ denote the wavenumbers of two long-wave harmonics propagating in the same direction with linear frequencies $\omega(k)$ and $\omega(\ell)$ respectively, then the three-layer closed system allows near-resonant triads of one mode only,

$$\omega(k) + \omega(\ell) - \omega(k+\ell) = 0(\mu^2), \qquad (4.1)$$

where μ is a measure of the ratio of fluid depth to wavelength. Such triads represent quadratic non-linear interactions between the harmonics of a single mode. For long waves, μ is small, and this relationship, (4.1), causes near-resonant growth of the $k + \ell$ harmonic to an amplitude of similar magnitude to the k and ℓ harmonics. The higher the harmonics the shorter the wavelength and hence the further from resonance the interaction. Thus, equation (4.1) allows the evolution of a wave system dominated by near-resonant interactions between the harmonics composing it, and as μ becomes smaller the number of harmonics making a significant contribution will increase.

For a uniform single shallow layer of fluid, only one mode exists and long periodic waves of permanent form are approximated by cnoidal waves, tending towards solitary waves in the limit as $\mu \to 0$, or to Stokes' waves for short wavelengths [BRYANT (1973) and (1974a)].

For two layers with a free surface PETERS and STOKER (1960) have shown fast free-surface permanent waves and slow interfacial permanent waves exist. Application of the near-resonant condition (4.1) is appropriate for either mode alone. When both modes are present, significant interactions occur between them when [see BRYANT (1977)]

$$\omega_1 (k+\ell) - \omega_1 (k) - \omega_2 (\ell) \simeq 0 \qquad (4.2)$$

where ω_1 is the faster mode and ω_2 the slower. For the open two layer system it is found that most interaction occurs when $\ell \ll k$, so writing $\ell = \Delta k$,

$$\omega_1 (k+\Delta k) - \omega_1 (k) \simeq \omega_2 (\Delta k). \qquad (4.3)$$

Rewriting this in the limit, Δk becomes very small compared to k ($\ell \ll k$), and we get the relation

$$\frac{d\omega_1(k)}{dk} \simeq \frac{\omega_2(\Delta k)}{\Delta k} \tag{4.4}$$

Equation (4.2) describes the interaction of a fast mode harmonic of large wavenumber with a slow mode harmonic of small wavenumber to modify another fast mode harmonic of large wavenumber. This generates fast mode harmonics with wavenumbers over a waveband to form a group. Alternatively, (4.2) can be interpreted as two fast mode harmonics interacting to modify a slow-mode harmonic, or, in the open two-layer context, the generation of interfacial waves in the presence of a surface group. From (4.4) this type of interaction occurs near where the group velocity of a fast mode harmonic of wavenumber k equals the phase velocity of a slow mode harmonic of low wavenumber (Δk).

In the closed three-layer system, resonant triads of the type described in (4.2) are found to occur. One type of triad is described by

$$\omega_2(\ell) = \omega_1(k+\ell) - \omega_1(k) \tag{4.5}$$

where ℓ and k can now be of comparable magnitude. This interaction still follows the pattern described in (4.4) and can be seen to lead to a permanent wave structure comprising a "carrier" wave in the slower mode and a group in the faster mode travelling at the same speed.

Another type of triad found to be significant is described by

$$\omega_2(k) + \omega_2(\ell) = \omega_1(k+\ell) \qquad (4.6)$$

which is peculiar to the interaction of closely related internal waves. This represents the interaction of two harmonics of the slower mode to modify a faster mode harmonic. As will be seen, this interaction introduces a complicating singularity into the analysis. It means that at certain wavenumbers a permanent wave in the slower mode only will not exist because at these values of k and ℓ a faster mode harmonic is generated. For example, a slow mode harmonic may interact with itself when $\ell = k$, for a particular k, to generate the fast mode harmonic of wavenumber 2k, or

$$2\omega_2(k) = \omega_1(2k).$$

In a paper by BRYANT and LAING (1978) a good deal of attention is paid to this particular type of interaction.

The resonant interactions described in (4.1), (4.5), and (4.6) suggest that if a range of harmonics of one mode is present then there will also be harmonics of the other mode generated by the quadratic interactions. This is a consequence of the aforementioned similarities in the two modes and means that separate evolution equations for each mode are not necessarily obtainable. The general evolution equations derived contain both modes, and for accuracy it is necessary to include all non-linear interactions between the modes to cover the possible resonances. It turns out, nevertheless, that the most significant are those described in (4.1), (4.5) and (4.6) above.

Once the permanent wave equations have been obtained from the general evolution equations, a Newton-Raphson

method of successive approximation can be used to find the permanent wave and permanent wave structure solutions. The starting values for this method are obtained, in the case of the permanent waves, by successive reduction in μ from a shortwave approximation, and, in the case of permanent wave structures, from the eigenvectors and eigenvalues derived for the group when the carrier wave is approximated by the permanent waves in absence of a group.

Another possible method, which has been employed by BRYANT and LAING (1978) is based on the observation that a resonant triad in which the energy of each of the three harmonics is constant is an elementary form of permanent wave. This observation is derived from BRETHERTON (1964) who investigated the more general form of resonant triad in which the energy is conserved within the triad but can be transferred between the harmonics. This triad is embedded in a whole set of harmonics with wavenumbers in its vicinity and so the structure can be solved.

It should be pointed out that aspects of the material contained in the following two chapters has been published in the paper by BRYANT and LAING (1978) mentioned above.

§4.2. *The General Equations.*

The closed three layer system comprises a rigid base and lid between which are confined three uniform layers of depths h_1, h_2, and h_3, and densities ρ_1, ρ_2, and ρ_3, for the lowest, middle, and uppermost layers respectively. This configuration is the same as in §3.1 (and figure (3.1)). The theory, however, is now extended to include quadratic non-linear terms.

The layer depths and the horizontal and vertical components, x and y, are non-dimensional multiples of $h_1 + h_2 + h_3$, and the origin of y is the channel floor. Time t is in units of $\sqrt{g(h_1 + h_2 + h_3)}$ where g is gravity. The fundamental wavelength is $2\pi\ell$, and the parameter μ is introduced as the ratio of channel height to wavelength: viz $\mu = (h_1 + h_2 + h_3)/\ell$. The amplitudes are measured in terms of a. Let the interfacial disturbances be ξ and η for the upper and lower interfaces respectively such that both are non-dimensional multiples of a, and also introduce velocity potentials ϕ_1, ϕ_2, and ϕ_3 for each layer, which are non-dimensional multiples of $a\sqrt{g(h_1 + h_2 + h_3)}$. The principal small parameter is $\varepsilon = a/(h_1 + h_2 + h_3)$ which is taken as much less than unity.

The governing equations and boundary conditions are then as in §3.1 which, taken to first order terms in ε, give

$$\phi_{1xx} + \phi_{1yy} = 0, \qquad 0 < y < h \tag{4.7a}$$

$$\phi_{2xx} + \phi_{2yy} = 0, \qquad h_1 < y < h_1 + h_2 \tag{4.7b}$$

$$\phi_{3xx} + \phi_{3yy} = 0, \qquad h_1 + h_2 < y < h_1 + h_2 + h_3 \tag{4.7c}$$

$$\phi_{1y} = 0 \qquad \text{on } y = 0 \tag{4.8a}$$

$$\phi_{1y} - \eta_t - \varepsilon\eta_x\phi_{1x} \qquad \text{on } y = h_1 + \varepsilon\eta$$

or $$\phi_{1y} = \varepsilon\eta\,\phi_{1xx} + \eta_t + \varepsilon\eta_x\phi_{1x} + 0(\varepsilon^2) \qquad \text{on } y = h_1$$

or $$\eta_t - \phi_{1y} + \varepsilon(\eta\phi_{1x})_x = 0(\varepsilon^2) \qquad \text{on } y = h_1 \tag{4.8b}$$

Similarly

$$\eta_t - \phi_{2y} + \varepsilon(\eta\phi_{2x})_x = 0(\varepsilon^2) \qquad \text{on } y = h_1. \tag{4.8c}$$

For pressure continuity across the interfaces

$$\rho_1\phi_{1t} + \tfrac{1}{2}\rho_1\varepsilon(\phi_{1x}^2 + \phi_{1y}^2) + \rho_1 g\eta$$

$$= \rho_2\phi_{2t} + \tfrac{1}{2}\rho_2\varepsilon(\phi_{2x}^2 + \phi_{2y}^2) + \rho_2 g\eta \text{ on } y = h_1 + \varepsilon\eta$$

or $\rho_1\phi_{1t} - \rho_2\phi_{2t} + (\rho_1 - \rho_2)g\eta + \varepsilon[\tfrac{1}{2}\rho_1(\phi_{1x}^2 + \phi_{1y}^2)$

$$- \tfrac{1}{2}\rho_2(\phi_{2x}^2 + \phi_{2y}^2) + \rho_1\eta\phi_{1yt} - \rho_2\eta\phi_{2yt}] = 0(\varepsilon^2)$$

$$\text{on } y = h_1 . \qquad (4.9a)$$

Similarly

$$\rho_2\phi_{2t} - \rho_3\phi_{3t} + (\rho_2 - \rho_3)g\xi + \varepsilon[\tfrac{1}{2}\rho_2(\phi_{2x}^2 + \phi_{2y}^2)$$

$$- \tfrac{1}{2}\rho_3(\phi_{3x}^2 + \phi_{3y}^2) + \rho_2\xi\phi_{2yt} - \rho_3\xi\phi_{3yt}] = 0(\varepsilon^2)$$

$$\text{on } y = h_1 + h_2 . \qquad (4.9b)$$

Also,

$$\xi_t - \phi_{2y} + \varepsilon(\xi\phi_{2x})_x = 0(\varepsilon^2) \quad \text{on } y = h_1 + h_2 \qquad (4.10a)$$

$$\xi_t - \phi_{3y} + \varepsilon(\xi\phi_{3x})_x = 0(\varepsilon^2) \quad \text{on } y = h_1 + h_2 \qquad (4.10b)$$

and $\phi_{3y} = 0$ on $y = h_1 + h_2 + h_3$. (4.10c)

Spatially periodic solutions are sought to satisfy equations (4.7), (4.8a) and (4.10c), whence the interfacial disturbances η and ξ are written as Fourier series

$$\eta(x,t) = \tfrac{1}{2}\sum_{k=1}^{\infty} B(k,t)\exp i\{\mu kx - \omega(k)t\}$$

$$+ \text{ complex conjugate} \qquad (4.11a)$$

$$\xi(x,t) = \tfrac{1}{2}\sum_{k=1}^{\infty} A(k,t)\exp i\{\mu kx - \omega(k)t\}$$

$$+ \text{ complex conjugate} \qquad (4.11b)$$

and the velocity potentials

$$\phi_1(x,t) = \tfrac{1}{2}\sum_{k=1}^{\infty} C(k,t)\cosh \mu k y \exp i\{\mu kx - \omega(k)t\}$$

$$+ \text{ complex conjugate} \qquad (4.11c)$$

$$\phi_2(x,t) = \tfrac{1}{2} \sum_{k=1}^{\infty} [D(k,t) \cosh \mu k y + E(k,t) \sinh \mu k y]$$

$$\times \exp i\{\mu k x - \omega(k) t\} + \text{complex conjugate} \qquad (4.11d)$$

$$\phi_3(x,t) = \tfrac{1}{2} \sum_{k=1}^{\infty} F(k,t) \cosh \mu k(1-y) \exp i\{\mu k x - \omega(k) t\}$$

$$+ \text{complex conjugate} \qquad (4.11e)$$

where wavenumber k and frequency $\omega(k)$ are nondimensional multiples of $1/\ell$, $\sqrt{g/(h_1 + h_2 + h_3)}$ respectively, and the Fourier coefficients $A(k,t) - F(k,t)$ are only slowly time dependent and henceforth written as $A(k) - F(k)$.

Substitution of (4.11) into equations (4.8), (4.9) and (4.10) correct to $0(\varepsilon)$ yields the *linear* theory of §3.1 and hence the relation

$$[(\rho_2 - \rho_3)\mu k - \omega^2(\rho_2 \coth \mu k h_2 + \rho_3 \coth \mu k h_3)]$$

$$\times [(\rho_1 - \rho_2)\mu k - \omega^2(\rho_1 \coth \mu k h_1 + \rho_2 \coth \mu k h_2)]$$

$$= \rho^2 \omega^4 / \sinh^2 \mu k h_2 \qquad (4.12)$$

which determines two positive frequencies $\omega = \omega_1(k)$ and $\omega = \omega_2(k)$, where $\omega_1(k) > \omega_2(k)$. Also the linear ratios of the amplitudes $A(k) - F(k)$ are found:

$$\frac{B(k)}{\rho_2 \omega^2} = -A(k)/\{\sinh \mu k h_1 [(\rho_1 - \rho_2)\mu k -$$

$$\omega^2(\rho_1 \coth \mu k h_1 + \rho_2 \coth \mu k h_2)]\}$$

$$= i\, C(k)\, \mu k \sinh \mu k h_1 / \{\rho_2 \omega^3\}$$

$$= i\, D(k)\, \mu k / \{\cosh \mu k h_1 [(\rho_1 \coth \mu k h_1$$

$$- \rho_2 \tanh \mu k h_1)\omega^2 - \mu k(\rho_1 - \rho_2)]\}$$

$$= i\, E(k)\, \mu k / \{\sinh \mu k h_1 [(\rho_1 - \rho_2)\mu k$$

$$- \omega^2(\rho_1 - \rho_2) \coth \mu k h_1]\}$$

$$= i\,F(k)\,\mu k \sinh kh_3 / \{\sinh \mu k h_2 \,[\,(\rho_1 - \rho_2)\,\mu k - \omega^2(\rho_2 \coth kh_2 + \rho_1 \coth \mu k h_1)\,]\}. \qquad (4.13)$$

To keep the theory general, all amplitudes and frequencies must be subscripted to show which mode they refer to. Hence (4.11) must be rewritten as

$$\eta = \tfrac{1}{2} \sum_{\alpha=1}^{2} \sum_{k=1}^{\infty} B_\alpha(k) \exp i\{\mu k x - \omega_\alpha(k) t\} + \text{complex conjugate} \qquad (4.14)$$

and similarly for ξ, ϕ_1, ϕ_2 and ϕ_3.

Henceforth it is convenient to denote the linear ratios of the amplitudes $B_\alpha(k)$ and $A_\alpha(k)$ as

$$r_\alpha(k) = \frac{B_\alpha(k)}{A_\alpha(k)} \qquad \alpha = 1,2 \qquad (4.15)$$

and equations (4.12) and (4.13) can be manipulated to show that

$$r_1(k)\, r_2(k) = -\frac{\rho_2 - \rho_3}{\rho_1 - \rho_2}\,. \qquad (4.16)$$

The equations correct to $0(\varepsilon^2)$ yield the *quadratic* approximation.

The linear solutions in equations (4.13) may be used freely to substitute in the quadratic terms for the velocity potential amplitudes $C_\alpha(k)$, $D_\alpha(k)$, $E_\alpha(k)$, and $F_\alpha(k)$. Lengthy algebra, however, is necessary to eliminate these amplitudes from the linear terms. After this has been done and the coefficients of the exponential terms $\exp i\{\mu k x\}$, $k = 1,2,\ldots$ are separated, two differential equations result at each k for the interfacial amplitudes $A_\alpha(k)$ and $B_\alpha(k)$ (with $D = \frac{d}{dt}$):

$$\sum_{\alpha=1}^{2} D^2\Big[\{B_\alpha(k) - (\rho_2 \coth \mu k h_2 + \rho_3 \coth \mu k h_3)\, \frac{\sinh \mu k h_2}{\rho_2}\, A_\alpha(k)\}$$

$$\times \exp -i\omega_\alpha(k)t\Big] - \sum_{\alpha=1}^{2} \frac{\rho_2 - \rho_3}{\rho_2}\, \mu k \sinh \mu k h_2\, A_\alpha(k) \exp -i\omega_\alpha(k)t$$

$$= \tfrac{1}{2}\, \varepsilon \sum_{\beta=1}^{2} \sum_{\gamma=1}^{2} \sum_{\ell=1}^{k-1} U_{\beta\gamma}(k,-\ell) B_\beta(\ell) B_\gamma(k-\ell) \exp -i\{\omega_\beta(\ell) + \omega_\gamma(k-\ell)\}t$$

$$+ \varepsilon \sum_{\beta=1}^{2} \sum_{\gamma=1}^{2} \sum_{\ell=1}^{\infty} U_{\beta\gamma}(k,\ell) B^*_\beta(\ell) B_\gamma(k+\ell) \exp -i\{\omega_\gamma(k+\ell) - \omega_\beta(\ell)\}t$$

$$+ O(\varepsilon^2), \qquad k = 1,2,... \tag{4.17a}$$

$$\sum_{\alpha=1}^{2} D^2\Big[\{\frac{\rho_1 \coth \mu k h_1}{\rho_2}\, B_\alpha(k)$$

$$+ (\rho_2 + \rho_3 \coth \mu k h_3 \coth \mu k h_2)\, \frac{\sinh \mu k h_2}{\rho_2}\, A_\alpha(k)\}$$

$$\times \exp -i\omega_\alpha(k)t + \sum_{\alpha=1}^{2} \Big[\frac{\rho_1 - \rho_2}{\rho_2}\, \mu k B_\alpha(k)$$

$$+ \frac{(\rho_2 - \rho_3)}{\rho_2}\, \mu k \cosh \mu k h_2\, A_\alpha(k)\Big]$$

$$\times \exp -i\omega_\alpha(k)t$$

$$= \tfrac{1}{2}\, \varepsilon \sum_{\beta=1}^{2} \sum_{\gamma=1}^{2} \sum_{\ell=1}^{k-1} V_{\beta\gamma}(k,-\ell) B_\beta(\ell) B_\gamma(k-\ell) \exp -i\{\omega_\beta(\ell) + \omega_\gamma(k-\ell)\}t$$

$$+ \varepsilon \sum_{\beta=1}^{2} \sum_{\gamma=1}^{2} \sum_{\ell=1}^{\infty} V_{\beta\gamma}(k,\ell) B^*_\beta(\ell) B_\gamma(k+\ell) \exp -i\{\omega_\beta(\ell) + \omega_\gamma(k+\ell)\}t$$

$$+ O(\varepsilon^2), \qquad k = 1,2,... \tag{4.17b}$$

where the coefficients U and V are given in the appendix, the complex conjugates of the amplitudes are denoted by "*", and the frequencies $\omega_\alpha(\ell)$ are defined for negative ℓ by $\omega_\alpha(-\ell) = -\omega_\alpha(\ell)$, $\ell > 0$. Note that

$U_\alpha(k,-\ell) = U_\alpha(k,-(k-\ell))$, $V_\alpha(k,-\ell) = V_\alpha(k,-(k-\ell))$, $0 < \ell < k$.

When there are quadratic interactions which contribute significantly to both the modes, no further reduction of the governing equations (4.17) is possible.

§4.3. *Single mode equations.*

Supposing the quadratic interactions can be divided into those which contribute to each mode separately, then equations (4.17) may be modified into equations separately describing the evolution of faster-mode waves and slower-mode waves respectively. To do this, drop the summation over α on the left hand side of (4.17) to obtain four differential equations at each k. After some manipulation these yield

$$(D - i\omega_\alpha(k))(D + i\omega_\alpha(k))[\{B_\alpha(k) - \tilde{r}_\alpha(k)A_\alpha(k)\}\exp -i\omega_\alpha(k)t]$$

$$= \tfrac{1}{2}\,\varepsilon \sum_{\beta,\gamma} \sum_{\ell=1}^{k-1} P_{\alpha\beta\gamma}(k,-\ell)B_\beta(\ell)B_\gamma(k-\ell)\exp -i\{\omega_\beta(\ell)+\omega_\gamma(k-\ell)\}t$$

$$+ \varepsilon \sum_{\beta,\gamma} \sum_{\ell=1}^{\infty} P_{\alpha\beta\gamma}(k,\ell)B^*_\beta(\ell)B_\gamma(k+\ell)\exp -i\{\omega_\gamma(k+\ell)-\omega_\beta(\ell)\}t$$

$$+ \ O(\varepsilon^2) \qquad \text{for } \alpha = 1,2\ ;\ k = 1,2,... \qquad (4.18a)$$

$$(D - i\tilde{\omega}_\alpha(k))(D + i\tilde{\omega}_\alpha(k))[\{B_\alpha(k) - r_\alpha(k)A_\alpha(k)\}\exp -i\omega_\alpha(k)t]$$

$$= \tfrac{1}{2}\,\varepsilon \sum_{\beta,\gamma} \sum_{\ell=1}^{k-1} \tilde{P}_{\alpha\beta\gamma}(k,-\ell)B_\beta(\ell)B_\gamma(k-\ell)\exp -i\{\omega_\beta(\ell)+\omega_\gamma(k-\ell)\}t$$

$$+ \varepsilon \sum_{\beta,\gamma} \sum_{\ell=1}^{\infty} \tilde{P}_{\alpha\beta\gamma}(k,\ell)B^*_\beta(\ell)B_\gamma(k+\ell)\exp -i\{\omega_\gamma(k+\ell)-\omega_\beta(\ell)\}t$$

$$+ \ O(\varepsilon^2) \qquad \text{for } \alpha = 1,2\ ;\ k = 1,2,... \qquad (4.18b)$$

where the notation $\tilde{\omega}_\alpha(k)$, $\tilde{r}_\alpha(k)$ and $\tilde{P}_{\alpha\beta\gamma}(k,\ell)$ has been introduced to refer to "the other mode", that is,

$\tilde{\omega}_\alpha(k) = \omega_1(k)\omega_2(k)/\omega_\alpha(k)$, $\tilde{r}_\alpha(k) = r_1(k)r_2(k)/r_\alpha(k)$, and $\tilde{P}_{\alpha\beta\gamma}(k,\ell) = P_{1\beta\gamma}(k,\ell)P_{2\beta\gamma}(k,\ell)/P_{\alpha\beta\gamma}(k,\ell)$. The β,γ summation in equations (4.18) is over all significant quadratic interactions contributing to mode α. The coefficients P are given in the appendix.

Equation (4.18a) has a complementary function which when substituted into (4.11a) gives a series of harmonics with exponents $\exp i\{\mu kx \pm \omega_\alpha(k)t\}$. Thus (4.18a) describes waves of one mode propagating in both directions but modified by the non-linear terms on the right hand side. Similarly (4.18b) yields a series of harmonics with exponents $\exp i\{\mu kx \pm \tilde{\omega}_\alpha(k)t\}$ and so represents modified waves of the other mode. Since both sets of equations hold for $\alpha = 1$ and 2, then they both represent waves of both modes in both directions.

The significant quadratic interactions contributing to the summations in β,γ on the right hand side of (4.18) are the resonant or near-resonant triads for which either

$$\omega_\alpha(k) - \omega_\beta(\ell) - \omega_\gamma(k-\ell) = 0(\varepsilon) \qquad (4.19a)$$

or

$$\omega_\alpha(k) + \omega_\beta(\ell) - \omega_\gamma(k+\ell) = 0(\varepsilon). \qquad (4.19b)$$

The criterion of this section is that these cannot contribute simultaneously to both modes at significant levels. That is, the other mode must not also form a resonant or near-resonant triad. Consequently the conditions

$$\tilde{\omega}_\alpha(k) - \omega_\beta(\ell) - \omega_\gamma(k-\ell) = 0(1) \qquad (4.20a)$$

$$\tilde{\omega}_\alpha(k) + \omega_\beta(\ell) - \omega_\gamma(k+\ell) = 0(1) \qquad (4.20b)$$

are stipulated.

Conditions (4.19) and (4.20) allow integration of (4.18b) twice but (4.18a) only once. The resulting equations are

$$(D + i\omega_\alpha(k))[\{B_\alpha(k) - \tilde{r}_\alpha(k)A_\alpha(k)\}\exp -i\omega_\alpha(k)t]$$

$$= \tfrac{1}{2} i \varepsilon \sum_{\beta,\gamma} \sum_{\ell=1}^{k-1} \frac{P_{\alpha\beta\gamma}(k,-\ell)}{\omega_\alpha(k) + \omega_\beta(\ell) + \omega_\gamma(k-\ell)} \cdot B_\beta(\ell)B_\gamma(k-\ell)$$

$$\times \exp -i\{\omega_\beta(\ell) + \omega_\gamma(k-\ell)\}t$$

$$+ i \varepsilon \sum_{\beta,\gamma} \sum_{\ell=1}^{\infty} \frac{P_{\alpha\beta\gamma}(k,\ell)}{\omega_\alpha(k) - \omega_\beta(\ell) + \omega_\gamma(k+\ell)} \cdot B^*_\beta(\ell)B_\gamma(k-\ell)$$

$$\times \exp -i\{\omega_\gamma(k+\ell) - \omega_\beta(\ell)\}t$$

$$+ 0(\varepsilon^2) \qquad \text{for } \alpha = 1,2 \; ; k = 1,2,... \qquad (4.21a)$$

and,

$$\{B_\alpha(k) - r_\alpha(k)A_\alpha(k)\}\exp -i\omega_\alpha(k)t$$

$$= \tfrac{1}{2} \varepsilon \sum_{\beta,\gamma} \sum_{\ell=1}^{k-1} \frac{\tilde{P}_{\alpha\beta\gamma}(k,-\ell)}{\tilde{\omega}^2_\alpha(k) - \{\omega_\beta(\ell) + \omega_\gamma(k-\ell)\}^2} \; B_\beta(\ell)B_\gamma(k-\ell)$$

$$\times \exp -i\{\omega_\beta(\ell) + \omega_\gamma(k-\ell)\}t$$

$$+ \varepsilon \sum_{\beta,\gamma} \sum_{\ell=1}^{\infty} \frac{\tilde{P}_{\alpha\beta\gamma}(k,\ell)}{\tilde{\omega}^2_\alpha(k) - \{\omega_\gamma(k+\ell) - \omega_\beta(\ell)\}^2} \; B^*_\beta(\ell)B_\gamma(k+\ell)$$

$$\times \exp -i\{\omega_\gamma(k+\ell) - \omega_\beta(\ell)\}t$$

$$+ 0(\varepsilon^2) \qquad \text{for } \alpha = 1,2 \; ; k = 1,2,... \qquad (4.21b)$$

After reorganising (4.21b) and differentiating it, the resulting equation and (4.21a) can be used to find the evolution equations for each of the Fourier amplitudes. Thus

$$D\,A_\alpha(k) = \tfrac{1}{2} i \varepsilon \sum_{\beta,\gamma} \sum_{\ell=1}^{k-1} R_{\alpha\beta\gamma}(k,-\ell)B_\beta(\ell)B_\gamma(k-\ell)\exp i\{\omega_\alpha(k) - \omega_\beta(\ell)$$

$$-\omega_\gamma(k-\ell)\}t + i \varepsilon \sum_{\beta,\gamma} \sum_{\ell=1}^{\infty} R_{\alpha\beta\gamma}(k,\ell)B^*_\beta(\ell)B_\gamma(k+\ell)$$

$$\times \exp i\{\omega_\alpha(k) + \omega_\beta(\ell) - \omega_\gamma(k+\ell)\}t$$

$$+ 0(\varepsilon^2) \qquad \text{for } \alpha = 1,2 \; ; k = 1,2,... \qquad (4.22a)$$

$$D\,B_\alpha(k) = \tfrac{1}{2} i \varepsilon \sum_{\beta,\gamma} \sum_{\ell=1}^{k-1} S_{\alpha\beta\gamma}(k,-\ell) B_\beta(\ell) B_\gamma(k-\ell)$$

$$\times \exp i\{\omega_\alpha(k) - \omega_\beta(\ell) - \omega_\gamma(k-\ell)\}t$$

$$+ i \varepsilon \sum_{\beta,\gamma} \sum_{\ell=1}^{\infty} S_{\alpha\beta\gamma}(k,\ell) B^*_\beta(\ell) B_\gamma(k+\ell)$$

$$\times \exp i\{\omega_\gamma(k) + \omega_\beta(\ell) - \omega_\gamma(k+\ell)\}t$$

$$+ 0(\varepsilon^2) \qquad \text{for } \alpha = 1,2 \; ; k = 1,2,... \qquad (4.22b)$$

where the β,γ summation is as described for equations (4.18), and the coefficients R and S are given in the appendix. It will be noted on reference to R and S in the appendix that the terms in $\tilde{P}_{\alpha\beta\gamma}(k,\ell)$ have a coefficient of $\omega_\alpha(k) + \omega_\beta(\ell) - \omega_\gamma(k+\ell)$, which by condition (4.19) is $0(\varepsilon)$. Hence, these terms should be omitted. However, since some of the calculations included triads in a wide range and not necessarily near resonance, these terms were retained.

A convenient stage has been reached in the analysis to relate the evolution equations obtained to previous parallel theories. BENNEY (1966) has derived equations for the time evolution of long non-linear waves. His theory suggests that in the long wave approximation both interfacial disturbances η and ξ should satisfy Korteweg - de Vries type equations. This is readily tested in the present case by applying the approximation $\mu^2 \sim \varepsilon$ to equations (4.22). The dominant interaction in these equations is that for which $\alpha = \beta = \gamma$, since there is very little interaction between harmonics of different modes under the assumptions of this section.

The long wave velocity, as a multiple of $\sqrt{g(h_1 + h_2 + h_3)}$, is $c_\alpha = \lim_{\mu\to 0} \omega_\alpha(k)/\mu k, \qquad \alpha = 1,2.$ which is determined from the small μ version of equation (4.12), namely the positive roots of

$$(\rho_1\rho_2 h_3 + \rho_2\rho_3 h_1 + \rho_3\rho_1 h_2)c_\alpha^4 - \{\rho_1(\rho_2-\rho_3)h_2h_3 + \rho_2(\rho_1-\rho_3)h_1h_3 + \rho_3(\rho_2-\rho_1)h_1h_2\}c_\alpha^2 + (\rho_1-\rho_2)(\rho_2-\rho_3)h_1h_2h_3 = 0. \quad (4.23)$$

Again from (4.12), the dispersion relation for $\omega_\alpha(k)/\mu k$ may now be written as

$$\omega_\alpha(k)/\mu k = c_\alpha - \mu^2 k^2 s_\alpha + 0(\mu^4) \quad (4.24)$$

where $$s_\alpha = \frac{c_\alpha}{b}\,\frac{c_\alpha^2 n_1 \ell_1 + n_2}{2c_\alpha^2\,\ell_1 - \ell_2}\,, \quad (4.25a)$$

The constants n_1, n_2, ℓ_1, ℓ_2 being given by

$$n_1 = 3\rho_2^2 + \rho_1\rho_2(h_1^2+h_2^2)/h_1h_2 + \rho_2\rho_3(h_2^2+h_3^2)/h_2h_3 + \rho_1\rho_3(h_1^2+h_3^2)/h_1h_3,$$

$$n_2 = (\rho_2-\rho_3)(\rho_1h_1 + \rho_2h_2) + (\rho_1-\rho_2)(\rho_2h_2 + \rho_3h_3),$$

$$\ell_1 = \rho_1\rho_2/h_1h_2 + \rho_2\rho_3/h_2h_3 + \rho_1\rho_3/h_1h_3,$$

$$\ell_2 = (\rho_2-\rho_3)(\rho_1/h_1 + \rho_2/h_2) + (\rho_1-\rho_2)(\rho_2/h_2 + \rho_3/h_3).$$

Taking $\alpha = \beta = \gamma$, the coefficients $S_{\alpha\beta\gamma}(k,\ell)$ in (4.22b) reduce to

$$-\frac{3\mu k\, c_\alpha}{4h}\{\rho_2h_1c_\alpha^2/h_1^2.W_{23} + \rho_3h_2^2/\rho_2h_3^2.W_{12}^2 - Y_{23}Y_{12} - Y_{12}^2\} \div [(\rho_2-\rho_3)W_{12} + (\rho_1-\rho_2)W_{23}].(1 + 0(\mu^2)) \quad (4.25b)$$

where $$W_{ij} = (\rho_i - \rho_j) - c_\alpha^2\left(\frac{\rho_i}{h_i} + \frac{\rho_j}{h_j}\right), \quad i,j = 1,2;2,3.$$

and $$Y_{ij} = (\rho_i - \rho_j) - c_\alpha^2\,\frac{\rho_\ell}{h_\ell}, \quad i,j = 1,2;2,3 \quad \ell \in \{i,j\}\ \ell \neq 2.$$

Write the quantity in (4.25b) as $\mu k f_\alpha$, then equation (4.22b) becomes

$$D\,B_\alpha(k) = \tfrac{1}{2}\, i\,\varepsilon\, f_\alpha \sum_{\ell=1}^{k-1} \mu\ell\, B_\alpha(\ell) B_\alpha(k-\ell)\, \exp i\{\omega_\alpha(k)-\omega_\alpha(\ell)-\omega_\alpha(k-\ell)\}t$$

$$+ i\,\varepsilon\, f_\alpha \sum_{\ell=1}^{\infty} \mu\ell\, B^*_\alpha(\ell) B_\alpha(k+\ell)\, \exp i\{\omega_\alpha(k)+\omega_\alpha(\ell)-\omega_\alpha(k+\ell)\}t$$

$$+ 0(\varepsilon^2) \qquad \text{for } \alpha = 1,2 \;;\; k = 1,2,3,... \qquad (4.26)$$

Multiplying through by $\exp i\{\mu kx - \omega_\alpha(k)t\}$ and writing $B_\beta(k) \exp i\{\mu kx - \omega_\alpha(k)t\}$ as $\eta_\alpha(k)$, equation (4.26) yields

$$\eta_\alpha(k)_t + i\,\omega_\alpha(k)\,\eta_\alpha(k) = \tfrac{1}{2}\, i\,\varepsilon\, f_\alpha \sum_{\ell=1}^{k-1} \mu\ell\, \eta_\alpha(\ell)\eta_\alpha(k-\ell)$$

$$+ i\,\varepsilon\, f_\alpha \sum_{\ell=1}^{\infty} \mu\ell\, \eta^*_\alpha(\ell)\eta_\alpha(k+\ell) + 0(\varepsilon^2)$$

$$\text{for } \alpha = 1,2 \;;\; k = 1,2,...$$

Using equation (4.24), and summing over k, where $\eta_\alpha = \tfrac{1}{2} \sum_k \eta_\alpha(k)$ (refer to (4.11a)), results in

$$\eta_{\alpha t} + c_\alpha\, \eta_{\alpha x} + s_\alpha\, \eta_{\alpha xxx} - 2\,\varepsilon\, f_\alpha\, \eta_\alpha\, \eta_{\alpha x} = 0(\varepsilon^2,\ \varepsilon\mu^2,\ \mu^4)$$

$$\text{for } \alpha = 1,2. \qquad (4.27)$$

Equation (4.27) is a Korteweg - de Vries equation and describes the evolution of long waves of either mode at the lower interface. At the upper interface similar equations are obtained for ξ_α by dividing (4.27) by r_α, the long wave limit of $r_\alpha(k)$ [the reduced form of $R_{\alpha\beta\gamma}(k,\ell)$ in equation (4.22a) differs from f_α by a factor of $\frac{1}{r_\alpha}$] and substituting $\xi_\alpha = \eta_\alpha / r_\alpha$.

§4.4. Permanent waves in one mode.

A permanent periodic wave, travelling with velocity c, and consisting of the faster of the modes only, will have the form

$$\xi = \sum_{k=1}^{\infty} a(k) \cos \mu k(x - ct) \tag{4.29a}$$

$$\eta = \sum_{k=1}^{\infty} r_1(k) a(k) \cos \mu k(x - ct) \tag{4.29b}$$

at the upper and lower interfaces respectively, where the amplitudes a(k) have constant form, being propogated at the speed c. The ratio $r_1(k)$ is given by equations (4.13) and (4.15). On reference to (4.14) for $\alpha = 1$ only, it will be seen that the Fourier amplitudes in both expansions are related by

$$A_1(k) = a(k) \exp i\{\omega_1(k) - \mu kc\}t$$

$$B_1(k) = r_1(k) a(k) \exp i\{\omega_1(k) - \mu kc\}t$$

$$k = 1,2,3,... \tag{4.30}$$

It should be noted in the consideration of permanent waves that the left hand sides of equations (4.17) and (4.22) will now contain terms in $\omega_\alpha(k) - \mu kc$. For significant interactions these terms will be $0(\varepsilon)$ and so substitution of the linear ratio

$r_\alpha(k) A_\alpha(k) = B_\alpha(k) + 0(\varepsilon)$ may be made on both sides of the equations without loss of accuracy. Thus, in all further considerations the lower interface amplitudes will be written as $r_1(k)a(k)$ and b(k), and the upper interface amplitudes as a(k) and $b(k)/r_2(k)$ for the faster and slower modes respectively.

Setting the maximum displacement between a crest and a trough for the upper interface as 2a [where a is defined in §4.2 so that $\varepsilon = a/(h_1 + h_2 + h_3)$]

$$\sum_{k=1}^{\infty} a(2k-1) = 1 \quad , \tag{4.31}$$

and substituting (4.30) into equations (4.22a) gives

$$\{\omega_1(k) - \mu k c\} a(k) = \tfrac{1}{2} \varepsilon \sum_{\ell=1}^{k-1} R_{111}(k,-\ell) r_1(\ell) r_1(k-\ell) a(\ell) a(k-\ell)$$

$$+ \varepsilon \sum_{\ell=1} R_{111}(k,\ell) r_1(\ell) r_1(k+\ell) a(\ell) a(k+\ell)$$

$$k = 1,2,... \tag{4.32}$$

Equations (4.31) and (4.32) are sufficient to solve. A numerical method is used based on a Newton-Raphson technique. Firstly solutions are found at large μ (short wavelength) where the permanent waves are Stokes' waves for which the values $a(1) = -1$, $a(2) = 0(\varepsilon)$ can be used as a starting point. Once the solutions at this μ have been obtained they can be used as starting values for the next calculations with slightly reduced μ. At each value of μ the number of harmonics included in the calculation is altered until the addition of one more harmonic makes a difference of less than 10^{-4} between the solutions. As μ decreases (longer waves) the nonlinear interactions between harmonics lie nearer to resonance, so the number of harmonics to be included increases.

Solutions have been plotted for

$\rho_1 : \rho_2 : \rho_3 = 1.05 : 1.00 : 0.95$ [this density distribution

will be retained throughout all future calculations], and $\varepsilon = 0.05$, in figures (4.1). The two height distributions $(h_1, h_2, h_3) = (0.3, 0.4, 0.3)$ and $(0.4, 0.2, 0.4)$ have been used for each of the two values $\mu = 0.5$ and 0.1. For such permanent waves consisting of the fast mode only, any significant interaction is only for very long wavelengths. The number of harmonics exceeding 10^{-3} in magnitude does not exceed 10 unless $\mu < 0.035$ when the first height distribution is used, and $\mu < 0.025$ if the second is used. As a result, it was found necessary to scale the profiles in figure (4.1) considerably. A vertical magnification of 40π shows them up sufficiently, but also illustrates how long these waves really are.

It is noticable from comparing figures (4.1a) and (4.1b) with (4.1c) and (4.1d) that there is a major difference between the forms of the permanent waves for these two distributions. For $(h_1, h_2, h_3) = (0.4, 0.2, 0.4)$, clearly both interfaces are displaced in phase with the solutions peaked towards the crests, whereas for $(h_1, h_2, h_3) = (0.3, 0.4, 0.3)$ they are peaked towards the troughs. Furthermore, solutions obtained for intermediatery height distributions showed a decrease in the number of significant harmonics. A turning point exists at which the fundamental is the only important contributor, and so sinusoidal solutions exist here. This dependence on the height distribution of the interfaces can be predicted analytically. In all the present situations for fast-mode-only waves the wavelength parameter μ is small so the long wave approximations in equations (4.25) and (4.27) can be

Figure 4.1 Permanent waves in the faster mode with $\varepsilon = 0.05$ (Vertical magnification 40π).

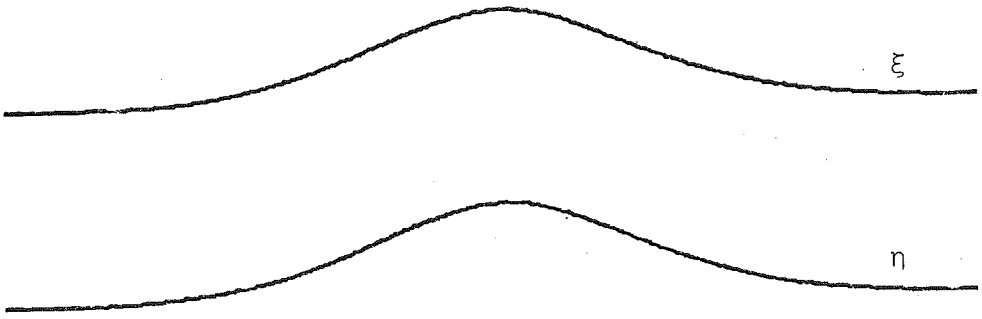

Figure 4.1a

One wavelength for $\mu = 0.05$, $(h_1, h_2, h_3) = (0.4, 0.2, 0.4)$.

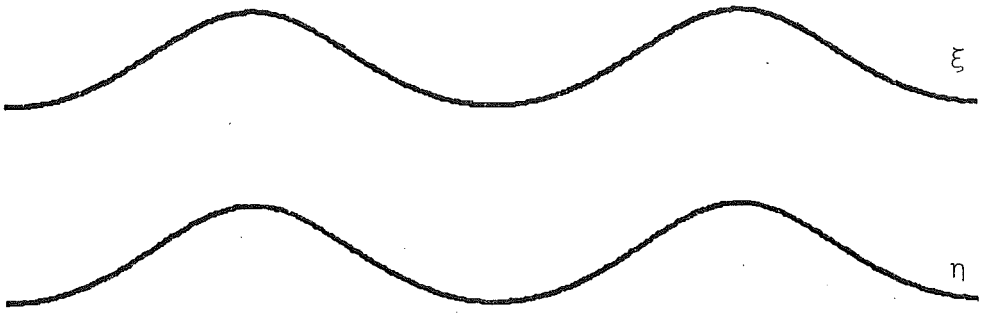

Figure 4.1b

Two wavelengths for $\mu = 0.1$, $(h_1, h_2, h_3) = (0.4, 0.2, 0.4)$.

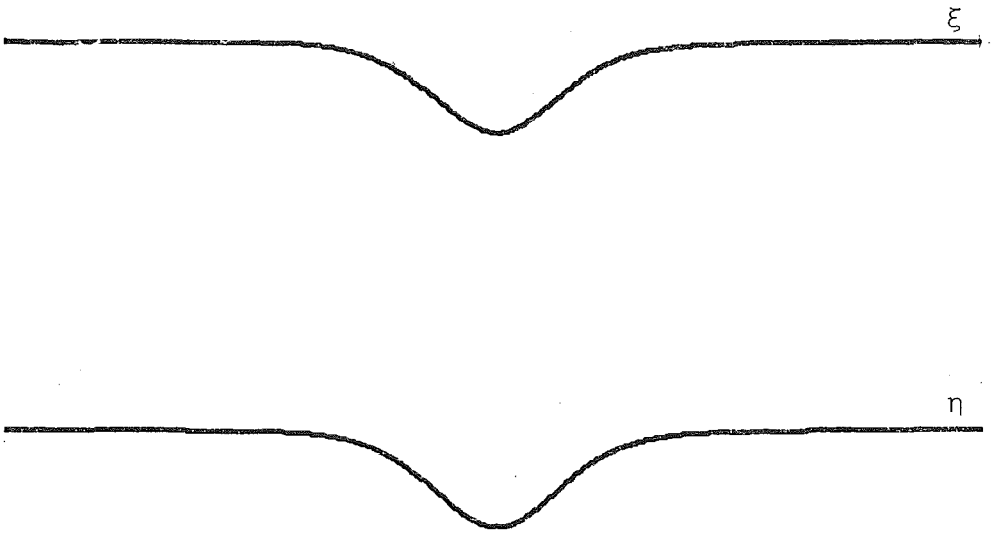

Figure 4.1c

One wavelength for $\mu = 0.05$, $(h_1, h_2, h_3) = (0.3, 0.4, 0.3)$.

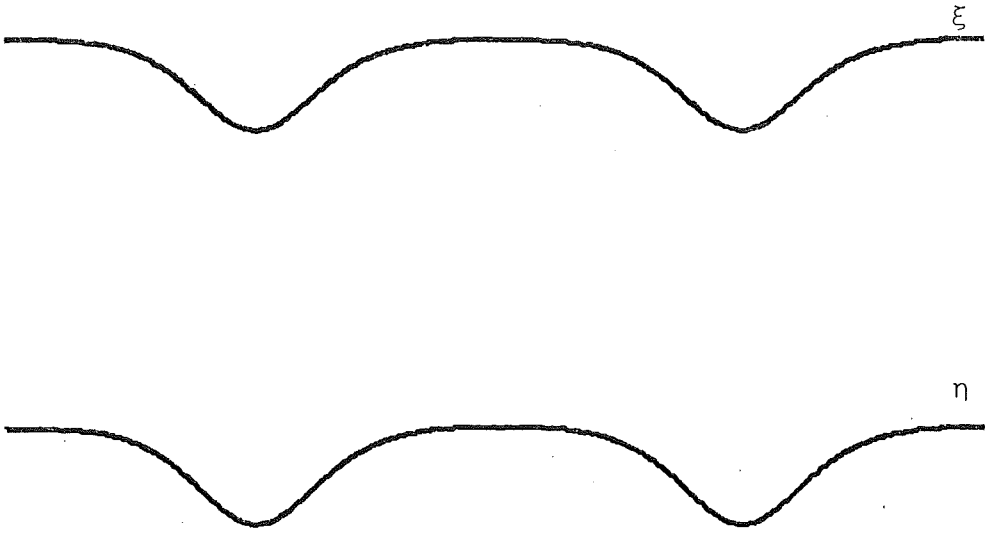

Figure 4.1d

Two wavelengths for $\mu = 0.1$, $(h_1, h_2, h_3) = (0.3, 0.4, 0.3)$.

used. In the limit as $\mu \to 0$ the amplitudes of the solitary waves are dependent on $-\frac{s_1}{f_1}$, where s_1 and f_1 are as in (4.25a and b). The sign of this term determines whether the solitary waves are of elevation or depression. For small μ then, the sign of this term determines whether the cnoidal waves are peaked at the crests or troughs: if positive, peaked crests are expected, whilst if negative, the peaking is towards the troughs. In each of the cases in figure (4.1a - d) the ratio of amplitudes of the interfacial disturbances has been calculated. These give $|\eta| = a \times |\xi|$ where a = 0.93, 0.94, 0.98 and 0.97 for (a) - (d) respectively. This serves to illustrate the minimal difference between the effects of the fast mode on the respective interfaces and hence the poor identification of mode with interface. Also, the number of harmonics exceeding 10^{-4} in magnitude in each case is 7, 4, 13 and 7 respectively.

In seeking solutions for periodic permanent waves consisting of the slower mode alone complications may occur. At most values of μ, especially large values, solutions exist, but it will be observed that in the regions of certain μ, the solutions suggest an influence by fast mode harmonics. For the time being assume wavelengths for which the slow-mode-only solutions are well behaved, then they will have the form

$$\eta = \sum_{\ell=1}^{\infty} b(k) \cos \mu k(x - ct) \qquad (4.33a)$$

$$\xi = \sum_{\ell=1}^{\infty} b(k)/r_2(k) \cos \mu k(x - ct). \qquad (4.33b)$$

The ratio $r_2(k)$ is negative and consequently the interfaces are displaced in antiphase. Taking the total displacement at the lower interface as 2a, in view of the phase difference we get

$$\sum_{k=1}^{\infty} b(2k-1) = -1 \,. \tag{4.34}$$

The amplitudes are related to those in (4.14), for $\alpha = 2$ only, by

$$A_2(k) = b(k)/r_2(k) \exp i\{\omega_2(k) - \mu kc\}t$$

$$B_2(k) = b(k) \exp i\{\omega_2(k) - \mu kc\}t$$

$$k = 1,2,... \tag{4.35}$$

Substitution into equations (4.22b) yields

$$\{\omega_2(k) - \mu kc\}b(k) = \tfrac{1}{2}\,\varepsilon \sum_{\ell=1}^{k-1} S_{222}(k,-\ell)b(\ell)b(k-\ell)$$

$$+ \varepsilon \sum_{\ell=1}^{\infty} S_{222}(k,\ell)b(\ell)b(k+\ell)$$

$$k = 1,2,... \tag{4.36}$$

Solutions can be found as for the fast-mode-only permanent waves.

Solutions for $\varepsilon = 0.05$ with $(h_1, h_2, h_3) = (0.3, 0.4, 0.3)$ and $\mu = 0.1$, 0.5 and 1.0 are sketched in figure (4.2) with a vertical magnification of 5π. The degree of interaction is obviously much greater for larger μ than in the case of the fast-mode-only solutions. At $\mu = 0.1$, there are 40 harmonics exceeding 10^{-4} in magnitude, at $\mu = 0.5$ there are 12, and at $\mu = 1.0$ there are 7. Thus, for any given wavelength there will be much more extensive resonant

Figure 4.2 Permanent waves in the slower mode with $\varepsilon = 0.05$ (vertical magnification 5π).

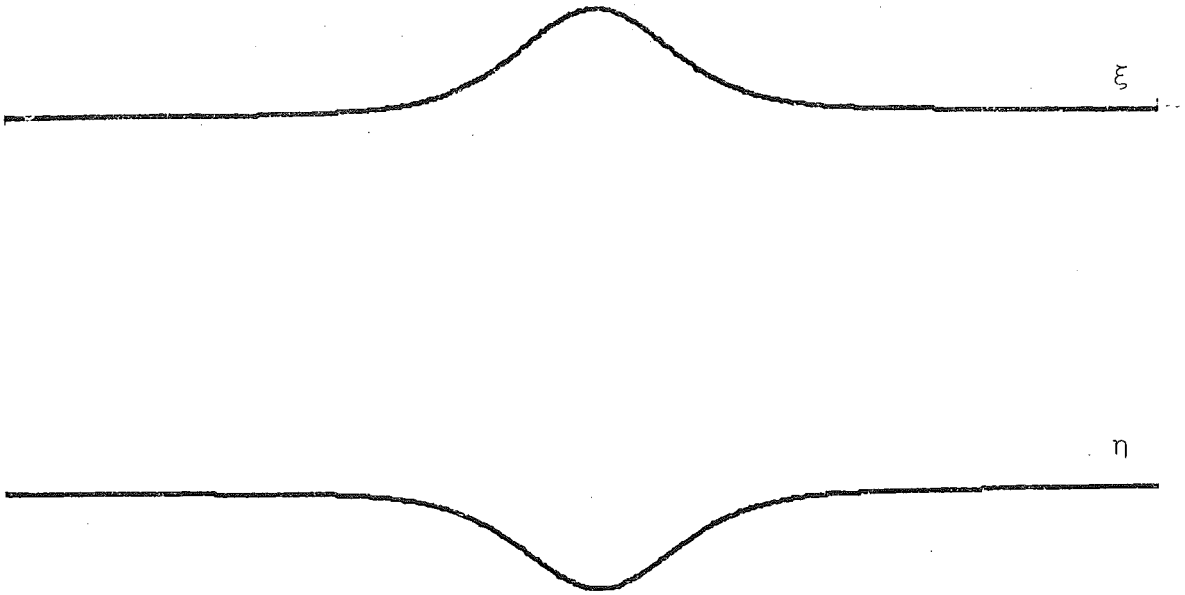

Figure 4.2a

The central 0.3 of a wavelength for $\mu = 0.1$

$(h_1, h_2, h_3) = (0.3, 0.4, 0.3)$.

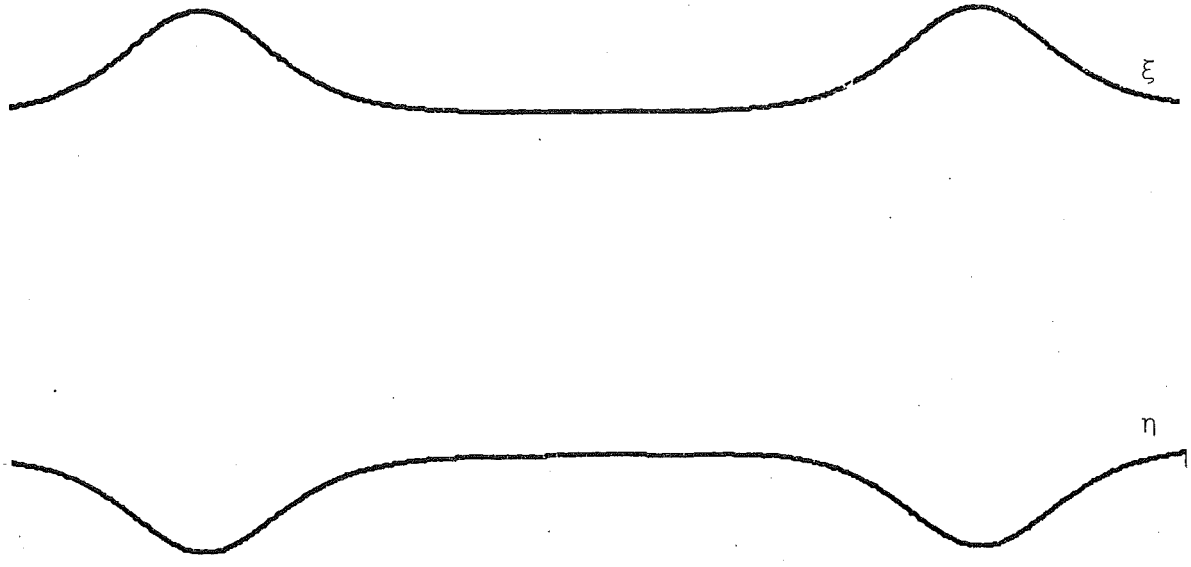

Figure 4.2b

One and a half wavelengths for $\mu = 0.5$

$(h_1, h_2, h_3) = (0.3, 0.4, 0.3)$.

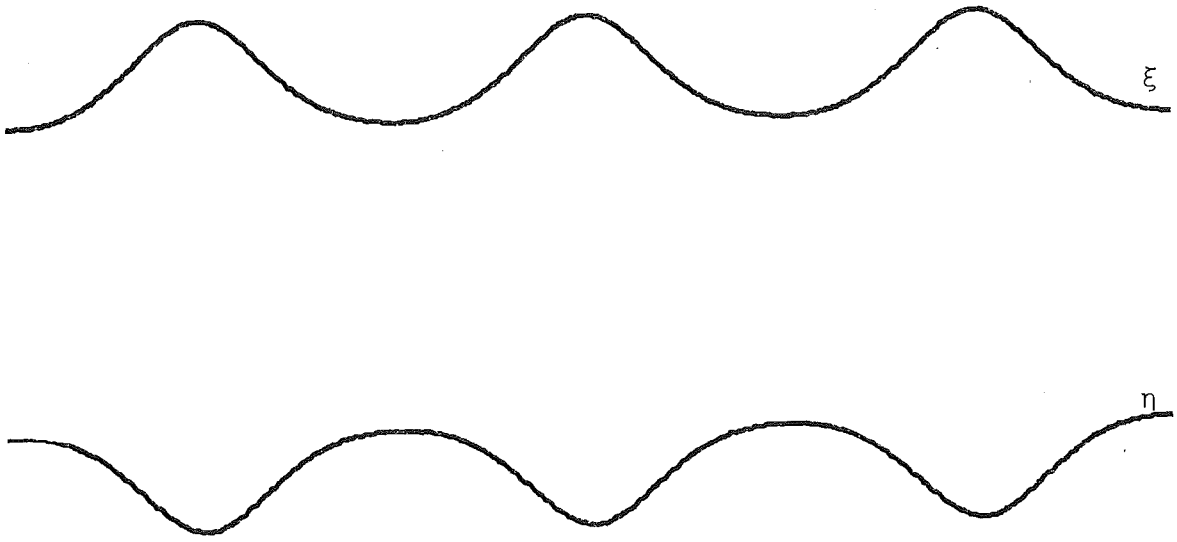

Figure 4.2c

Three wavelengths for $\mu = 1.0$, $(h_1, h_2, h_3) = (0.3, 0.4, 0.3)$

production of higher slow-mode harmonics than fast-mode harmonics. This is consistent with the results obtained when permanent wave structures are considered in the next chapter: allowing all types of interaction it is seen that a predominantly slow mode permanent wave is prominent as the "carrier wave" part of the structure while a fast mode permanent wave does not feature.

Calculations were also made for the height distributions $(h_1, h_3, h_3) = (0.4, 0.2, 0.4)$ and $(0.2, 0.6, 0.2)$, and it is noticed that the former and $(h_1, h_2, h_3) = (0.3, 0.4, 0.3)$ both result in waves peaked to the troughs at the lower interface accompanied by waves peaked to the crest at the upper interface, whilst the latter gives a pattern in which the lower interface bears waves peaked to the crests accompanied by waves peaked to the troughs at the upper interface. The phenomena is the same as occurred for the fast-mode-only permanent waves, the dependence being now on $-\frac{s_2}{f_2}$, where s_2 and f_2 are as in (4.25). In the limit as $\mu \to 0$ this term will determine whether the solitary wave is elevated at the upper interface $\left(-\frac{s_2}{f_2} < 0\right)$ and depressed at the lower interface, or vice versa. Once again a turning point is expected somewhere between $(h_1, h_2, h_3) = (0.2, 0.6, 0.2)$, and $(0.3, 0.4, 0.3)$ at which the solution is sinusoidal. Given $\mu = 0.3$ this occurs at $(h_1, h_2, h_3) = (0.25, 0.50, 0.25)$.

It was in obtaining solutions for equations (4.34) and (4.36) that the misbehaviour of the results in the neighbourhoods of certain values of μ was noticed. These values of μ were found to correspond to the breaking down of the conditions

(4.20), which were necessary for the development of single mode solutions.

Referring to (4.36), significant interactions occur when

$$\omega_2(\ell) - \mu\ell c = 0(\varepsilon) .$$

However, the breakdown of condition (4.20) implies that

$$\omega_1(k) - \mu k c = 0(\varepsilon) \qquad (4.37)$$

for some k. For the slow-mode-only permanent wave, the velocity c is approximated by the wave velocity for $\ell = 1$, that is

$$c \simeq \frac{\omega_2(1)}{\mu} ,$$

but from (4.37)

$$c \simeq \frac{\omega_1(k)}{\mu k} ,$$

so $\omega_1(k) \simeq k\omega_2(1)$

gives the condition for this singularity. Writing the μ-dependence of the frequency explicitly

$$\omega_1(\mu k) = k\,\omega_2(\mu) , \qquad (4.38)$$

and for integer values of k this equation determines values of μ near which slow permanent waves will resonantly generate a fast wave harmonic with the wavenumber k. At such values of μ, slow mode permanent waves must be accompanied by certain fast mode harmonics and a single mode theory breaks down. This resonance is that described in equation (4.6) [see BRYANT and LAING (1978)].

To keep the theory general then, fast mode harmonics must be included in (4.33), so rewrite

$$\eta = \sum_{k=1}^{\infty} \{b(k) + r_1(k)a(k)\} \cos \mu k(x - ct),$$

$$\xi = \sum_{k=1}^{\infty} \{b(k)/r_2(k) + a(k)\} \cos \mu k(x - ct)$$

$$k = 1,2,... \qquad (4.39)$$

where $A_1(k)$, $A_2(k)$, $B_1(k)$ and $B_2(k)$ are related to $a(k)$ and $b(k)$ by equations (4.30) and (4.35). Note that the relevant equations to be solved are now (4.17) since some of the interactions can make significant contributions to both modes. Thus

$$\mu^2k^2c^2\{[(\rho_2 \coth \mu kh_2 + \rho_3 \coth \mu kh_3) \sinh \mu kh_2/\rho_2][a(k)+b(k)/r_2(k)]$$

$$- [a(k)r_1(k)+b(k)]\} - \frac{(\rho_2-\rho_3)}{\rho_2}\mu k \sinh \mu kh_2[a(k)+b(k)/r_2(k)]$$

$$= \tfrac{1}{2}\varepsilon \sum_{\ell=1}^{k-1} U_{22}(k,-\ell)b(\ell)b(k-\ell) + \varepsilon \sum_{\ell=1}^{\infty} U_{22}(k,\ell)b(\ell)b(k+\ell)$$

$$+ 0(\varepsilon^2) \qquad k = 1,2,... \qquad (4.40a)$$

$$-\mu^2k^2c^2\{\frac{\rho_1 \coth \mu kh_1}{\rho_2}[b(k)+r_1(k)a(k)]+(\rho_2+\rho_3 \coth \mu kh_2 \coth \mu kh_3)$$

$$\times \sinh \mu kh_2/\rho_2[a(k)+b(k)/r_2(k)]\}+\frac{\rho_1-\rho_2}{\rho_2}\mu k[b(k)+r_1(k)a(k)]$$

$$+ \frac{\rho_2-\rho_3}{\rho_2}\mu k \cosh \mu kh_2[a(k)+b(k)/r_2(k)]$$

$$= \tfrac{1}{2}\varepsilon \sum_{\ell=1}^{k-1} V_{22}(k,-\ell)b(\ell)b(k-\ell) + \varepsilon \sum_{\ell=1}^{\infty} V_{22}(k,\ell)b(\ell)b(k+\ell)$$

$$+ 0(\varepsilon^2) \qquad k = 1,2,... \qquad (4.40b)$$

A little manipulation of these yields

$$\{\omega_2^2(k)-\mu^2k^2c^2\}b(k)[1-(\rho_2 \coth \mu kh_2 + \rho_3 \coth \mu kh_3)\frac{\sin \mu kh_2}{\rho_2 r_2(k)}]$$

$$+ \{\omega_1^2(k)-\mu^2k^2c^2\}a(k)[r_1(k)-(\rho_2 \coth \mu kh_2+\rho_3 \coth \mu kh_3)\frac{\sin \mu kh_2}{\rho_2}]$$

$$= \tfrac{1}{2}\varepsilon \sum_{\ell=1}^{k-1} U_{22}(k,-\ell)b(\ell)b(k-\ell) + \varepsilon \sum_{\ell=1}^{\infty} U_{22}(k,\ell)b(\ell)b(k+\ell)$$

$$+ 0(\varepsilon^2) \qquad k = 1,2,... \qquad (4.41a)$$

$$\{\omega_2^2(k) - \mu^2k^2c^2\}b(k)$$

$$\times \left[\frac{\rho_1 \coth \mu kh_1}{\rho_2} + (\rho_2+\rho_3 \coth \mu kh_2 \coth \mu kh_3)\frac{\sinh \mu kh_2}{\rho_2 r_2(k)}\right]$$

$$+ \{\omega_1^2(k) - \mu^2k^2c^2\}a(k)$$

$$\times \left[\frac{\rho_1 \coth \mu kh_1}{\rho_2} r_1(k) + (\rho_2+\rho_3 \coth \mu kh_2 \coth \mu kh_3)\frac{\sinh \mu kh_2}{\rho_2}\right]$$

$$= \tfrac{1}{2}\varepsilon \sum_{\ell=1}^{k-1} V_{22}(k,-\ell)\, b(\ell)b(k-\ell) + \varepsilon \sum_{\ell=1}^{\infty} V_{22}(k,\ell)b(\ell)b(k+\ell)$$

$$+ 0(\varepsilon^2) \qquad k = 1,2,... \qquad (4.41b)$$

Equations (4.41) and (4.34) can be solved, by the numerical method described previously, for a(k), b(k) $k = 1,2,...$, and c. Solutions were obtained in this case for $(h_1, h_2, h_3) = (0.3, 0.4, 0.3)$ at $\varepsilon = 0.05$ over a range of values for μ. At most wavelengths, especially the shorter ones, the contribution from the faster mode is negligible, that is, $a(k) = 0(\varepsilon)$, and the same solutions as in the previous set of calculations were obtained. As the wavelength is increased the points are reached at which each of the fast harmonics in turn are resonantly generated to significant levels. For example, at $\mu = 2.5$ the first point of resonance occurs, at which the second harmonic of the fast mode is generated. Here a(2) is significant whilst a(k) for all other k are insignificant. For the higher harmonics a(3), a(4), a(5) and a(6), the values of μ near which they are significant are $\mu = 1.55, 1.15, 0.90$

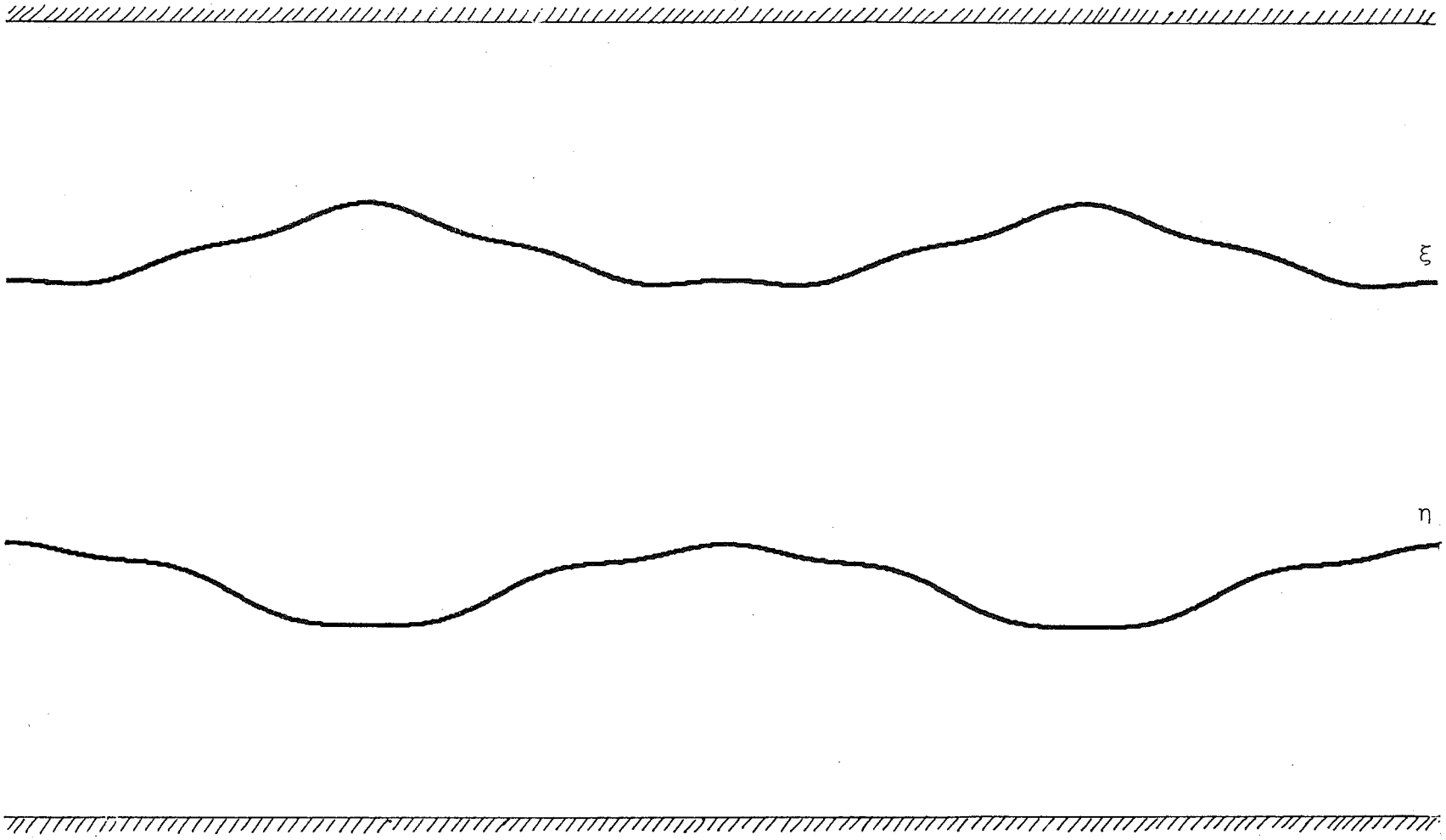

Figure 4.3

Two wavelengths of the slower mode permanent wave at $\mu = 1.15$ (Vertical magnification 2π). The presence of the fast mode harmonic a(4) is noticeable.

and 0.75 respectively.

For the first resonance $|a(2)| > 0.02$ for $\mu \in (2.2, 2.9)$, but the size of the neighbourhoods in which these harmonics are significant decreases with μ, so that in the limit as $\mu \to 0$ the solitary wave comprises slow mode harmonics only. This solitary wave is a wave of depression at the lower interface with an elevation at the upper interface.

It is notable from the solutions that the sign of the significant fast-mode harmonic differs depending on whether μ is slightly larger or smaller than the resonant value. It has been pointed out [BRYANT and LAING (1978)] that this implies the possibility of two forms of the fast mode harmonic, one differing from the other only in that it has a π phase difference.

The calculations have also been performed for the height distribution $(h_1, h_2, h_3) = (0.4, 0.2, 0.4)$. The features are identical except that the corresponding resonances occur for higher μ, for example, at $\mu \simeq 4.5$, 2.7 for the second and third fast mode harmonics respectively.

A solution for $(h_1, h_2, h_3) = (0.3, 0.4, 0.3)$, in the vicinity of the resonance of the fourth fast-mode harmonic with the slow fundamental has been sketched in figure (4.3). The cnoidal profile has been deformed by the significant size of a(4) viz:a(4) = 0.1273, and as the sketch shows there are four corresponding "bumps" appearing in each wavelength.

CHAPTER V

PERMANENT WAVE STRUCTURES

§5.1. It has been mentioned in §4.1 that the presence of two wave modes allows quadratic interactions involving harmonics of both modes. Two of these were described in equations (4.5) and (4.6), the latter being investigated in chapter four. The former interaction can be regarded as that occurring between a group of the faster mode and harmonics of the slower mode. This chapter investigates structures comprising a group of permanent envelope and a predominantly slower mode "carrier" wave of permanent form. These structures are largely due to the extent of this interaction.

Considering equation (4.5) with ℓ very small compared to k it is not difficult to anticipate an equality

$$c_{g1}(k) = c_2(1) \tag{5.1}$$

where c_g is the group velocity, c the phase velocity, and the numeric subscripts denote the mode. This equation provides a basis for seeking the above-mentioned structures. Even when the close relation of the modes means that ℓ and k in equation (4.5) can be similar, this equality (5.1) provides a good starting point, and to this end the phase velocities and group velocities of the two wave modes are drawn in figure (5.1) as functions of μk, for both $(h_1, h_2, h_3) = (0.4, 0.2, 0.4)$ and $(0.3, 0.4, 0.3)$.

Note that for large wavenumbers the dispersion relation (4.12) gives

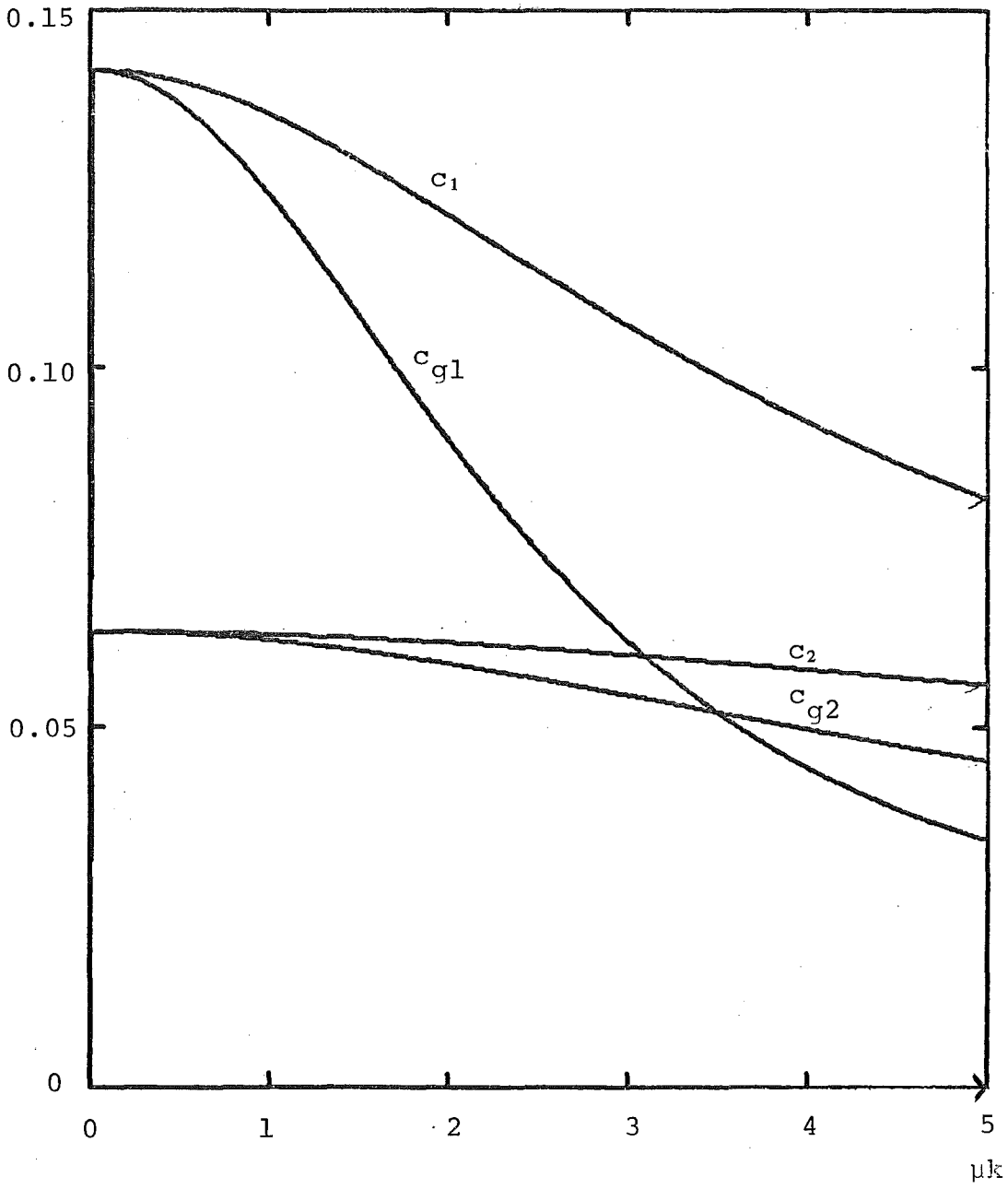

Figure 5.1a

Phase velocities and group velocities of the two wave modes for $(h_1, h_2, h_4) = (0.4, 0.2, 0.4)$.

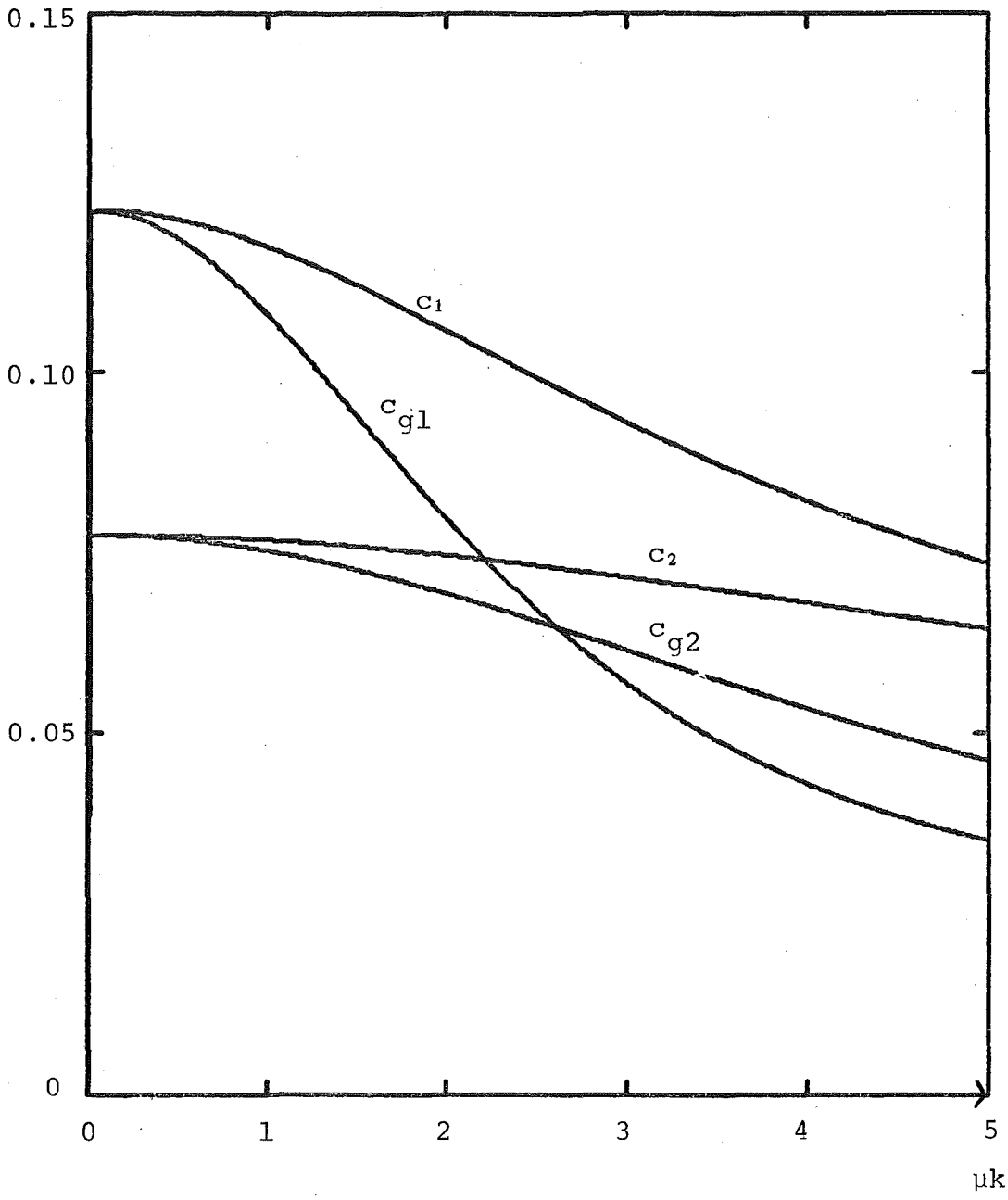

Figure 5.1b

Phase velocities and group velocities of the two wave modes for $(h_1, h_2, h_3) = (0.3, 0.4, 0.3)$.

$$\frac{\omega_\alpha^2(k)}{\mu k} = \frac{\rho_2 - \rho_3}{\rho_2 + \rho_3} \quad \text{or} \quad \frac{\rho_1 - \rho_2}{\rho_1 + \rho_2} \qquad \alpha = 1,2 \tag{5.2}$$

whence the frequency is parabolically related to k, for large k. For small wavenumbers equation (4.24) gives

$$\frac{\omega_\alpha(k)}{\mu k} \simeq c_\alpha , \qquad \alpha = 1,2.$$

which indicates a linear dependence.

The general equations (4.17) are used to seek solutions of permanent form such that

$$\eta(x,t) = \sum_{k=1}^{n} [b(k) + r_1(k)a(k)] \cos \mu k(x - ct)$$

$$+ \sum_{k=m_1}^{m_2} \bar{a}(k) r_1(k) \cos \{\mu k(x - ct) - \delta t\} \tag{5.3a}$$

$$\xi(x,t) = \sum_{k=1}^{n} [a(k) + b(k)/r_2(k)] \cos \mu k(x - ct)$$

$$+ \sum_{k=m_1}^{m_2} \bar{a}(k) \cos \{\mu k(x - ct) - \delta t\} \tag{5.3b}$$

where δ is the frequency of the fast group waves relative to the group envelope, and $\bar{a}(k)$ are the amplitudes of the group's component harmonics. The significant harmonics (of magnitude greater than 10^{-4}) only need be considered, so the series have been truncated to leave $b(k)$, $a(k)$, for $1 \leqslant k \leqslant n$, and $\bar{a}(k)$ for $m_1 \leqslant k \leqslant m_2$. These harmonics along with δ and c are the quantities to be determined.

The solutions in (5.3) represent permanent structures comprising a group of the faster mode and a permanent wave of predominantly the slower mode travelling together at a speed c, at both interfaces. The Fourier amplitudes

$A_\alpha(k)$ and $B_\alpha(k)$ are related to $a(k)$ and $b(k)$ respectively as in (4.30) and (4.35), and in addition

$$A_1(k) = \bar{a}(k) \exp i\{\omega_1(k)-\mu kc-\delta\}t \qquad m_1 \leqslant k \leqslant m_2 \quad (5.4a)$$

$$B_1(k) = r_1(k)a(k) \exp i\{\omega_1(k)-\mu kc-\delta\}t \qquad m_1 \leqslant k \leqslant m_2 \quad (5.4b)$$

are possible substitutions. The use of (5.4) or (4.30) for $A_1(k)$ and $B_1(k)$ depends on the particular interaction. All interactions are included.

Substitution for the amplitudes $A_1(k)$, $A_2(k)$, $B_1(k)$ and $B_2(k)$ into equations (4.17) quickly shows that there are two cases to be considered. Firstly, there are the equations in which no phase term $\exp\{-i\delta t\}$ appears on the left hand side. The balance on the right hand side is achieved by using (4.30) and (4.35) in the substitutions. However, on the right hand side it is possible to include an $\bar{a}(\ell)\bar{a}(k+\ell)$ term since one is a complex conjugate and so the exponentials in $i\delta t$ cancel. Thus, two sets of equations result, similar to (4.41) with the difference that all interactions are included:

$$\{\omega_2^2(k)-\mu^2k^2c^2\}b(k)\left[1-(\rho_2 \coth \mu kh_2 + \rho_3 \coth \mu kh_3)\frac{\sinh \mu kh_2}{\rho_2 r_2(k)}\right]$$

$$+ \{\omega_1^2(k)-\mu^2k^2c^2\}a(k)$$

$$\times \left[r_1(k)-(\rho_2 \coth \mu kh_2 + \rho_3 \coth \mu kh_3)\frac{\sinh \mu kh_2}{\rho_2}\right]$$

$$= \tfrac{1}{2}\varepsilon \sum_{\ell=1}^{k-1}\sum_{\beta=1}^{2}\sum_{\gamma=1}^{2} U_{\beta\gamma}(k,-\ell)b_\beta(\ell)b_\gamma(k-\ell)$$

$$+ \varepsilon \sum_{\ell=1}^{n}\sum_{\beta=1}^{2}\sum_{\gamma=1}^{2} U_{\beta\gamma}(k,\ell)b_\beta(\ell)b_\gamma(k+\ell)$$

$$+ \varepsilon \sum_{\ell=m_1}^{m_2} U_{11}(k,\ell)r_1(\ell)r_1(k+\ell)\bar{a}(\ell)\bar{a}(k+\ell)$$

$$+ 0(\varepsilon^2) \qquad k = 1,2,\ldots n \quad (5.5a)$$

$$\{\omega_2^2(k)-\mu^2k^2c^2\}b(k)$$

$$\times\left[\frac{\rho_1\coth\mu kh_1}{\rho_2}+(\rho_2+\rho_3\coth\mu kh_2\coth\mu kh_3)\frac{\sinh\mu kh_2}{\rho_2 r_2(k)}\right]$$

$$+\{\omega_1^2(k)-\mu^2k^2c^2\}a(k)$$

$$\times\left[\frac{\rho_1\coth\mu kh_1}{\rho_2 r_1(k)}+(\rho_2+\rho_3\coth\mu kh_3\coth\mu kh_2)\frac{\sinh\mu kh_2}{\rho_2}\right]$$

$$=\tfrac{1}{2}\varepsilon\sum_{\ell=1}^{k-1}\sum_{\ell=1}^{2}\sum_{\ell=1}^{2}V_{\beta\gamma}(k,-\ell)b_\beta(\ell)b_\gamma(k-\ell)$$

$$+\varepsilon\sum_{\ell=1}^{n}\sum_{\ell=1}^{2}\sum_{\ell=1}^{2}V_{\beta\gamma}(k,\ell)b_\beta(\ell)b_\gamma(k+\ell)$$

$$+\varepsilon\sum_{\ell=m_1}^{m_2}V_{11}(k,\ell)r_1(\ell)r_1(k+\ell)\bar{a}(\ell)\bar{a}(k+\ell)$$

$$+0(\varepsilon^2)\qquad k=1,2,\ldots n \tag{5.5b}$$

where $b_1(\ell)=r_1(\ell)a(\ell)$ and $b_2(\ell)=b(\ell)$.

Secondly, there are the equations in which the coefficients of the term $\exp\{-i\delta t\}$ are collected. These are the evolution equations for the group amplitudes and, since only the faster mode terms will appear on the left hand side, can be treated as the special case in §4.4. Thus, equations like (4.22a) result where $A_1(k)$ and $B_1(k)$ are as given by (5.4), but $A_2(k)$ and $B_2(k)$ as by (4.35). This yields the set of equations

$$\{\omega_1(k)-\mu kc-\delta\}\bar{a}(k)$$

$$=\tfrac{1}{2}\varepsilon\sum_{\ell=1}^{\min(n,k-m_1)}\sum_{\beta=1}^{2}R_{1\beta1}(k,-\ell)b_\beta(\ell)\bar{a}(k-\ell)r_1(k-\ell)$$

$$+\tfrac{1}{2}\varepsilon\sum_{\ell=1}^{\min(n,k-m_1)}\sum_{\beta=1}^{2}R_{11\beta}(k,-\ell)\bar{a}(\ell)b_\beta(k-\ell)r_1(\ell)$$

$$+\varepsilon\sum_{\ell=1}^{\min(n,m_2-k)}\sum_{\ell=1}^{2}R_{1\beta1}(k,\ell)b_\beta(\ell)\bar{a}(k+\ell)r_1(k+\ell)$$

$$k=m_1,\ m_1+1,\ldots\ m_2.$$

The first two summations on the right hand side are equal since $R_{1\beta 1}(k,-\ell) = R_{11\beta}(k,-\ell)$, thence

$$\{\omega_1(k) - \mu kc - \delta\}\bar{a}(k)$$

$$= \varepsilon \sum_{\ell=1}^{\min(n,k-m_1)} \sum_{\beta=1}^{2} R_{1\beta 1}(k,-\ell) b_\beta(\ell) \bar{a}(k-\ell) r_1(k-\ell)$$

$$+ \varepsilon \sum_{\ell=1}^{\min(n,m_2-k)} \sum_{\beta=1}^{2} R_{1\beta 1}(k,\ell) b_\beta(\ell) \bar{a}(k+\ell) r_1(k+\ell)$$

$$k = m_1, \ldots m_2. \qquad (5.6)$$

It turns out that all significant contributions are made when $\beta = \gamma = 2$ in equations (5.5), and when $\beta = 2$ in equations (5.6), with some contribution from $\beta = \gamma = 1$ in the former. For generality the other combinations are retained.

In addition to the above equations, it is necessary to impose a condition on the carrier wave's amplitude

$$\sum_{k=1}^{\infty} b(2k-1) = -1 \qquad (5.7)$$

so that the vertical difference between a crest and trough is 2ε.

The amplitude of the group envelope may be assigned independently. Taking the maximum displacement as ε then there are two possibilities: either the envelope maximum coincides with a crest or a trough of the carrier wave. In the former case

$$\sum_{k=m_1}^{m_2} \bar{a}(k)(-1)^{k-1} = 1 \qquad (5.8a)$$

whilst for the latter

$$\sum_{k=m_1}^{m_2} \bar{a}(k) = 1 \quad . \qquad (5.8b)$$

Equations (5.5) - (5.8) suffice to solve.

§5.2. *The method of solution* is as follows. For a given wavelength the values obtained for $b(\ell)$, $a(\ell)$ and c, using the method of §4.4 in the absence of any group, are substituted into equations (5.6). The resulting $m_2 - m_1 + 1$ linear algebraic equations can be regarded as an eigenvalue-eigenvector problem in which δ is the eigenvalue and the associated eigenvector is $[\bar{a}(m_1), \bar{a}(m_1+1), \ldots \bar{a}(m_2)]$. Standard eigenvalue techniques determine the $m_2 - m_1 + 1$ eigenvalues and eigenvectors. These together with the original values for $b(\ell)$, $a(\ell)$ and c are then used as starting values for a Newton-Raphson method of solution for (5.6) - (5.8). The number of harmonics included in this final calculation is altered progressively so that all harmonics with a magnitude larger than 10^{-4} are included. This involves increasing or decreasing n and m_2 for the higher limit on harmonics for the group and carrier wave respectively, and m_1 for the lower limit on harmonics in the group ($m_1 \geqslant 1$ always).

An alternative method is to firstly make a short wave approximation for which $b(1) = -1$ and $b(\ell) = 0(\varepsilon)$, $\ell > 1$ with the speed c approximated by $\omega_2(1)/\mu$. The eigenvalues and eigenvectors can now be determined providing a reasonably accurate solution at large μ. Successive reduction in μ to that desired, using the Newton-Raphson method at each step, now achieves the solution required.

Yet another method, using a different approach but in the long run not much different in practice from the second

method above, is that used by BRYANT and LAING (1978) for shorter wavelengths. Solutions are found for particular resonant triads (at the desired wavelength) using equations derived from the evolution equation (4.22). For example, taking a triad

$$\omega_\alpha(k) + \omega_\beta(\ell) - \omega_\gamma(k+\ell) = 0(\varepsilon) \qquad \alpha,\beta,\gamma \in \{1,2\}$$

then

$$DB_\alpha(k) = i\,\varepsilon\, S_{\alpha\beta\gamma}(k,\ell) B^*_\beta(\ell) B_\gamma(k+\ell) \times \exp i\{\omega_\alpha(k) + \omega_\beta(\ell) - \omega_\gamma(k+\ell)\}t \tag{5.9}$$

and similarly for $DB_\beta(\ell)$ and $DB_\gamma(k+\ell)$. This triad is regarded as an elementary permanent wave structure for which

$$\eta = b_\alpha \cos \mu k(x-ct) + b_\beta \cos\{\mu\ell(x-ct) - \delta t\} + b_\gamma \cos\{\mu(k+\ell)(x-ct) - \delta t\}.$$

Rewriting the amplitudes $B_\alpha(k)$, $B_\beta(\ell)$ and $B_\gamma(k+\ell)$ from (5.9) in terms of b_α, b_β, b_γ, and substituting, a set of equations results:

$$\{\omega_\alpha(k) - \mu kc\}b_\alpha = \varepsilon\, S_{\alpha\beta\gamma}(k,\ell) b_\beta b_\gamma,$$

$$\{\omega_\beta(\ell) - \mu\ell c - \delta\}b_\beta = \varepsilon\, S_{\beta\alpha\gamma}(\ell,k) b_\alpha b_\gamma,$$

$$\{\omega_\gamma(k+\ell) - \mu(k+\ell)c - \delta\}b_\gamma = \varepsilon\, S_{\gamma\beta\alpha}(k+\ell,-\ell) b_\alpha b_\beta,$$

the last equation having a factor of ½ on the right hand side if $\alpha = \beta$ and $k = \ell$. The carrier wave amplitude b_α, and the group envelope amplitude $b_\beta + b_\gamma$, are given, so that solutions can be obtained for the triad $(b_\alpha, b_\beta, b_\gamma)$, the speed c, and the phase δ. These solutions can be used now as starting points for including the range of harmonics with wavenumbers near to those of the components $(k,\ell,k+\ell)$

of this resonant triad. Thus the solutions are obtained. This method is similar in practice to the previous one because for short wavelengths the number of significant harmonics in the group is small. The final solution is therefore not much different from the traid first considered. By the other method of approach, with b(1) = -1 and say $\bar{a}(k)$, $\bar{a}(k+1)$ as the only significant harmonics in the group, we effectively have the triad with $\omega_2(1) + \omega_1(k) - \omega_1(k+1) \simeq 0$.

For the following results and discussion a wide range of wavelengths is considered and so the first two methods, based on eigenanalysis, have been used.

§5.3. *Results.*

Using the same densities and amplitude scalings as in chapter four viz: $\rho_1 : \rho_2 : \rho_3 = 1.05 : 1.00 : 0.95$ with $\varepsilon = 0.05$, firstly the system with layer thicknesses $(h_1, h_2, h_3) = (0.3, 0.4, 0.3)$ was solved. As stated in §5.2 the solutions for a(k), b(k), and c in the absence of a group (from §4.4) were substituted into equations (5.6). The resulting eigenvalues for $\mu = 0.3$ were then ordered, the largest being $\delta_1 = 0.0570$, followed by $\delta_2 = 0.0551$, $\delta_3 = 0.0533$, $\delta_4 = 0.0508$, $\delta_5 = 0.0488$ etc. The eigenvectors $\bar{a}_1, \bar{a}_2, \ldots$ respectively were scaled to satisfy equation (5.8). For the largest eigenvalue δ_1 the associated eigenvector, to an accuracy of 10^{-4}, is

$$\bar{a}_1 = (0, -0.0001, -0.0010, 0.0037, -0.0328, 0.2566, -0.4545, 0.2176, -0.0267, 0.0068, -0.0006, 0.0000). \qquad (5.10)$$

The centre of the group represented by this eigenvector is obviously in the vicinity of the wavenumber 7. On reference

to figure (5.1b), if $\mu = 0.3$ then

$$c_2(1) = c_{g1}(k)$$

is satisfied for $\mu k \simeq 2.1$, that is, $k \simeq 7$. This is obtained by drawing a line in the direction of the μk axis. This line is raised or lowered until the intercept with the c_2-curve is at $\mu k = 0.3$ $(k = 1)$. The intercept with the c_{g1}-curve gives the above result. It is evident that this rough method gives a reasonably accurate estimate of the central wave-number for the group, thus endorsing the use of (5.1).

It is interesting to consider the spectra of these eigenvectors. Since the maxima of the envelopes of the groups they represent are at $x = 0$, to present the spectra more clearly we shift the whole group along by π so that the maximum is at $x = \pi$. Now the group is

$$\sum_{k=m_1}^{m_2} \bar{a}(k)\cos\{\mu k(x - ct) - \delta t + \pi\}$$

$$= \sum_{k=m_1}^{m_2} \bar{a}'(k)\cos\{\mu k(x - ct) - \delta t\}$$

where $\bar{a}'(k) = \bar{a}(k)(-1)^{k+1}$ $\quad k = 1,2,\ldots m_2$.

Consider the spectrum of harmonics $\bar{a}'(k)$. The first five vectors $[\bar{a}'(m_1),\ldots, \bar{a}'(m_2)]$ are shown in figure (5.2) along with the associated carrier wave [some rescaling has been necessary so that $\sum_{k=m_1}^{m_2} |\bar{a}'(k)| = 1$ rather than equation (5.8) for which individual $\bar{a}'(k)$'s can be larger than 1]. There is a clear correspondence between the nth eigenvector and the number of "turning points" in the spectral representation. These distinctive patterns were encountered

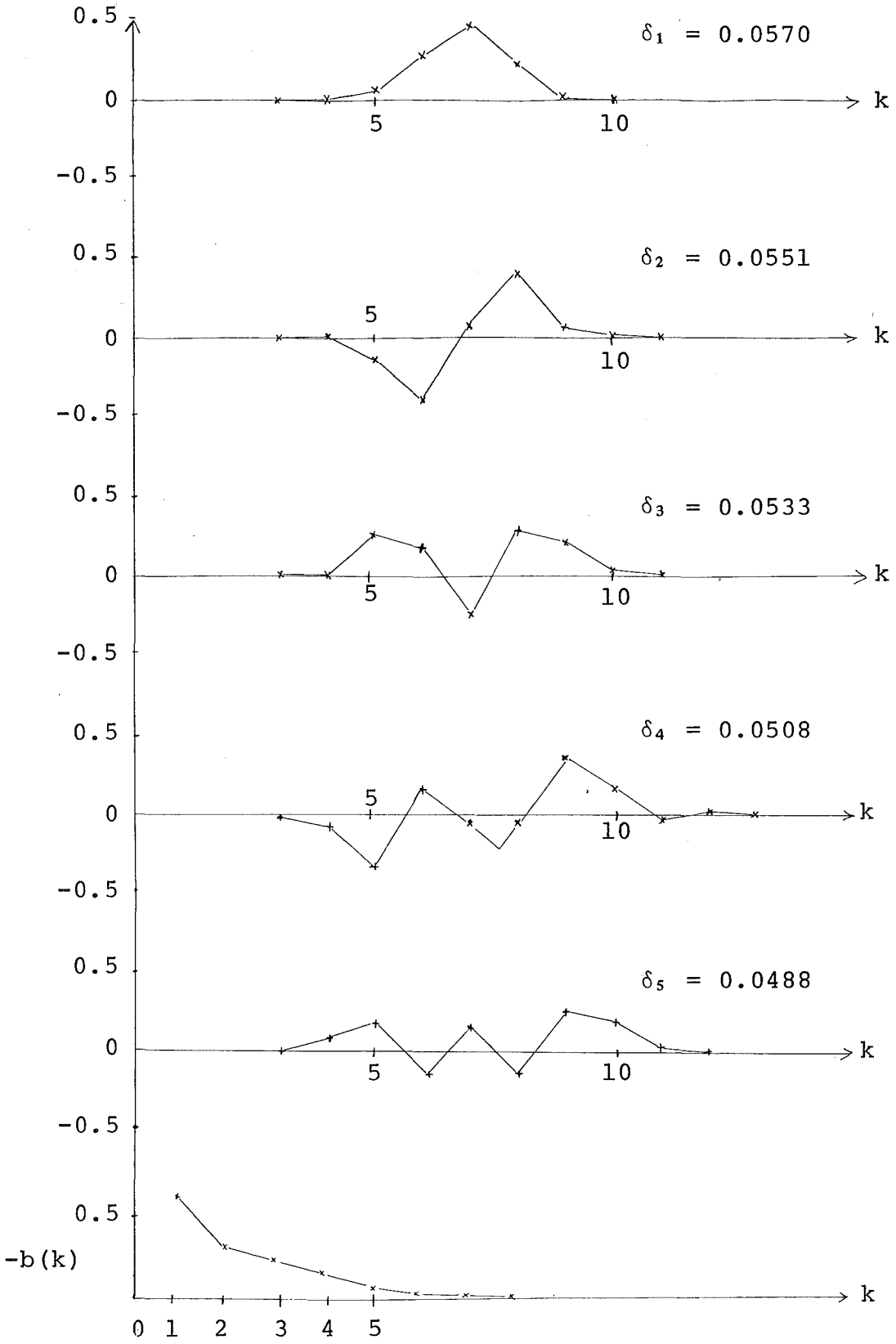

Figure 5.2

Wave spectra for the first five eigenvectors at $\mu = 0.3$, given the carrier wave b and $(h_1, h_2, h_3) = (0.3, 0.4, 0.3)$.

by BRYANT (1977) for the open two layered fluid. For short wavelengths, under the approximation $b(1) = -1$, $b(\ell) = 0(\varepsilon)$, $\ell > 1$, he gives an explanation for these patterns and observes that they persist as the wavelength increases. In the present case for relatively long waves the same explanation is valid. If k is the central wavenumber for the group then the first form is clearly dominated by $\bar{a}'(k-1)$, $\bar{a}'(k)$ and $\bar{a}'(k+1)$. Considering the first five forms the only other harmonics which have much influence are $\bar{a}'(k\pm2)$, but since $b(2)$ is considerably smaller than $b(1)$ a reasonable approximation to equation (5.6) [especially for the first few forms of solution] is given by

$$\{\omega_1(k)-\mu kc-\delta\}\bar{a}'(k) = \varepsilon R_{121}(k,-1)b(1)\bar{a}'(k-1)r_1(k-1) + \varepsilon R_{121}(k,1)b(1)\bar{a}'(k+1)r_1(k+1), \quad m_1 \leqslant k \leqslant m_2 .$$

Calculation of $R_{121}(k,\ell)$ for various k and ℓ confirms that

$$R_{121}(k,-1)r_1(k-1) \simeq R_{121}(k,1)r_1(k+1)$$

whence, writing μc as $\omega_2(1)$,

$$\{\omega_1(k)-k\omega_2(1)-\delta\}\bar{a}'(k) - \varepsilon R_{121}(k,1)b(1)r_1(k+1)[\bar{a}'(k+1)+\bar{a}'(k-1)] = 0, \quad m_1 \leqslant k \leqslant m_2 .$$

This allows the difference equations

$$\bar{a}'(k+1) - 2\bar{a}'(k) + \bar{a}'(k-1) + f(k)\bar{a}'(k) = 0 \qquad m_1 \leqslant k \leqslant m_2 \qquad (5.11)$$

to be written. [At short wavelengths $r_1(k+1)\ R_{121}(k,\ell)$ behaves like $k^{3/2}$ and $\omega_1(k)$ like $k^{1/2}$ so $f(k)$ will behave approximately like $Ak^{-3/2} + Bk^{-1} + Ck^{-1/2} + D$]. Comparison of (5.11) with

$$\frac{d^2y}{dx^2} + f(x)y = 0$$

implies oscillatory solutions for $\bar{a}(k)$, provided $f(k) > 0$, and convergent or divergent solutions for $f(k) < 0$. The only stationary value of $f(k)$ is where a maximum occurs near

$$\frac{df(k)}{dk} \simeq \frac{d}{dk}\{\omega_1(k) - k\omega_2(1) - \delta\} = 0$$

$$\text{i.e.} \quad \omega_2(1) = \frac{d\omega_1(k)}{dk} = c_{g1}(k). \tag{5.12}$$

Thus $\bar{a}'(k)$ is oscillatory near the centre of each group where (5.12) holds and decreases monotonically to zero at each end. Higher δ implies lower $f(k)$ and hence a decrease in both the range of oscillation and the number of oscillations of $\bar{a}'(k)$ as a function of k. Figure (5.2) displays all these characteristics.

The eigenvector $\bar{a}_i$, eigenvalue δ_i, and the values for $a(\ell)$, $b(\ell)$, and c are now used as starting values in solving equations (5.5) - (5.8) for the ith form of solution. The range of harmonics contributing to the group, $m_1 \leqslant k \leqslant m_2$, is chosen about the central wavenumber (found above as 7) large enough so as to obtain accuracy to 10^{-4}. In this case m_1 and m_2 were initially set at 1 and 12 respectively.

The first form of solution, corresponding to the largest eigenvalue δ_1, is sketched in figure (5.3a). The group envelope which has permanent shape is dotted. The group itself and the carrier wave have been first sketched separately at the upper interface and then superimposed to give the resultant profile of the structure at each interface.

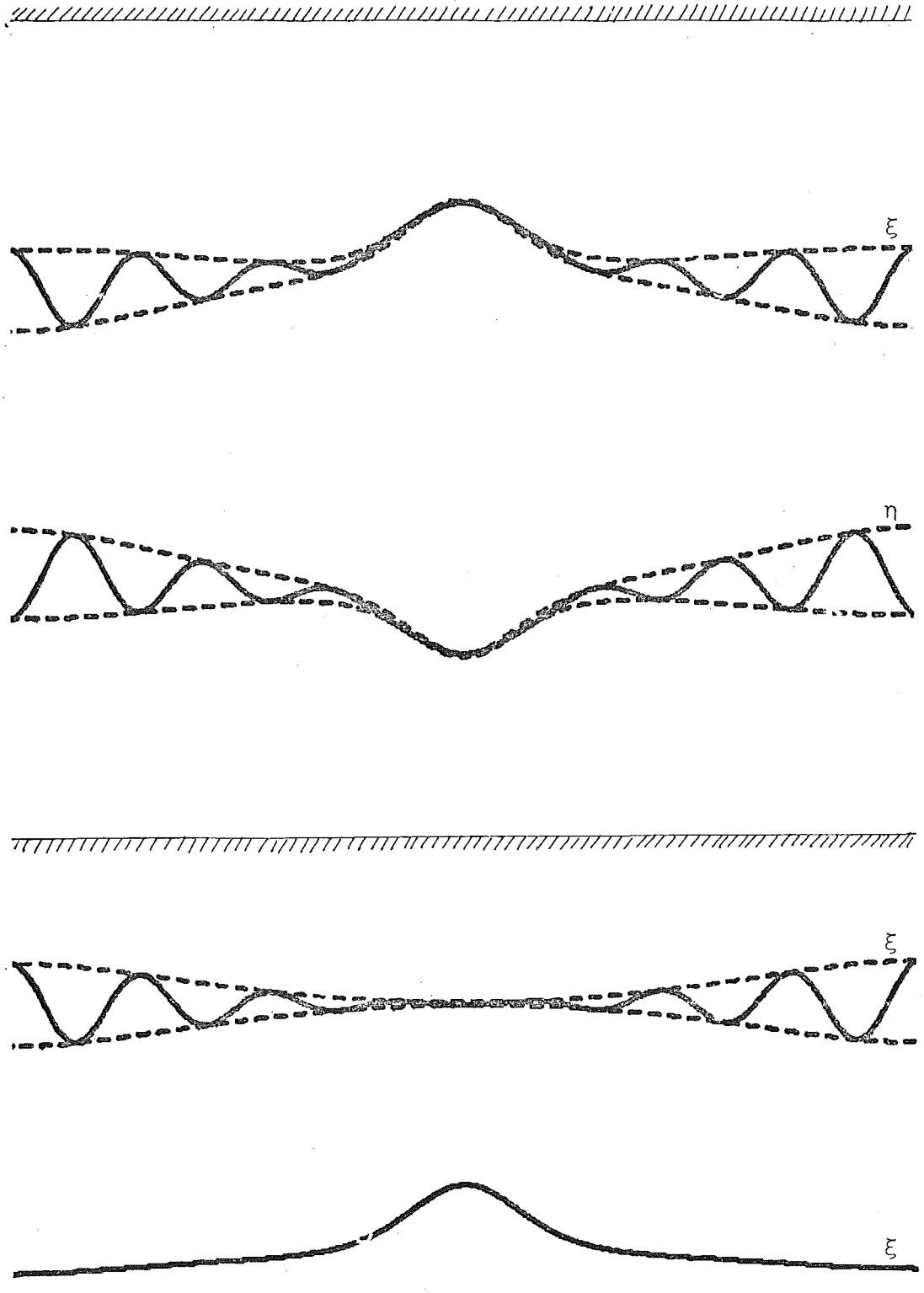

Figure 5.3a

One wavelength of the first form of permanent wave structure at $\mu = 0.3$ (Vertical magnification 6π).
$(h_1, h_2, h_3) = (0.3, 0.4, 0.3)$, $\delta_1 = 0.0570$ and $c = 0.0782$.
The carrier wave and group at the upper interface are shown separately.

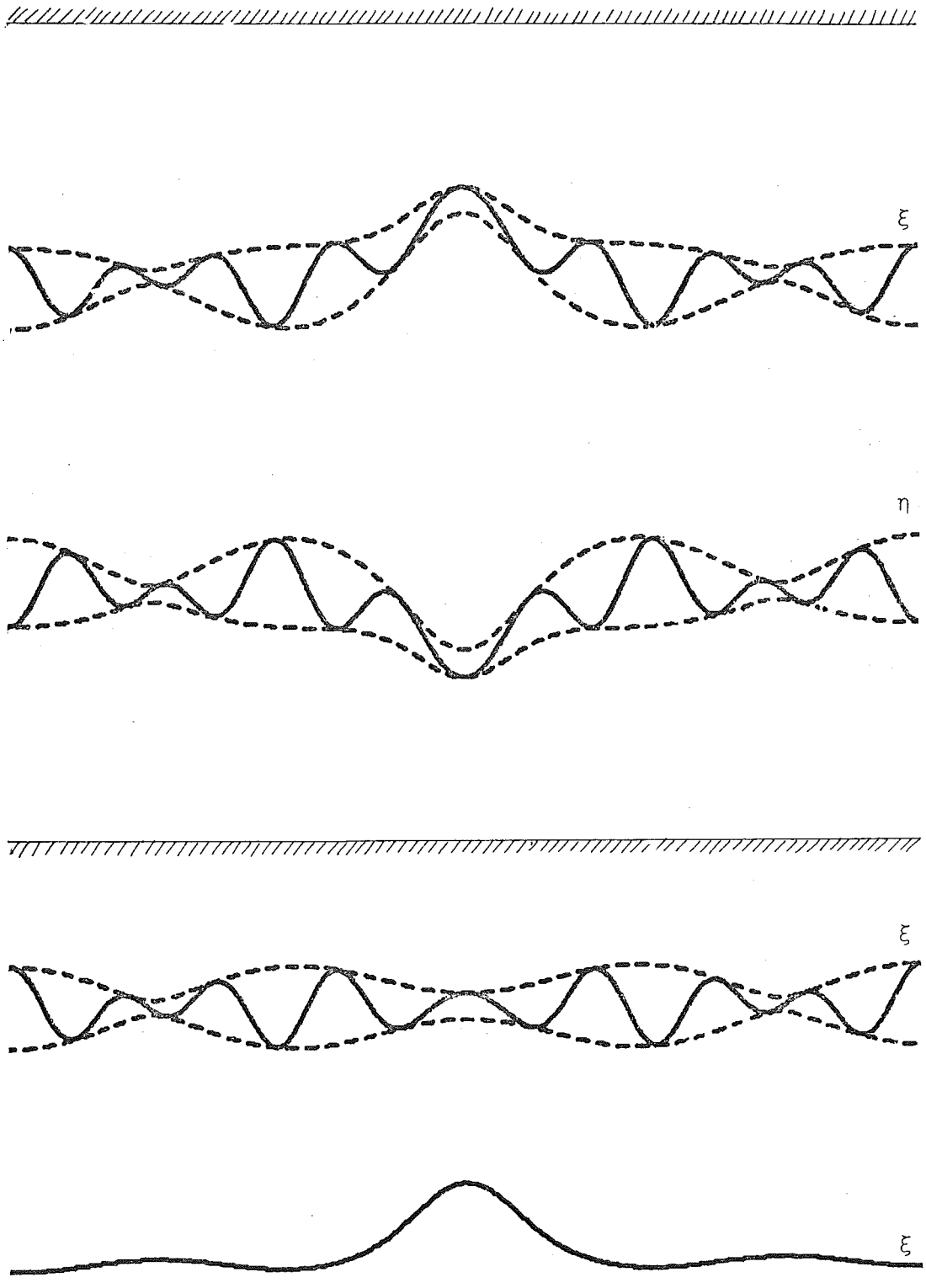

Figure 5.3b

One wavelength of the third form of the same structure.

$\delta_3 = 0.0551.$

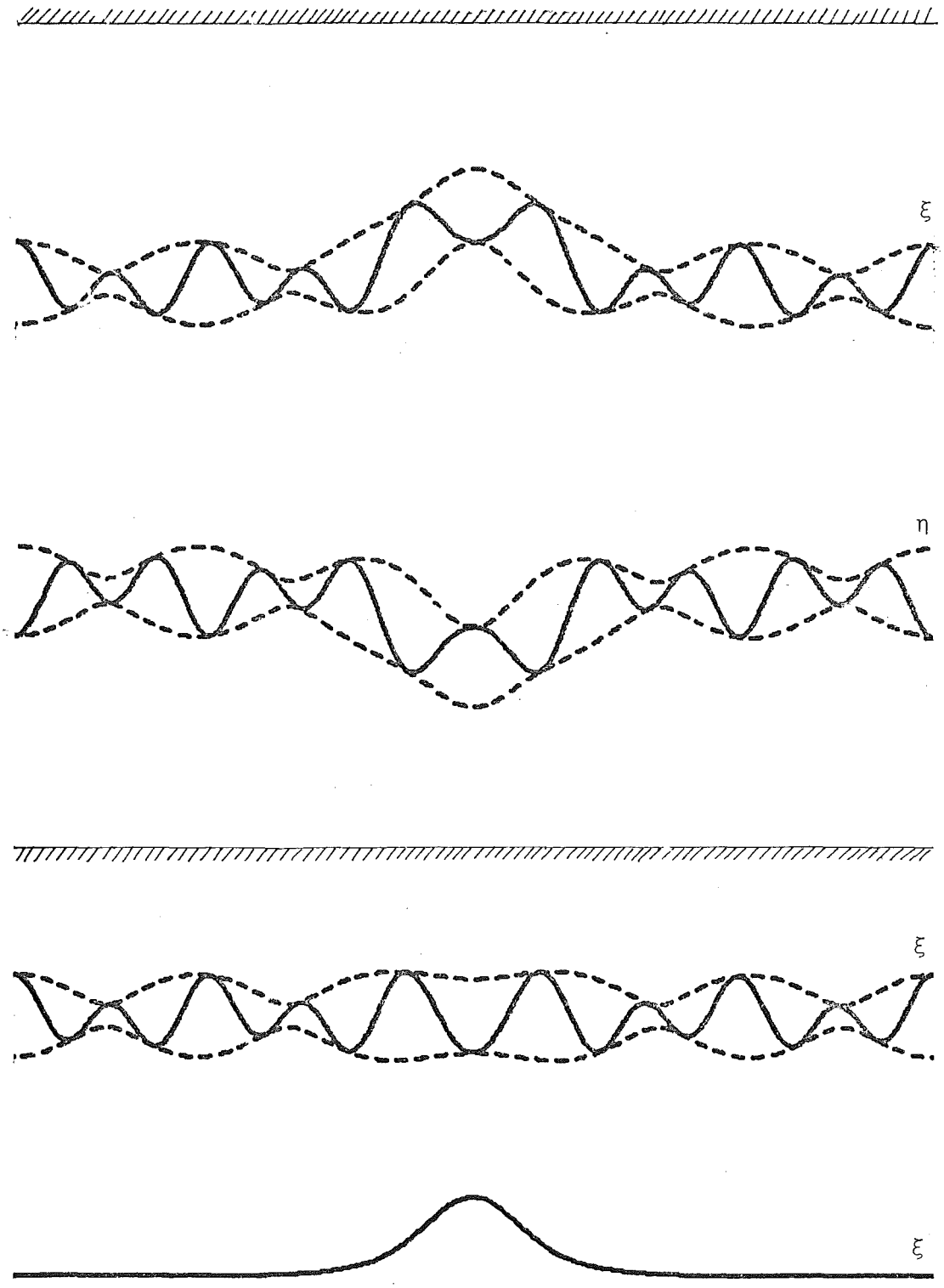

Figure 5.3c

One wavelength of the fifth form of the same structure.

$\delta_s = 0.0533.$

The third and fifth forms of solution, corresponding to the eigenvalues δ_3 and δ_5 respectively, are sketched in a similar manner in figures (5.3b) and (5.3c) respectively.

Note that if $\bar{a}(\ell)\,(m_1 \leqslant \ell \leqslant m_2)$ is a solution for the group then $-\bar{a}(\ell)\,(m_1 \leqslant \ell \leqslant m_2)$ is also a solution. Reference to equations (5.5) and (5.6) make this obvious, and it is also noted that both solutions will have the same envelope.

For the first form of solution the wavelength was altered in small steps of μ using the Newton-Raphson method at each step, so that this form of solution was found for μ between 0.3 and 3.0. As with the solutions in §4.4 the larger μ became (the shorter the wavelength), then the fewer the number of contributing harmonics both to the carrier wave and to the group. Also, as the wavelength decreases the central wavenumber of the group decreases until at about $\mu = 1.5$ the most significant contributor to the group is $\bar{a}(1)$. Reference to figure (5.1b) will confirm this since at $\mu = 1.5$

$$c_2(1) = c_{gl}(k) \quad \text{for} \quad k \simeq 1.4.$$

At very small wavelengths $b(1)$ and $\bar{a}(1)$ become the only significant harmonics so that there is no difference in wavelength between the group envelope and the fast mode waves within the envelope. A wavelength of the first forms of solution at $\mu = 1.3$ and 1.7 are sketched in figure (5.4). At $\mu = 1.3$ the second harmonic $\bar{a}(2)$ is dominant with a significant contribution from $\bar{a}(1)$. However at $\mu = 1.7$ this situation is reversed.

At small wavelengths (in terms of the number of harmonics involved) a distinct pattern, representing

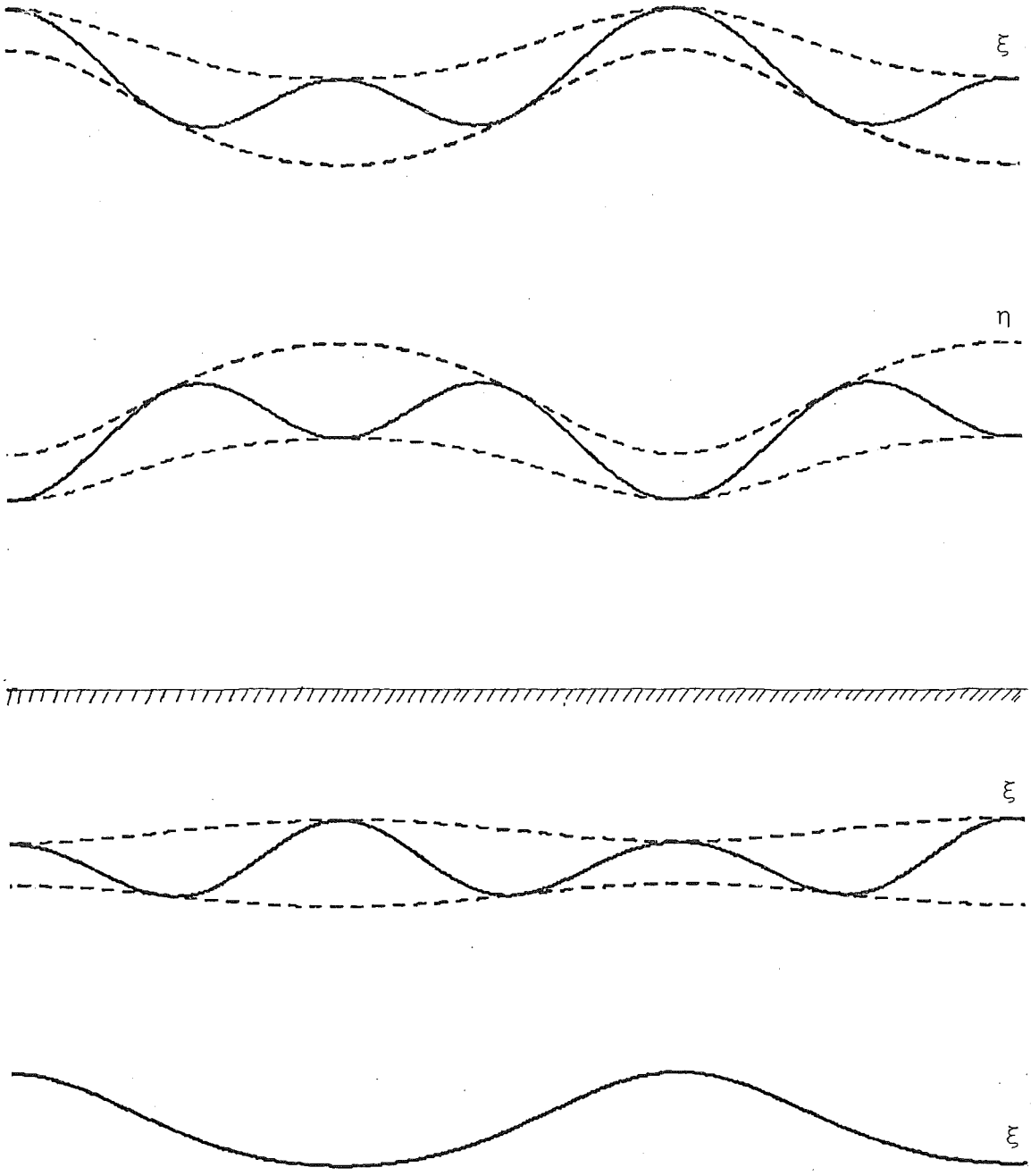

Figure 5.4a

One and a half wavelengths of the first form of permanent wave strucutre at $\mu = 1.3$ (vertical magnification 2π). $\delta_1 = 0.0575$ amd $c = 0.0762$.

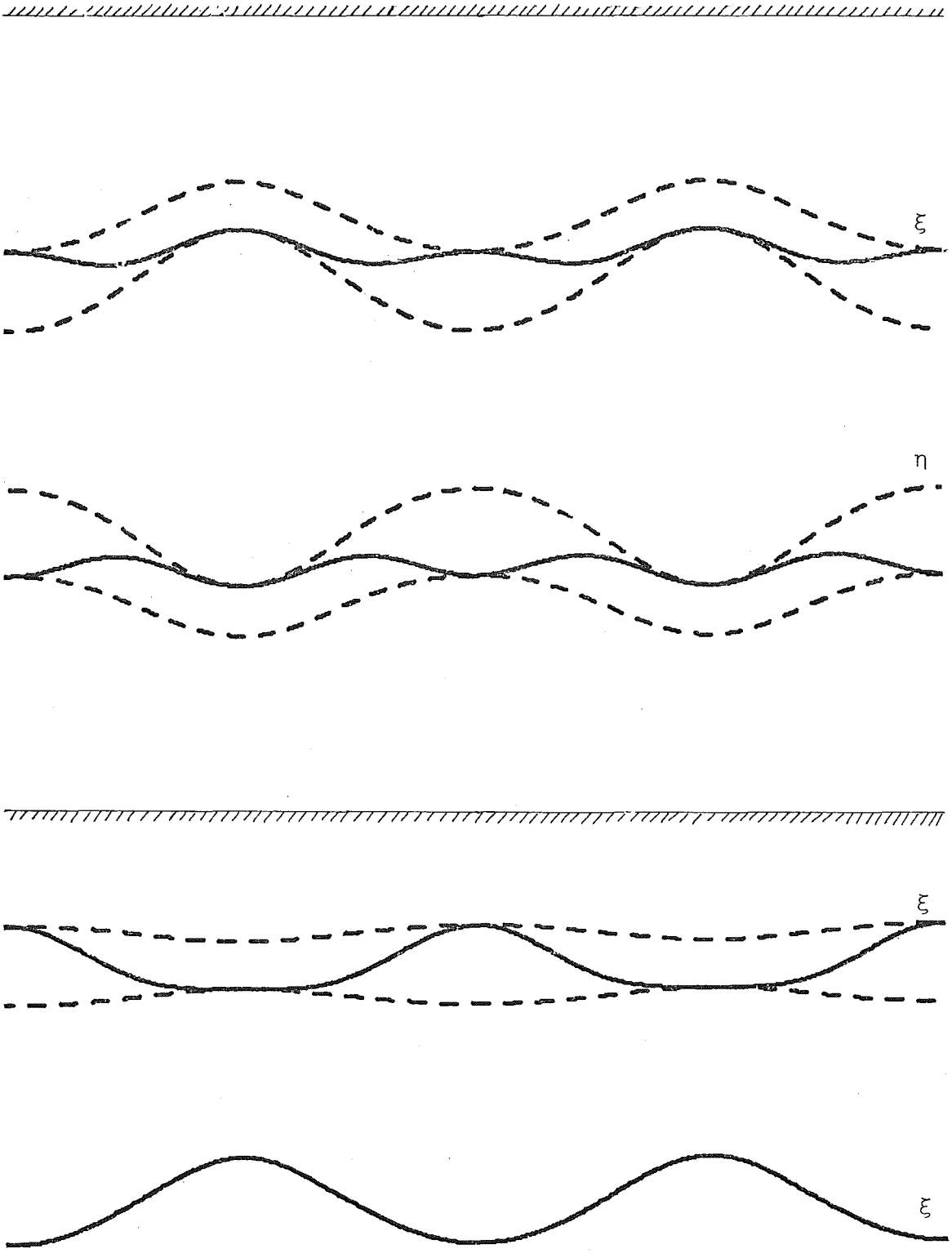

Figure 5.4b

Two wavelengths of the first form of permanent wave structure at $\mu = 1.7$ (Vertical magnification 2π). $\delta_1 = 0.0587$ and $c = 0.0754$.

degenerate sinusoidal solutions, emerges for the higher forms of solution. It has been observed for $\mu > 1.5$ that the first form becomes effectively a two harmonic structure comprising $\bar{a}(1)$ and $b(1)$ with minor influence due to $\bar{a}(2)$. The speed c will be fairly accurately described by $c = \omega_2(1)/\mu$, and since $b(1)$ is the only slower mode harmonic the rest of the harmonics satisfy equation (5.6), that is

$$\{\omega_1(k) - k\omega_2(1) - \delta\}\bar{a}(k) = 0(\varepsilon) \qquad m_1 \leqslant k \leqslant m_2 . \qquad (5.13)$$

In this case for the first form of solution, $k = 1$ only, whence $\omega_1(1) - \omega_2(1) \simeq \delta_1$, a relation which agrees with the obtained values for $\omega_1(1)$, $\omega_2(1)$ and δ_1. Naturally for $k = 2$, $\{\omega_1(2) - 2\omega_2(1) - \delta_1\}$ will be of greater magnitude and hence, by (5.13), $\bar{a}(2)$ will be much smaller. Suppose that $\delta_2 = \omega_1(2) - 2\omega_2(1)$ is another eigenvalue, then the associated eigenvector would have its major contribution from $\bar{a}(2)$, with $\bar{a}(1)$ and $\bar{a}(3)$ of smaller magnitudes. This is in fact what the results at large μ indicate, quite accurately. The third eigenvalue is $\delta_3 \simeq \omega_1(3) - 3\omega_2(1)$ which has an eigenvector featuring the third fast mode harmonic $\bar{a}(3)$, and so on. Thus when $\mu > 1.5$, $\omega_1(k) - k\omega_2(1)$ decreases monotonically for $k \geqslant 1$ and so the kth harmonic $\bar{a}(k)$ dominates the kth form of solution.

At lower values of μ the second or a higher harmonic dominates the first form of solution, and there is a turning point in $\omega_1(k) - k\omega_2(1)$ for which $k > 1$ [here, $\left.\frac{d\omega_1(k)}{dk}\right|_{k=k_0} = \omega_2(1)$, i.e. (5.1) holds]. In this case, for $k > k_0$, the kth harmonic will dominate the kth form of solution as before.

A situation has been described above where $b(1)$, $\bar{a}(k)$, and $\bar{a}(k\pm1)$ are the only harmonics of any significance in the kth form of solution, and the resonance

$$\omega_2(1) + \omega_1(k) - \omega_1(k+1) = 0 \qquad k = 1,2,...$$

dominates the proposed structure.

These degenerate solutions can be identified with the resonant triads of BRYANT and LAING (1978) explained in §5.2. However, it should be noted that only one of these triads will represent the type of interaction between a fast group and a slow carrier wave to which this chapter is devoted. The other forms are not fast group solutions, but rather, fast mode solutions for phase velocities $c_1(k) = c + \delta_k/\mu k$.

At long wavelengths (small μ) the bandwidth of wavenumbers increases for both group and carrier wave, and the central wavenumber for the group also increases. The dependence of significant harmonics in the group on wavelength is a logical consequence of the same dependence of significant harmonics in the carrier wave. As the latter increases, each slow mode harmonic will interact near resonance with a pair of fast group harmonics according to equation (5.6), with a subsequent increase in the number of group harmonics. Furthermore the number of harmonics in the carrier wave will be increased as a result of the presence of the group.

It is suggested by the sketches in figure (5.3a) that for very long wavelengths ($\mu < 0.1$) the solutions of the

first form would be characterised by a nearly uniform sinusoidal wavetrain which deforms in the vicinity of the solitary carrier wave, at which point the envelope of the wavetrain would decrease to a minimum coinciding with the point of maximum displacement of the carrier wave. The higher forms do not suggest such simple extrapolation. Although it is clear from figures (5.3b and c) that the group envelope is no longer minimum at the point of maximum displacement of the carrier wave, the group does seem to have divided itself into a number of "packets", the exact number depending on how high the form of solution.

There is obvious difference in scale and, more important, in shape of the permanent wave structures in figures (5.3) and (5.4) respectively. Figure (5.3) for $\mu = 0.3$ represents quite long waves and a large vertical magnification (or horizontal reduction) is used. This is necessary to show the structures to best effect. From a mathematical point of view this choice of wavelength is justifiable. Long wavelengths are necessary to increase the number of harmonics in both the group and the carrier wave and so provide a reasonably clearly defined situation in terms of the theory. The greater the number of interactions and harmonics, the more distinct the behaviour of the structure. This then enables us to discern and comprehend the less obvious structures obtained at shorter wavelengths. To be realistic from a practical or experimental point of view, the wavelengths under study should be comparable to the channel height where μ would have to be about 2π, that is, more

than 6. However, as figure (5.4) shows, for μ as low as 1.3 the structure becomes difficult to follow: the carrier wave has a distinctly sinusoidal shape whilst there is diminishing difference between a group wave and its envelope. At $\mu = 1.3$ the wavelength of a group wave is half that of the envelope whilst at $\mu = 1.7$ it is identical. The distinctive group structure of figure (5.3) is not present in figure (5.4). This, then, is why the emphasis throughout is on longer wavelengths.

For the calculations done so far [at $\mu = 0.3$ in particular, and at all other long wavelengths ($\mu < 1.0$)], convergence of the solutions using the Newton-Raphson technique was good when the odd numbered eigenvalues δ_1, δ_3 etc and their eigenvectors were used as starting points. However, attemps to find a second form of solution had no success. Using $\bar{a}_2$ and δ_2 no convergence could be obtained. There is no obvious reason for this and it can only be suggested that the velocity field will simply not permit certain solutions. As BRYANT (1977) found in the limiting case as $\rho_3 \to 0$ this second form of solution can exist, and so the density distribution must have some bearing on the existence. This "absence" is supported by the results of the resonant triad approach of BRYANT and LAING (1978). Equations (5.10) were found to yield two solutions for a group structure, which correspond to the first and third forms of solution. No second form appears. Higher forms also do not appear in this approach as they are all approximated as being sinusoidal.

Using the eigenvalue approach, in most cases some higher forms can be found using the appropriate eigenvalues and eigenvectors as starting points. Convergence cannot be assured although the second form is consistently absent and the third form consistently converges.

In addition to the solution for $(h_1, h_2, h_3) = (0.3, 0.4, 0.3)$, the system was also solved for closer interfaces. Firstly for the symmetric case $(h_1, h_2, h_3) = (0.4, 0.2, 0.4)$ and secondly for the unsymmetric case $(h_1, h_2, h_3) = (0.6, 0.2, 0.2)$. In both cases $\mu = 0.3$.

The proximity of the interfaces has a marked effect on the number of significant harmonics present. An increase in the velocity field at each interface due to waves at the other increases the degree of interaction and hence the number of harmonics. In each case the carrier wave contained about 40 harmonics of magnitude greater than 10^{-4}, and the group nearly 30, compared to the previous example in which each had less than 20. Also there is an increase in the central wavenumber of the group to about $k = 9$ for the symmetric case and $k = 10$ for the unsymmetric case.

Solutions for the first and third forms are sketched in figures (5.5) and (5.6) for each height distribution respectively. Individual profiles for the group and carrier wave are included. For the latter case $[(h_1, h_2, h_3) = (0.6, 0.2, 0.2)]$ the results indicated a resonance of the type mentioned in §4.4 at which

$$\omega_1(k) = k\omega_2(1) \quad \text{for} \quad k \simeq 24.$$

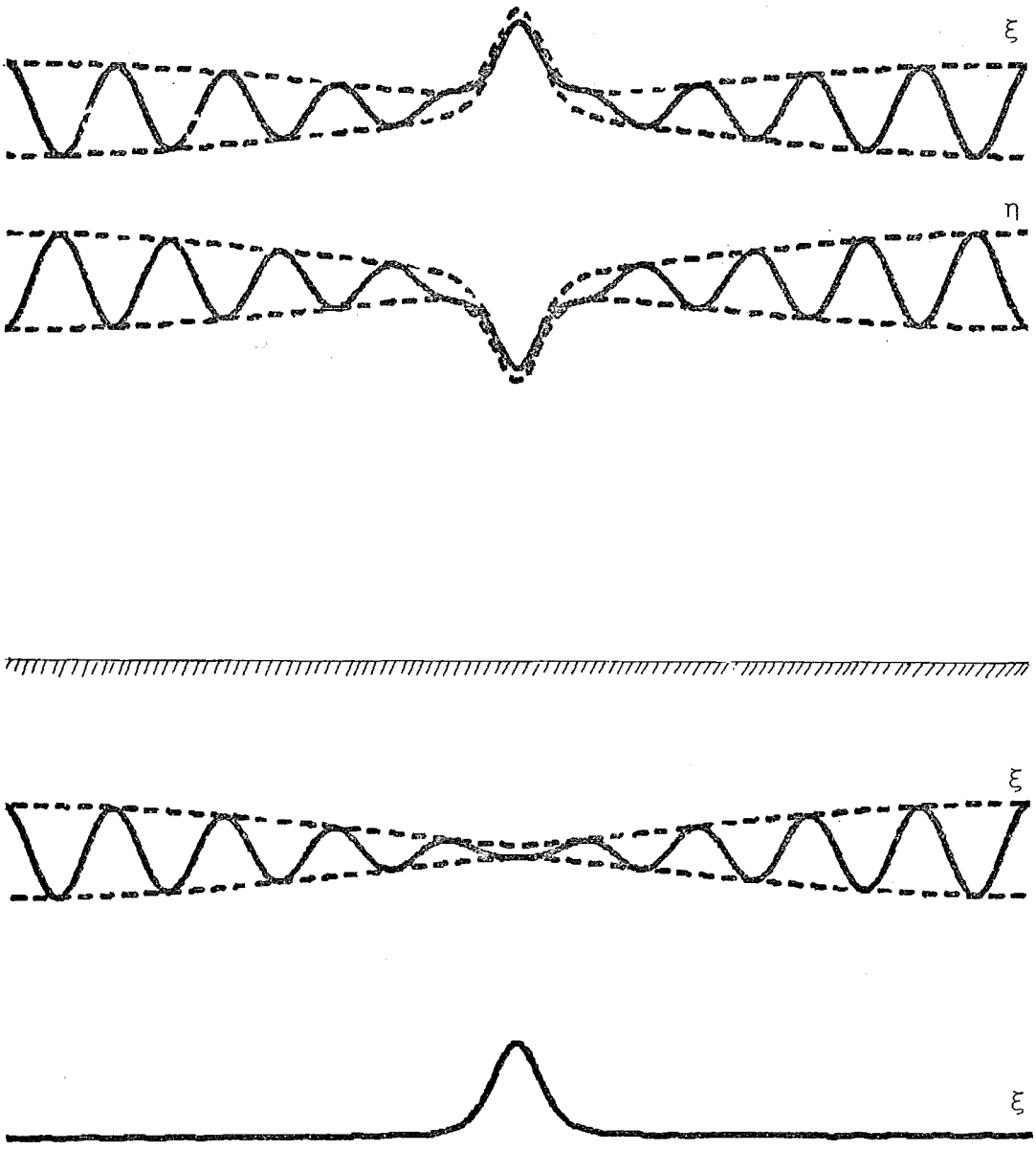

Figure 5.5a

One wavelength of the first form of permanent wave structure at $\mu = 0.3$ (Vertical magnification 6π).

$(h_1, h_2, h_3) = (0.4, 0.2, 0.4)$, $\delta_1 = 0.1177$ and $c = 0.0668$.

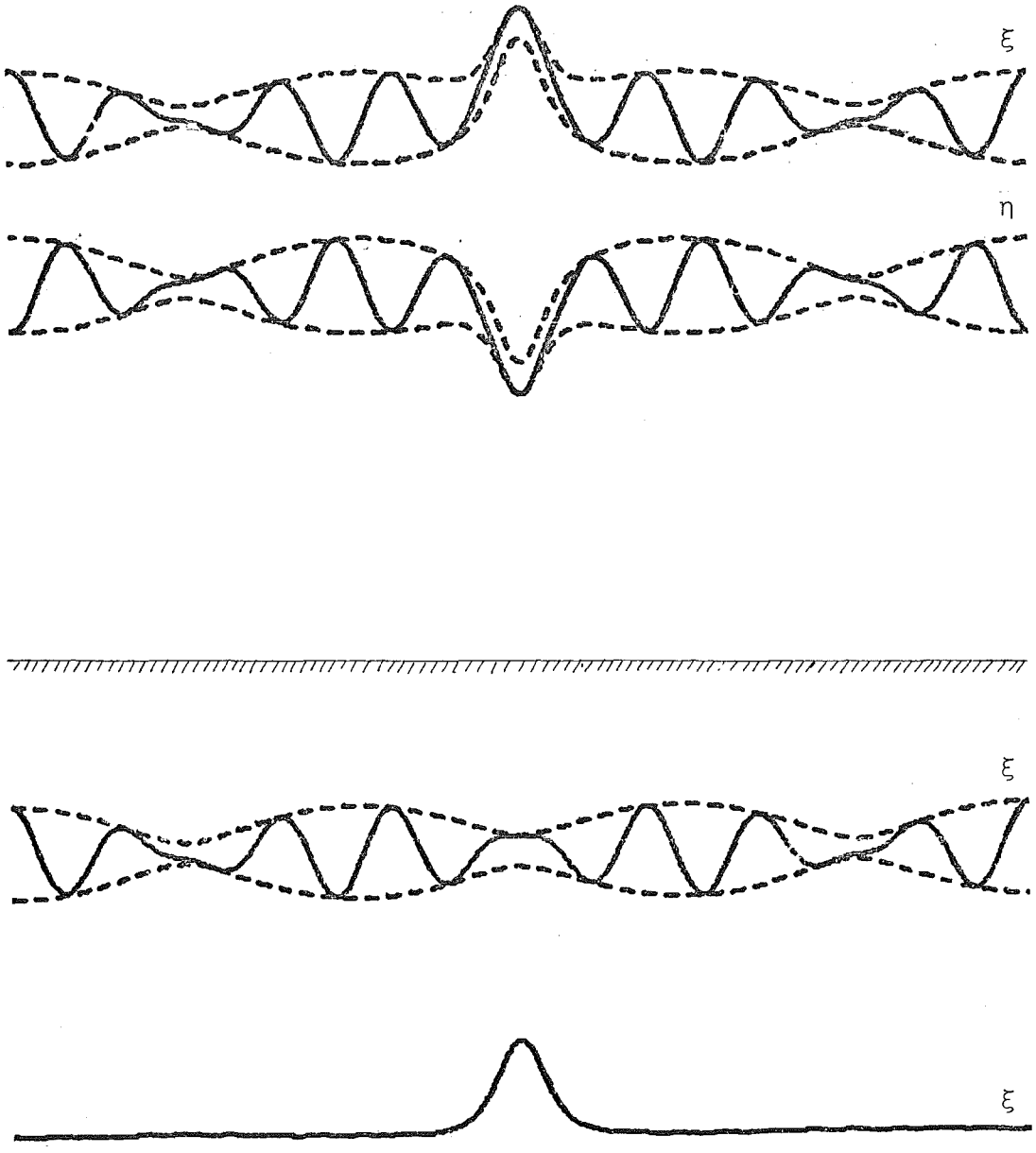

Figure 5.5b

One wavelength of the third form of the same structure.

$\delta_3 = 0.1157.$

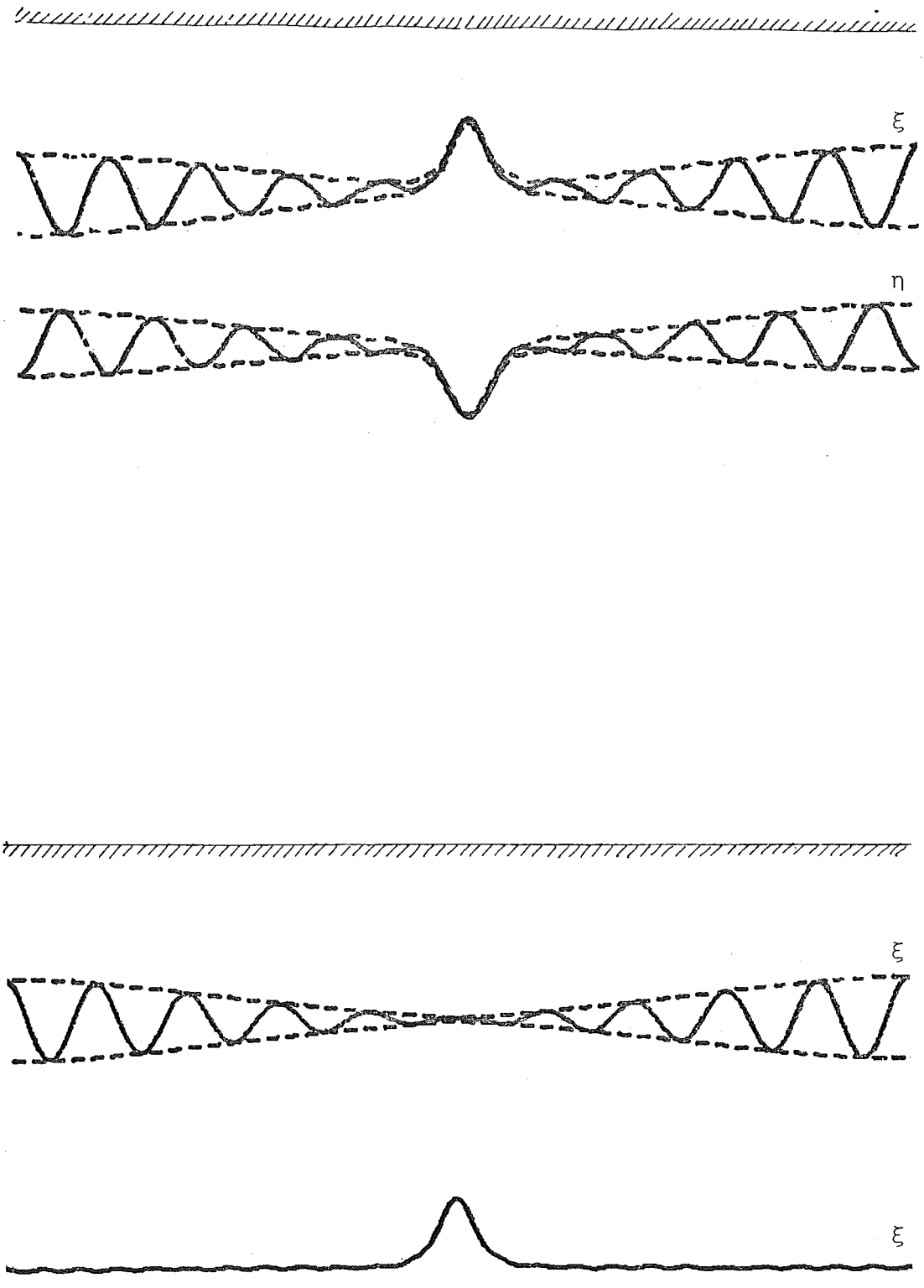

Figure 5.6a

One wavelength of the first form of permanent wave structure at $\mu = 0.3$ (Vertical magnification 6π).

$(h_1, h_2, h_3) = (0.6, 0.2, 0.2)$, $\delta_1 = 0.1067$ and $c = 0.0639$

The presence of the fast mode harmonic a(24) is noticeable.

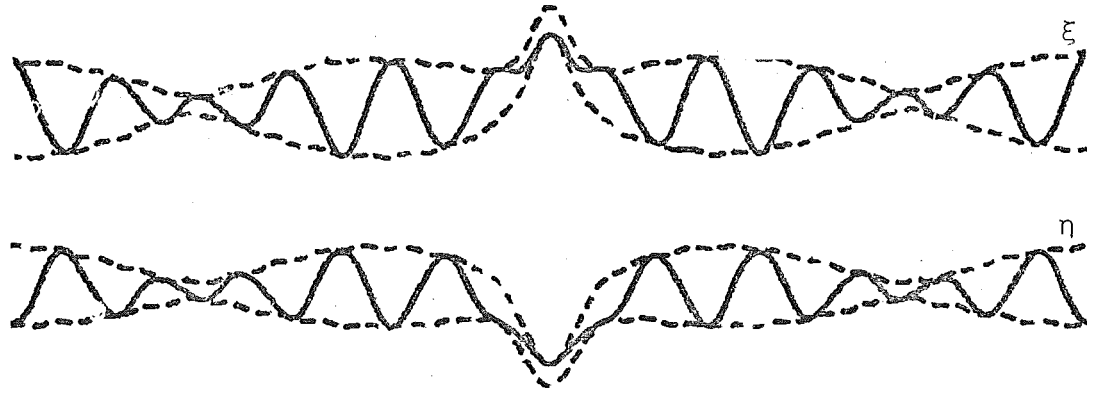

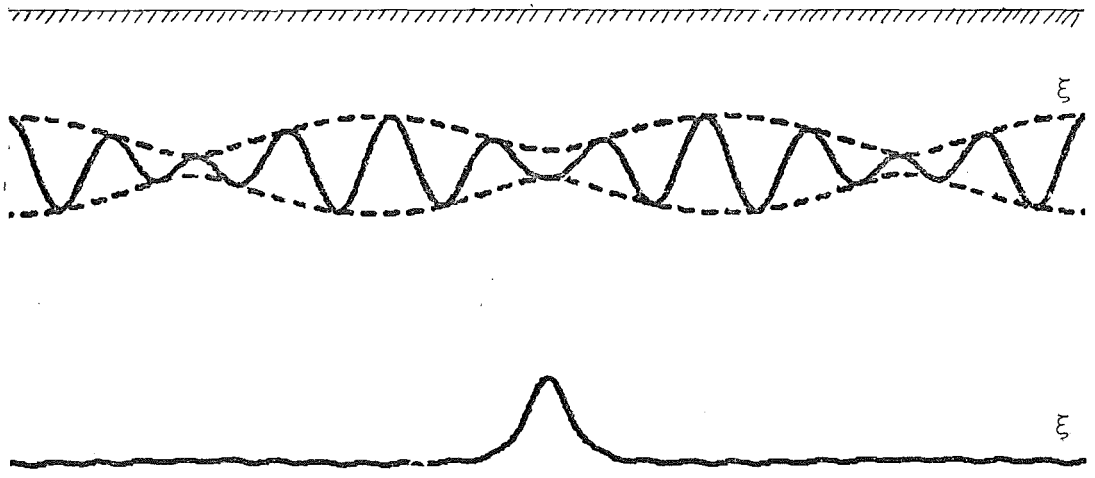

Figure 5.6b

One wavelength of the third form of the same structure.

$\delta_3 = 0.1050.$

This means the twenty-fourth fast mode harmonic is generated near resonantly and figure (5.6) shows this with the small "vibrations" on the carrier wave. Each vibration has a wavelength 1/24th of that of the carrier wave.

§5.4. *Conclusion.*

The permanent wave structures which have been found as solutions to the closed three-layer system comprise waves of unchanging shape at both interfaces, consisting predominantly of harmonics of the slower mode, and wave groups of faster mode waves whose envelopes are of permanent form, also at both interfaces. The close relation of the two modes ensures the whole structure is present at each interface almost equally. It is also responsible for several other features. The "carrier" wave part of the structure is only *predominantly* of the slower mode harmonics because at certain wavelengths the interaction of two such harmonics can cause near-resonant growth of faster mode harmonics to significant levels. This is illustrated by the profiles in figures (4.3) and (5.6), and is not in evidence when the modes are less closely related as in the two layer free-surface problem.

The permanence of the group envelope and carrier wave results from a balancing of linear dispersion effects and non-linear distortions. The horizontal velocity profiles interact in a rather complicated way, but the general argument is that whenever the horizontal velocity field set up by one part of the structure tends to cause non-linear stretching or compressing of the waves in another part, then the wavelengths, and hence the wave speeds, must change, and this dispersive effect acts to negate the non-linear distortion.

As the number of layers is increased the problem becomes much more complicated and algebraically formidable. However,

certain deductions from this study should remain valid. For a number of layers there will be a finite number of closely related internal wave modes. Consequently all features of permanent structures will be significant at all the interfaces. For the fastest of these modes, permanent waves will exist comprising harmonics of this mode only. For the slower modes the permanent wave solutions will be dominated by harmonics of one of these modes, but at certain wavelengths resonant interactions of the type described by equation (4.3) will introduce significant contributions from harmonics of the other modes. Group structures should also exist in which the "carrier" wave is the permanent wave consisting predominantly of harmonics of the slowest mode. Groups of permanent envelope will probably exist for each of the faster modes such that their group velocities all match the phase velocity of the carrier wave. Thus, these groups would have central wave-numbers which are larger for faster modes.

In theory there is apparently a variety of forms the structures may take. Each form depends on one of the various eigenvalues δ_i obtained for the phase of the waves within a group. It can be seen that the higher the form of solution, the more complex the shape of the group, and so the energy of the group would be expected to be higher too. This suggests that the higher forms are less stable, and that the first form of permanent wave structure is the most likely to occur in practice.

A feature of the analysis in chapters four and five is the generality provided by the freedom of the wavelength

parameter μ. The results generally describe *periodic* permanent structures of *finite* wavelengths - a logical consequence of the use of Fourier series as the means of solving. It is not a difficult matter to consider special cases as μ becomes very small and the wavelengths long. At such wavelengths the solutions represent "solitary structures" or, in the special case of Chapter four [§4.3, §4.4], for one mode only, "solitary waves". For the latter, in the region $\mu^2 \sim \varepsilon$ we have already seen that the system can be described by Korteweg - de Vries type evolution equations. However, the permanent structures do not reduce so conveniently to Korteweg - de Vries type systems and their behaviour at long wavelengths is subject to more tenuous conjecture. It is known that the cubic-Schrödinger equation describes soliton envelopes [see WHITHAM (1974) §17.7] something similar to the wave packets we have found in Chapter five, but the link between our evolution equations at small μ and the Schrödinger equation has yet to be established.

The importance of permanent solutions in a more general context can be summed up by reference to the findings of GARDINER, GREENE, KRUSKAL and MIURA (1974). Using the inverse scattering method for finding asymptotic solutions to the Korteweg - de Vries equation they conclude that in a non-linear dispersive medium acceptable initial data will evolve into a discrete set of permanent waves (solitons) and a train of dispersive waves. By virtue of their persistence the permanent waves assume considerable importance. Hopefully the existence of permanent features in the

internal system of chapters four and five can be seen in this light.

ACKNOWLEDGEMENTS

I would like to express my thanks to Dr Peter Bryant for his assistance and supervision over the years taken for this research. His discussion, suggestions and encouragement have been much appreciated.

I would also like to thank Shelley Climo for doing an excellent job in typing the final manuscript.

REFERENCES

BENJAMIN, T.B. 1966: "Internal waves of finite amplitude and permanent form". J. Fluid Mech. 25: 241.

BENNEY, D.J. 1966: "Long non-linear waves in fluid flows". J. Math. & Phys. 45: 52.

BENNEY, D.J. 1970: "Non-linear waves". Lect. Appl. Math 13: 103.

BENNEY, D.J. 1973: "Some properties of long non-linear waves". Stud. Appl. Math. 52: 45.

BENNEY, D.J. 1974a: "Interaction and dispersion of long waves". Stud. Appl. Math. 53: 137.

BENNEY, D.J. 1974b: "Long waves". Lect. Appl. Math. 15: 49.

BENNEY, D.J. 1976: "Significant interactions between small and large scale surface waves". Stud. Appl. Math. 55: 93.

BENNEY, D.J. 1977: "A general theory for interactions between short and long waves". Stud. Appl. Math. 56: 81.

BOUSSINESQ, J. 1871: "Théorie de l'intumescence liquide appelée onde solitaire ou de translation se propogeant dans un canal rectangulaire". Inst. Fr. acad. Sci. Comples Rendus. 79: 755.

BRETHERTON, F.P. 1964: "Resonant interactions between waves. The case of discrete oscillations". J. Fluid Mech. 20: 457.

BRYANT, P.J. 1973: "Periodic waves in shallow water". J. Fluid Mech. 59: 625.

BRYANT, P.J. 1974a: "Stability of periodic waves in shallow water". J. Fluid Mech. 66: 81.

BRYANT, P.J. 1974b: "Flow of a layered fluid from a reservoir". Proc. 5th Australasian Conf. Hydraul. and Fluid Mech. Vol 2: 421.

BRYANT, P.J. and WOOD, I.R. 1976: "Selective withdrawal from a layered fluid". J. Fluid Mech. 77: 581.

BRYANT, P.J. 1977: "Permanent wave structures on an open two layer fluid". Stud. Appl. Math 57: 225.

BRYANT, P.J. and LAING, A.K. 1978: "Permanent wave structures and resonant triads in a layered fluid". To appear in Stud. Appl. Math.

GARDINER, C.S., GREENE, J.M., KRUSKAL, M.D. and MIURA, R.M. 1970: "Korteweg - de Vries equation and generalisations". Comm. Pure Appl. Math. 27: 97.

GARGETT, A.E. and HUGHES, B.A. 1972: "On the interaction of surface and internal waves". J. Fluid Mech. 52: 179.

KEULEGAN, G.H. 1953: "Characteristics of internal solitary waves". J. Res. Nat. Bureau of Standards, 51: 133.

KORTEWEG, D.J. and DE VRIES, G. 1985: "On the change in form of long waves advancing in a rectangular channel, and a new type of long stationary waves". Phil. Mag. (5), 39: 422.

KRUSKAL, M.D. 1974: "The Korteweg - de Vries equation and related evolution equations". Lect. Appl. Math. 15: 61.

LAI, K.K. and WOOD, I.R. 1973: "A two layer flow through a contraction". J. Hydraul. Res. 13: 19.

LAING, A.K. 1975: "Flow of stratified fluids past obstacles". M.Sc. Thesis: Univ. of Canterbury.

LEWIS, J.E., LAKE, B.M. and KO, D.R.S. 1974: "On the interaction of internal and surface gravity waves". J. Fluid Mech. 63: 773.

LONG, R.R. 1956: "Solitary waves in one- and two-fluid systems". Tellus 8: 460.

LONGUET-HIGGINS, M.S. and STEWART, R.W. 1960: "Changes in the form of short gravity waves on long waves and tidal currents". J. Fluid Mech. 8: 565.

PETERS, A.S. and STOKER, J.J. 1960: "Solitary waves on liquids having non-constant density". Comm. Pure Appl. Math 13: 115.

RAYLEIGH, J.W.S. LORD. 1876: "On waves". Phil. Mag.(5) 1: 257.

SCOTT-RUSSELL, J. 1844: "Report on waves". British Association Report.

WHITHAM, G.B. 1974: "Linear and non-linear waves". publ. John Wiley and Sons.

WOOD, I.R. 1968: "Selective withdrawal from a stably stratified fluid". J. Fluid Mech. 32: 209.

WOOD, I.R. 1970: "A lock exchange flow". J. Fluid Mech. 42: 671.

WOOD, I.R. and LAI, K.K. 1972a: "Flow of a layered fluid over a broadcrested weir". J. Hydraul. Div. A.S.C.E. 98 HY1: 87.

WOOD, I.R. and LAI, K.K. 1972b: "Selective withdrawal from a two layered fluid". J. Hydraul. Res. 10: 475.

YIH, C.S. 1965: "Dynamics of non-homogeneous fluids". Publ. The MacMillan Co. New York.

APPENDIX

Denote $\omega_k = \omega_\alpha(k)$, $\omega_\ell = \omega_\beta(\ell)$, $\omega_{k\ell} = \omega_\gamma(k+\ell)$,

$$y_1 = \frac{\omega_\ell}{\tanh\ \mu\ell h_1} + \frac{\omega_{k\ell}}{\tanh\ \mu(k+\ell)h_1}$$

$$y_2 = \frac{\mu\ell}{\omega_\ell} + \frac{\mu(k+\ell)}{\omega_{k\ell}}$$

$$y_3 = \omega_\ell^{\,2} + \omega_{k\ell}^{\,2} - \omega_\ell\ \omega_{k\ell},$$

$$y_4 = \frac{\omega_\ell\ \omega_{k\ell}}{\tanh\ \mu\ell h_1\ \tanh\ \mu(k+\ell)h_1}$$

$$y_5 = \left(\frac{\rho_1\omega_\ell}{\rho_2\ \tanh\ \mu\ell h_1} - \frac{(\rho_1-\rho_2)\mu\ell}{\rho_2\ \omega_\ell}\right) \times \left(\frac{\rho_1\omega_{k\ell}}{\rho_2\ \tanh\ \mu(k+\ell)h_1} - \frac{(\rho_1-\rho_2)\mu(k+\ell)}{\rho_2\ \omega_{k\ell}}\right)$$

$$y_6 = \frac{\omega_\ell}{\tanh\ \mu\ell h_3} + \frac{\omega_{k\ell}}{\tanh\ \mu(k+\ell)h_3}$$

$$y_7 = \frac{\omega_\ell\ \omega_{k\ell}}{\tanh\ \mu\ell h_3\ \tanh\ \mu(k+\ell)h_3}$$

$$y_8 = \left(\frac{\rho_3\omega_\ell}{\rho_2\ \tanh\ \mu\ell h_3} - \frac{(\rho_1-\rho_2)\mu\ell}{\rho_2\omega_\ell}\right) \times \left(\frac{\rho_3\omega_{k\ell}}{\rho_2\ \tanh\ \mu(k+\ell)h_3} - \frac{(\rho_2-\rho_3)\mu(k+\ell)}{\rho_2\ \omega_{k\ell}}\right).$$

Then
$$U_{\beta\gamma}(k,\ell) = \frac{1}{2}\mu k\ (\omega_{k\ell}-\omega_\ell)\left(\frac{\rho_1-\rho_2}{\rho_2}\ y_2 - \frac{\rho_1}{\rho_2}\ y_1\right)$$
$$+ \frac{\mu k(\rho_2-\rho_3)\ \cosh\{\mu k h_2\}(\omega_{k\ell}-\omega_\ell)}{2\ \rho_2\ r_\beta(\ell)r_\gamma(k+\ell)}\ y_2$$
$$- \frac{\mu k\ \rho_3\ (\omega_{k\ell}-\omega_\ell)}{2\ \rho_2\ r_\beta(\ell)r_\gamma(k+\ell)}\left(\cosh\ \mu k h_2 + \frac{\sinh\ \mu k h_2}{\tanh\ \mu k h_3}\right) y_6$$
$$+ \frac{\mu k\ \sinh\ \mu k h_2}{2\ r_\beta(\ell)r_\gamma(k+\ell)}\left(y_8 - \frac{\rho_2-\rho_3}{\rho_2}\ y_3 - \frac{\rho_3}{\rho_2}\ y_7\right),$$

$$V_{\beta\gamma}(k,\ell) = -\frac{\mu k\ \rho_1\ (\omega_{k\ell}-\omega_\ell)}{2\ \rho_2\ \tanh\ \mu k h_1}\ y_1$$
$$+ \frac{1}{2}\mu k\left(\frac{\rho_1-\rho_2}{\rho_2}\ y_3 - \frac{\rho_1}{\rho_2}\ y_4 + y_5\right)$$

$$- \frac{\mu k(\rho_2 - \rho_3)\ \sinh\{\mu k h_2\}(\omega_{k\ell} - \omega_\ell)}{2\ \rho_2\ r_\beta(\ell) r_\gamma(k+\ell)}\ y_2$$

$$+ \frac{\mu k\ \rho_3\ (\omega_{k\ell} - \omega_\ell)}{2\ \rho_2\ r_\beta(\ell) r_\gamma(k+\ell)}\ \sinh\ \mu k h_2 + \frac{\cosh\ \mu k h_2}{\tanh\ \mu k h_3}\ y_6$$

$$+ \frac{\mu k\ \cosh\ \mu k h_2}{2\ r_\beta(\ell) r_\gamma(k+\ell)}\ \frac{\rho_2 - \rho_3}{\rho_2}\ y_3 - y_8 + \frac{\rho_3}{\rho_2}\ y_7\ ,$$

$$P_{\alpha\beta\gamma}(k,\ell) = \left(1 - \frac{\rho_1\ \omega_k^{\,2}}{(\rho_1 - \rho_2)\mu k\ \tanh\ \mu k h_1}\right) U_{\beta\gamma}(k,\ell)$$

$$+ \frac{\rho_2\ \omega_k^{\,2}}{(\rho_1 - \rho_2)\mu k}\ V_{\beta\gamma}(k,\ell)\ ,$$

$$R_{\alpha\beta\gamma}(k,\ell) = \frac{1}{r_\alpha(k) - \tilde{r}_\alpha(k)} \left(\frac{P_{\alpha\beta\gamma}(k,\ell)}{(\omega_k + \omega_{k\ell} - \omega_\ell)}\right.$$

$$\left. - \frac{\omega_k + \omega_\ell - \omega_{k\ell}}{\tilde{\omega}_k^{\,2} - (\omega_{k\ell} - \omega_\ell)^2}\ \tilde{P}_{\alpha\beta\gamma}(k,\ell)\right)\ ,$$

$$S_{\alpha\beta\gamma}(k,\ell) = \frac{1}{r_\alpha(k) - \tilde{r}_\alpha(k)} \left(\frac{r_\alpha(k)\ P_{\alpha\beta\gamma}(k,\ell)}{(\omega_k + \omega_{k\ell} - \omega_\ell)}\right.$$

$$\left. + \frac{\omega_k + \omega_\ell - \omega_{k\ell}}{\tilde{\omega}_k^{\,2} - (\omega_{k\ell} - \omega_\ell)^2}\ \tilde{r}_\alpha(k) \tilde{P}_{\alpha\beta\gamma}(k,\ell)\right).$$